UNIVERSITY *of*
TASMANIA

INVESTIGATION OF NEOPLASTIC TRANSITION OF THE COLONIC EPITHELIUM IN THE WINNIE MOUSE MODEL OF SPONTANEOUS CHRONIC COLITIS

Sarron Randall-Demllo, BHlthSc (Hons)

Submitted in fulfilment of the requirements
for the Degree of Doctor of Philosophy

School of Health Sciences
University of Tasmania August,
2016

This thesis contains no material which has been accepted for a degree or diploma by the University or any other institution, except by way of background information and duly acknowledged in the thesis, and that, to the best of my knowledge and belief, this thesis contains no material previously published or written by another person, except where due acknowledgement is made in the text of the thesis, nor does the thesis contain any material that infringes on copyright.

Signed:

_____

Sarron Randall-Demllo

Date: 08/09/2016

Signed:

_____

Sarron Randall-Demllo

Date: 08/09/2016

The research associated with this thesis abides by the international and Australian codes on human and animal experimentation, the guidelines by the Australian Government's Office of the Gene Technology Regulator and the rulings of the Safety, Ethics and Institutional Biosafety Committees of the University.

Paper: *Characterisation of colonic dysplasia-like epithelial atypia in murine colitis*, World Journal of Gastroenterology, 2016
Located in: Chapters 3 and 5
Sarron Randall-Demllo[1], Ruchira Fernando[2], Terry Brain[2], Sukhwinder Singh Sohal[5], Anthony L. Cook[3], Nuri Guven[4], Dale Kunde[1], Kevin Spring[678] and Rajaraman Eri[1]

1 School of Health Sciences, University of Tasmania, Launceston, Tasmania, Australia

2 Department of Pathology, Launceston General Hospital, Launceston, Tasmania, Australia

3 Wicking Dementia Research and Education Centre, University of Tasmania, Hobart, Tasmania, Australia

4 Division of Pharmacy, School of Medicine, University of Tasmania, Hobart, Australia

5 Breathe Well Centre of Research Excellence for Chronic Respiratory Disease and Lung Ageing, School of Medicine, University of Tasmania, Hobart, Australia

6 Medical Oncology, Ingham Institute for Applied Medical Research, Liverpool, NSW, Australia

7 Liverpool Clinical School, Western Sydney University, NSW, Australia

8 South West Sydney Clinical School, University of New South Wales, NSW, Australia

Author contributions:
Randall-Demllo S and Eri R conceived and designed the experiments.
Randall-Demllo S performed experiments and collected data
Randall-Demllo S, Fernando R, Brain T analysed the data. Fernando R, Brain T, Sohal SS, Cook AL, Gueven N, Kunde D and Eri R contributed reagents and materials.
Randall-Demllo S, Fernando R, Brain T, Sohal SS, Cook AL, Gueven N, Kunde D, Spring K, Eri R contributed to writing the manuscript.

Signed:

Sarron Randall-Demllo	Nuri Guven
Ruchira Fernando	Dale Kunde
Terry Brain	Kevin Spring
Sukhwinder Singh Sohal	Rajaraman Eri
Anthony Cook	

ABSTRACT

Inflammatory bowel diseases (IBD) include a range of pathologies, with ulcerative colitis (UC) and Crohn's disease (CD) representing the bulk of IBD cases. Both UC and CD are life-long immune disorders which are the cause of significant morbidity with the incidences of both diseases increasing globally. Chronic inflammation of the colon, such as that occurring in ulcerative colitis or Crohn's colitis is associated with an increased risk of colorectal cancer. The mechanisms responsible for the transition from chronically inflamed tissue and colorectal cancer remain largely unknown.

Defects in the formation of a colonic mucous lining impermeable to bacterial penetration have been associated with inflammatory bowel diseases. Genetic ablation of the predominant gel-forming mucin in the colon, mucin-2 (Muc2), produces a chronic colitis by permitting contact between the host tissues and the micro-organisms resident within the colon. Animals with defects in mucus synthesis also display an increased incidence of intestinal tumours, the development of which may accelerated by the severity of the concomitant chronic inflammation.

The present study therefore aimed to investigate the utility of using the Winnie mouse to model the progression of chronic colitis to colonic cancer. Winnie carry a homozygous missense mutation in Muc2, resulting in spontaneous colitis and ER stress due to Muc2 misfolding. Since Winnie display features of UC, we intended to characterise the molecular mechanisms mediating the transition from chronically inflamed mucosa to early pre-cancerous lesions in these animals.

Administration of the colonic irritant dextran sulphate sodium (DSS) in a regimen of three, seven-day cycles in Winnie mice to simulate bouts of severe inflammation was trialled. The distal colon of Winnie mice after completion of the DSS protocol revealed hyperplastic mucosa with glandular morphological abnormalities resembling pre-cancerous change. Architectural derangement consistent with high-grade dysplasia was present in 55% of Winnie receiving DSS whereas these features were absent untreated Winnie or wild-type mice (χ^2 = 6.667, P ¡ 0.01). Penetration of crypts beyond the muscularis mucosae was observed infrequently (27% of Winnie mice after DSS) but was absent in wild-type (WT) animals irrespective of treatment. Although dysplasia-like changes were evident after the completion of five DSS cycles, cessation of DSS administration allowed a return to a uniform crypt morphology.

Three cycles of DSS increased expression of *Ccl5*, *Trp53* by 10% and 28% ($P < 0.05$) but *Cav1* decreased 44% in Winnie + DSS relative to WT + DSS. Expression of *Myc* was unchanged in Winnie with or without DSS, but increased in WT following three cycles of DSS. Changes in distribution of vimentin and N-cadherin were not observed in the colon of Winnie suggesting that EMT was not involved in the manifestation of the observed pathology in the Winnie colon.

Though the cancerous potential of the lesions observed in Winnie was unclear, the described model may be useful in exploring the progression from chronic colitis to dysplasia. Persistent alterations to Cav1 and p53 expression in particular, may be associated with an abnormal regenerative response to pro-inflammatory stimuli in the colonic mucosa.

ACKNOWLEDGEMENTS

Thanks to my primary supervisor Dr. Raj Eri for the opportunity to pursue this fascinating and challenging project, and for his boundless optimism. I would also like to thank Dr. Anthony Cook, Associate Professor Heinrich Körner and Associate Professor Kevin Spring for their expert advice and supervision over the course of my studies. Thanks to Dr. Dale Kunde, Dr. Sukhwinder Singh Sohal, Mr. Dane Hayes for their generous provision of time, knowledge and resources all of which was crucial for this project.

A special thank you is reserved for Dr. Ruchira Fernando and Dr. Terry Brain and pathology staff of Launceston General Hospital and Launceston Pathology for their specialist skills, advice and the provision of valuable specimens.

I would also like to thank Puneet Singh and David Wescott at the Ingham Institute for all their valuable assistance. Thanks to all the technical and administrative staff at the School of Health Sciences over the years whose technical assistance and accommodating nature made life that much easier. Thanks to Paul Scowen and staff at the University of Tasmania Lab Animal Services, and the Monash Animal services for their help in breeding and re-deriving the mice for this project.

I am very grateful for the School of Health Sciences, Australian Rotary Health and the Rotary clubs of Tasmania, without whom this work would not have happened, and for their support of my development as a scientist and as person.

Finally, thanks to all my friends and colleagues, particularly Waheedha Basheer, Nicole Ranson and Qi Ying Lean who have lent me both their practical support and encouragement.

PUBLICATIONS

Randall-Demllo S, Fernando R, Brain T, Sohal SS, Cook AL, Guven N, Kunde D, Spring K, Eri R, Characterisation of colonic dysplasia-like epithelial atypia in murine colitis, World Journal of Gastroenterology, 2016; In press.

Lean QY, Eri RD, **Randall-Demllo S**, Sohal SS, Stewart N, Peterson GM, Gueven N, Patel RP, Orally Administered Enoxaparin Ameliorates Acute Colitis by Reducing Macrophage-Associated Inflammatory Responses, PLoS One, 2015, 10, doi:10.1371/journal.pone.0134259

Alkadhi S, Kunde D, Cheluvappa R, **Randall-Demllo S**, Eri R. The murine appendiceal microbiome is altered in spontaneous colitis and its pathological progression, Gut pathogens, 2014, 6, doi:10.1186/1757-4749-6-25

Randall-Demllo S, Chieppa M, Eri RD, Intestinal epithelium and autophagy: partners in gut homeostasis, Frontiers in Immunology, 2013, 4:1-14

Shabala L, Walker EJ, Eklund A, **Randall-Demllo S**, Shabala S, Guven N, Cook AL, Eri RD, “Exposure of colonic epithelial cells to oxidative and endoplasmic reticulum stress causes rapid potassium efflux and calcium influx, Cell Biochemistry and Function, 2013, 31:603-611

LIST OF ABBREVIATIONS

8-OHdG	8-hydroxyl-deoxyguanosine
A	Adenine
ACF	Aberrant crypt focus
ANOVA	Analysis of variance
AOM	Azoxymethane
APC	Adenomatous polyposis coli
BER	Base-excision repair
CACC	Colitis-associated colorectal cancer
CARD	Caspase-recruitment domain family member
C	Cytosine
CCL	C-C motif-containing chemokine ligand
CCN	Cyclin
CCR	C-C motif-containing chemokine ligand
CD	Crohn's disease
CDH	Cadherin
CDKN	Cyclin-dependent kinase inhibitor
CpG	Cytosine-phosphodiester-guanosine
COX	Cyclooxygenase
CRC	Colorectal cancer
CXCL	C-X-C motif-containing chemokine ligand
Da	Dalton
DAB	3,3'-diaminobenzidine
DC	Distal colon
DCC	Deleted in colorectal carcinoma
DPC4	Homozygously deleted in pancreatic cancer, locus 4
dNTP	Dinucleotide triphosphate

DNMT	DNA cytosine-5-methyltransferase
DPX	Dibutylphthalate polystyrene xylene
DNA	Deoxyribonucleic acid
DSS	Dextran sodium sulphate
ECM	Extracellular matrix
EMT	Epithelial-mesenchymal transition
ER	Endoplasmic reticulum
eNOS	Endothelial nitric oxide synthase
G	Guanine
G-CSF	Granulocyte-colony-stimulating factor
GSK	Glycogen-synthase kinase
H&E	Haematoxylin and eosin
HGD	High-grade dysplasia
IBD	Inflammatory bowel diseases
IFN	Interferon
IL	Interleukin
iNOS	Inducible nitric oxide synthase
JAK	Janus kinase
KRAS	Kirsten rat sarcoma viral oncogene
LGD	Low-grade dysplasia
LP	Lamina propria
LPS	Lipopolysaccharide
MAPK	Mitogen-activated protein kinase
MC	Middle colon
MGMT	O^6-methylguanine-DNA-methyltransferase
MHC	Major histocompatiblity complex
MMR	DNA mismatch repair
mPAS	Mild periodic acid-Schiff
miRNA	Micro-RNA
mRNA	Messenger ribonucleic acid
MSI	Microsatellite instability

MUC	Mucin
MLH	DNA mismatch repair protein, mutL homologue
MSH	DNA mismatch repair protein, mutS homologue
MUTYH	mutY adenine DNA glycosylase homologue
MYC	Myelocytomatosis viral oncogene
NADPH	Nicotinamide diphosphate, reduced
NBF	Neutral buffered formalin
NF-$\varkappa$B	Nuclear factor-$\varkappa$B
NLRP	NOD-containing, leucine-rich repeat, pyrin domain-containing
nNOS	Neuronal nitric oxide synthase
NOD	Nucleotide-binding oligomerisation domain
NO	Nitrous oxide
NOX	Nicotinamide diphosphate oxidase
OGG	8-oxo-guanine-excising DNA glycosylase
PAMP	Pathogen-associated molecular pattern
PRR	Pattern-recognition receptor
PBS	Phosphate-buffered saline
PC	Proximal colon
PCR	Polymerase chain reaction
PPARγ	Peroxisome proliferator-activated receptor-γ
PMN	Polymorphonuclear cells
PSC	Primary sclerosing cholangitis
RAG1	Recombination-activating gene 1
RNS	Reactive nitrogen species
ROS	Reactive oxygen species
RT-qPCR	Real-time quantitative polymerase chain-reaction
RNA	Ribonucleic acid
SD	Standard deviation
SFRP	Secreted Frizzled-related protein
SMAD	Mothers-against *Drosophila* homologue
SNP	Single-nucleotide polymorphism

SPF	Specific pathogen-free
STAT	signal transducer and activator of transcription
TBS	Tris-buffered saline
TBST	Tris-buffered saline with Tween-20
T	Thymine
TCF	T-cell transcription factor
TGF	Transforming growth factor
TLR	Toll-like receptor
TNF	Tumour necrosis factor
TP53	Transformation-related protein-53, human
TRP53	Transformation-related protein-53, murine
UC	Ulcerative colitis
UPR	Unfolded-protein response
WNT	Wingless/int-1
WT	Wild-type

TABLE OF CONTENTS

LIST OF TABLES

LIST OF FIGURES

CHAPTER 1

LITERATURE REVIEW

1.1 Epidemiology of UC, CD and IBD

Inflammatory bowel diseases (IBD), which include Crohn's disease (CD) and ulcerative colitis (UC), are a growing global health problem. Both diseases feature a chronic, relapsing and remitting inflammation of the gastrointestinal tract which causes significant morbidity for those affected. Since neither CD nor UC can be cured at present, life-long management of the disease through pharmacological and dietary intervention is necessary to maintain remission. Although a subset of patients experience the onset of IBD during childhood, the peak age at which diagnosis of CD or UC typically occurs is during the late teen years to early twenties. Presently, treatment for IBD involves inducing and maintaining a remission of symptoms, therefore, patients with IBD must endure chronic, relapsing illness for the remainder of their lives.

1.1.1 Incidence and prevalence

Incidence and prevalence of both CD and UC has historically been highest in the industrialised Western nations, particularly northern and central Europe, North America and the United Kingdom [1, 2]. Canada for example has, for CD and UC, 20.2 and 19.2 per 100,000 incident cases respectively, and a prevalence of 319 and 248 per 100,000 for CD and UC.

Geographical variation

A considerable degree of variation in both incidence and prevalence of CD and UC exists between populations, seemingly related to geographical region. Although previous researchers have suggested a high–low gradient of IBD incidence and prevalence from the Northern Hemisphere to the Southern Hemisphere, recent studies in Australia and New Zealand provided evidence against this idea [3]. Incidences of IBD in both the Geelong region in Australia (12.5 and 17.4 per 100,000/year, UC and CD respectively) and in Canterbury, New Zealand (7.6 and 16.5 per 100,000/year, UC and CD respectively) [4, 5]. The incidence of IBD in Australasia therefore closely resembles that of the Norther Hemisphere, but stands in stark contrast to that of the remaining Asia-Pacific region. The incidence of IBD is generally low in all Asian populations studied to date, though China displays considerable variation in the estimated rates [6]. The Guangzhou region in China has an incidence of 1.09 and 2.05 per 100,000 for CD and UC respectively, whereas incident cases of IBD are relatively rare in less urbanised areas. Incident rates of 1.25 and 1.30 for CD and UC respectively, have been recorded in Hong Kong, suggesting that some variance may be explained by an association between IBD and urbanisation [6]. Regions with low incidences of IBD also display a higher incidence of UC cases than CD whereas the incidences of both diseases are presently close to equal in Europe, North America and Australasia [1, 7]. In contrast, the ratio between CD to UC incident cases in Hong Kong is close to parity, similar to high-incidence regions [6]. The few studies in Africa, and South America have also recorded low estimates of IBD incidence rates [1, 2].

Temporal variation

Recent systematic review of population-based studies into the temporal trends in IBD incidence and prevalence has revealed a global increase in the incidence of both CD and UC [2]. While annual increases in incidence were observed in most studies (70% of UC and

60% of CD), only 6% of UC and none of the CD studies reported a decrease in incidence. Several populations with a historically low incidence of IBD have shown a trend toward an increased incidence of IBD, particularly UC. Eastern Asia, particularly South Korea and Japan have experienced increases in the rate of newly diagnosised cases of IBD in recent decades [8–10]. Increased incidence of IBD in typically low-incidence regions appears to favour UC more than CD. The ratio of CD to UC diagnoses in Asia is thought to be increasing with time, a trend which may mirror the initial predominance in UC cases followed by an increase in CD similar to the trend observed in Europe and North America [6, 11, 12]. In contrast, the last three decades have seen a possible stabilisation or slight decline in annual incident cases of UC in regions of high-incidence such as Canada, Denmark and the Netherlands [2]. While UC incidence has stabilised in high-incidence regions, incident cases of CD has continued to increase to the point where the incidences of both diseases are approaching parity. It might be assumed that the predominance of diagnosed UC cases in Asia may also stabilise over time while CD cases increase [8].

1.1.2 Aetiological factors for UC, CD and IBD

Ethnicity

Studies in the United States have indicated differences in the susceptibility to IBD associated with certain ethnic groups. While African-Americans display an equivalent rate of incidence and prevalence to Americans of European heritage, peoples of Hispanic and Asian heritage have comparatively lower rates of IBD [13]. Similar to the regions from which these Hispanic and Asian populations originated from, UC was more prevalent than that of CD. Immigrants from southern Asia living in the UK or North America have been the subject of several studies. Indian immigrants in Leicestershire (78% of whom were first-generation) displayed a higher incidence of UC during 1972–1989 [14]. A subsequent multi-centre study in Leicestershire suggested an increase in the incidence of UC in both the indigenous and migrant populations (7.0 and 17.2 per 100,000 respectively) [15]. Second-generation

immigrants displayed comparable rates of disease, and with similar severity and extent to that reported in the indigenous population. In contrast, first-generation immigrants in Sweden were found to have a decreased risk of IBD relative to the Swedish population [16]. Immigrants from South Asia in Ontario, Canada, display a lower incidence of IBD than the local Western European/North American population following migration to Canada [17]. The age at arrival appears to be important in determining the risk of developing IBD in immigrants from low-incidence regions, with subsequent generations raised in Canada displaying a similar incidence to the indigenous population. While it is clear that the environment has considerable influence on susceptibility to IBD in early life, ethnicity remains a likely modifier. For example, in immigrants in Sweden the risk of developing IBD however was dependent on the origin of these immigrants, with second-generation migrants from Iran and Iraq being particularly susceptible to UC and CD respectively [16].

Age

The majority of CD cases are diagnosed between the ages of 20–30 years [1]. In contrast, UC is typically diagnosed later in life between the ages of 30–40 years, though it has been suggested a second peak may exist between 60–70 years of age. Less frequent are the cases of IBD arising prior to adolescence, often called paediatric IBD, which may account for between 7% and 20% of total IBD cases. Generally, paediatric CD is more common than paediatric cases of UC. Change in the incidence rates for paediatric IBD appear to reflect the trend in incidence for IBD overall. Cases of paediatric CD in European populations have been increasing in the last two to three decades whereas the incidence of paediatric UC has remained unchanged or slightly decreased [18, 19].

Sex

Occurrence of CD has been reported as being slightly more frequent in females than in males (10–30%) in populations with high incidences of CD [4, 20, 21]. However, the sex bias in

CD has not been observed in areas of Europe and North America, where the ratio may be equivalent [18, 22]. Occurrence of UC may be slightly more frequent in males [4, 20, 21].

1.1.3 Environmental factors

While genetic factors are likely to be involved in susceptibility to IBD, environmental factors are doubtless a major driving force in the increasing IBD incidence. Two environmental risk factors for IBD have consistently been identified in repeated aetiological studies: smoking and appendectomy.

Smoking

Multiple studies have identified smoking as a behaviour associated with both CD and UC. Meta-analysis of studies investigating a possible relationship between smoking and IBD has confirmed the increased risk of CD (odds ratio = 1.76) and habitual cigarette smoking at the time of diagnosis [23]. Former smokers may also be at a similarly increased risk of UC relative to control populations. Conversely, active smoking at the time of diagnosis appeared to be protective (odds ratio = 0.58) against UC. Interestingly, low incidences of IBD in Asia and Africa co-incide with high smoking rates within the given regions, whereas regions in which smoking rates are lower have high rates of IBD. The timing of exposure to smoking is likely to be important to its effect on IBD, with the strongest association occurring in adolescents [24]. Exposure to smoking *in utero* has also been associated the development of CD later in life although this observation has not been reported by every study [25–27].

Appendectomy

A number of observational studies have associated appendectomy with protection from UC. The course of disease for patients with UC appears to be modified significantly for those who have undergone appendectomy prior to diagnosis. For example, a multi-centre study in Japan observed a more limited anatomic extent and reduced relapsing disease in patients

with UC and prior appendectomy [28]. Studies involving Australian UC patients have associated appendectomy before diagnosis with lower rates of immunosuppressive therapy or colectomy [29, 30]. However, several studies, including a systematic review, have failed to observe the same associations between appendectomy and UC [31–33]. Recent study of North American UC patients has suggested that appendectomy prior to diagnosis had no significant effect on colectomy rates, whereas post-diagnosis appendectomy increased the rate of colectomy [34]. While the subsequent meta-analysis supported the lack of protection from colectomy attributable to appendectomy it appears likely that the onset of UC may be delayed by prior appendectomy [29, 31, 34].

1.2 Pathological features of UC and CD

Patients with IBD typically display various non-specific symptoms associated with inflammation or irritability of the bowel. Chronic diarrhoea is the symptom most often reported among patients with IBD and is the prevailing symptom that prompts consultation with a physician [35]. Eighty-five percent of patients with CD and 70% of patients with UC experience an increase in the number of bowel movements. In patients with UC, constipation associated with the acute phase of disease is also reported, albeit with considerably less frequency than diarrhoea [36]. Colonic inflammation is the most likely cause of diarrhoea in IBD, however, malabsorption of food and bile acids in the small intestine due to CD-associated inflammation may also result in diarrhoea. Rectal bleeding and haematochaezia are usually associated with distal colonic and rectal disease and hence are more common in UC [37]. Increased urgency to defaecate and cramps occurring during defaecation (known as tenesmus) are often associated with active inflammation of the anorectal region. Abdominal pain is commonly reported by patients with either CD or UC and the location may vary according to the extent of disease. Patients with UC often report lower left quadrant pain

whereas the ileal inflammation that typically occurs in patients with CD may result in pain and cramps in the right lower quadrant.

A number of local and extra-intestinal complicating diseases have been associated with IBD. Fistulae and intestinal strictures are associated with sites of severe intestinal inflammation in patients with IBD. Approximately 50%–60% of patients with IBD will develop at least one extra-intestinal manifestation, such as arthritis, cutaneous lesions and primary sclerosing cholangitis [35]. The large degree to which symptoms overlap between IBD and non-IBD enteropathies, and the lack of biomarkers specific for either disease means that histological examination is essential for diagnosis. Indeed, histological features are the basis for the distinction between CD and UC.

1.2.1 Crohn's disease

The majority of patients with CD experience episodic "flare-ups" of acute disease followed by periods of remission. Tissue damage caused by inflammation may take week to decades to manifest. Damage to the intestine may be reversed by anti-inflammatory therapy, or recovery may occur spontaneously.

Crohn's disease may affect any region from the oral cavity to the anus. At diagnosis, the proportion of patients with CD presenting with either ileal, colonic or ileocolonic inflammation is approximately equal [38, 39]. One to four percent of patients with CD display oesophageal, gastric or duodenal involvement [40]. Isolated perianal disease is also observed in 2%–5% of patients newly diagnosed with CD. Chronic inflammation associated with CD results in alterations to the intestine that are in most cases, histologically distinct from UC. Neutrophilic accumulation and lymphoid aggregates in the intestinal mucosa are present in the early stages of disease. In the ileum of patients with CD, areas of inflamed mucosa are often interspersed with uninflamed regions. In the ileum, chronic inflammation results in villous atrophy, reducing the absorptive function of the small bowel. Chronic

inflammation also results in the progressive disruption of crypt structure. As the disease progresses the characteristic transmural inflammation becomes evident. A defining feature of CD with ileal involvement, is the formation of deep, fissuring ulcers penetrating into the muscularis externa. A series of ulcers may also merge together to form lines that extend longitudinally, eventually forming the cobblestone mucosa pattern associated with CD. Variation in the anatomical location and disease activity of CD has made comparing clinical studies somewhat difficult. To address some of these difficulties, the Vienna classification of IBD clinical phenotypes was developed.

The Vienna classification identifies distinct clinical phenotypes of CD based on the age, extent and severity of disease (Table 1.1). Following the initial diagnosis with CD, there is little change in the involved regions of the gastro-intestinal tract within each patient. However, follow-up examination after diagnosis revealed significant variation in CD disease behaviour [41]. At diagnosis, approximately three quarters of patients studied presented with non-stricturing, non-penetrating disease (B1). After diagnosis, the occurrence of patients with B1-type disease declined, while a progressive increase in structuring and penetrating disease was observed. Five years after diagnosis, half of patients with CD displayed a B1 phenotype whereas 21% presented with stricturing disease (B2) and 27% with penetrating lesions (B3). After ten years the proportion of patients with stricturing and penetrating disease increased to 32% and 37% respectively. The gradual change in disease behaviour toward a penetrating/stricturing phenotype explains the prevalence of surgery among patients with CD.

Strictures are more common in the small intestine than the colon and as such are a common complication occurring in patients with CD [42]. Fistulae and perforations of the bowel are also associated with CD. As the aforementioned complications are unaffected by anti-inflammatory medication, surgical intervention is necessary. Surgical removal of segments of the inflamed bowel is also indicated in patients with refractory CD. Approximately

Table 1.1: **The modified Vienna classification (Montreal) for Crohn's disease**

Age at diagnosis	A1	<16 years of age
	A2	between 17 years and 40 years
	A3	>40 years
Location	L1	ileal
	L2	colonic
	L3	ileocolonic
	L4	isolated upper disease*
Behaviour	B1	non-stricturing, non-penetrating
	B2	stricturing
	B3	penetrating
	p	peri-anal disease modifier†

* L4 is a modifier that can be added to L1–L3 when concomitant upper gastrointestinal disease is present. † p is added to B1–B3 when concomitant peri-anal disease is present.

70%–80% of patients with CD will undergo intestinal resection at 20 years after diagnosis [1]. Furthermore, patients with stricturing disease are more likely to require recurrent surgeries after the initial operation.

If inflammation is initially confined to the terminal ileum, symptoms of CD may not be readily apparent. With increased spread of disease to distal sites in the intestine, or the occurrence of systemic the symptoms of CD become evident [1]. Differentiation between colonic CD and UC may be complicated by similar clinical features. Deep ulcerations, strictures and fistulae are less common in the colon than in the ileum. As a result, some patients with CD may be initially diagnosed with UC.

1.2.2 Ulcerative colitis

Chronic superficial inflammation limited to the colon and rectum is a key feature of UC. Similarly to CD, the disease course of UC involves episodes of acute disease followed by episodes of remission.

The anatomical extent of UC is far more limited than that of CD. Inflammation associated with UC typically begins in the distal colon and/or rectum. While rectal involvement is not always present in the paediatric subset of patients with UC, it is almost always present in adult patients [43]. Over time inflammation spreads proximally from the initial site in the colorectal region, potentially affecting the entire colon and caecum. It is estimated that 50% of patients with UC will have developed pancolitis 20 years after diagnosis [1]. Although inflammation of the terminal ileum is infrequent in patients with UC, pancolonic disease has been associated with ”backwash” ileitis. Backwash ileitis in UC was initially believed to be due to reflux of colonic contents through an inflamed and dysfunctional ileo-caecal valve. However, the aetiology of ileitis in UC may be more complex than first thought. A study by Haskell *et al*. suggested that colonic inflammation adjacent to the ileum although frequent, was not necessary for ileitis [44].

Even extensive, pancolonic CD rarely affects the rectum, a site that is commonly inflamed in patients with UC. Colonic inflammation associated with UC spreads proximally from the distal colon forming a continuous lesion. Similarity exists between the histological features of colonic CD and UC, especially in the early stages of disease. Chronic inflammation of the colon results in accumulation of neutrophils in the mucosa and the formation of lymphoid aggregates in the mucosa. Unlike CD, submucosal inflammation is minimal in UC and is instead confined to the mucosa. Superficial ulceration of the mucosa is present and extends proximally, and in a uniform fashion, along the colon as disease progresses. Crypt abscesses are also frequent though fistulae are rarer than in CD. Perforation of the colon and resultant haemorrhage is infrequent, affecting approximately 15% of patients with UC, but is seriously

life-threatening. With the advent of immunosuppressive therapies and improved treatment strategies, mortality of patients with UC is currently not significantly higher than the general population.

1.2.3 Intestinal complications of UC

An array of intestinal complications have been associated with long-standing UC including anaemia, fistulae, and more rarely, distension and perforation of the colon. Additionally, the disease may be associated with colonic pseudopolypoid features. Pseudopolypoid inflammatory polyps, are islands of non-ulcerated mucosa, submucosa, or muscularis, surrounded by deep mucosal ulceration and are thus associated with active inflammation [45]. The non-ulcerative mucosal projecting above the ulcerated bowel wall are typically prominences of inflammatory leukocytic infiltrates and/or oedema, or alternatively may be hamartomata. Unless the pseudopolypoid tissue contains glandular dysplasia, these lesions are otherwise recognised as an insignificant risk of developing neoplasia.

Pseudopolyps may also serve as the basis for the infrequently observed post-inflammatory or filiform polyp, usually within the distal colon and rectum. Filiform polyps are likely formed during the regeneration of the ulcerated mucosa after the induction of remission in UC [46]. Despite its association with UC, filiform polyps have also been observed in association with neuromuscular alterations indicative of hamartamatous change [47]. The non-ulcerated epithelium may expand outwards from the under-surface of the pseudopolyp while the ulcer is simultaneously regenerated from the base. In such cases a ”stalk” of submucosa supports a genuine, thin, polypoid projection with complete mucosa extends into the lumen. Due to their originating from normal regenerating mucosa, filiform polyps are also regarded as having no risk of neoplasia, despite a lack of quantitative data regarding the incidence of neoplastic transformation in these polyps [48]. Although these polyps may extend in a branched fashion and even bridge the lumen, they are rarely the cause of clinically significant

bowel obstruction [49, 50]. However, a small subset of patients may develop a ”giant” ($>$ 15 mm) pseudopolyposis which have been in turn associated with intestinal intussusception.

Intestinal intussusception involves the ”telescopic” invagination of a segment of the intestine into another intestinal segment. Intussusception most commonly involves the junctions of the freely moving intestinal segments or those fixed retroperitoneally or adhesionally [51]. Intussusception may therefore be classified into entero-enteric, i.e. involving only the small intestine; colo-colonic, confined to the large bowel; ileo-colonic, between ileum and ascending colon; or ileo-caecal, between ileum and caecum only. Paediatric cases account for the majority of cases of intussusception whereas adult cases account for only 5% of total cases [51]. In children, intussusception most often occurs idiopathically, with no identifiable cause, or subsequent to viral or bacterial infection of the intestine [52] . Conversely, aetiology of adult intussusception is identifiable in 90%–93% of cases [53–55]. Adult cases of intussusception are rare, however intussusception in adults with UC appear to be rarer still. Few cases of intussusception in adults with UC have been described in the literature, with one case of seemingly idiopathic colo-colonic intussusception, and another associated with giant pseudopolyposis [56, 57]. Cases of intussusception are rare in patients with CD and were associated with chronic haematoma, giant pseudopolyposis, fibroid polyps, active inflammation and surgical resection [58–63]. A variety of intra-intestinal abnormalities may therefore precede the occurrence of intussusception in adults with UC.

Though the exact mechanisms of intussusception aren’t well understood, a general pathogenesis has been proposed. Lesions arising from the wall of the bowel may initiate the intussusception by disrupting the normal peristaltic movement of local muscularis propria, or perhaps through distortion of the adjacent fibrous and/or muscular tissue. The lesion forms the leading point for the invagination or prolapse of the involved region of the bowel wall into the intestinal lumen, which is progressively distended and forced aborally through the propulsive motility of the surrounding musculature (Fig. 1.1A). The intussusception

thus forms the characteristic ”telescope-like” structure within the adjacent bowel segment. Constriction of the mesenteric blood vessels supplying the intussuscepted region of the bowel produces an ischaemia and intraluminal bleeding (Fig. 1.1B). Without medical intervention, adult intussusception is likely to progress, potentially resulting in strangulation, subsequent necrosis of the intussusceptum and sepsis.

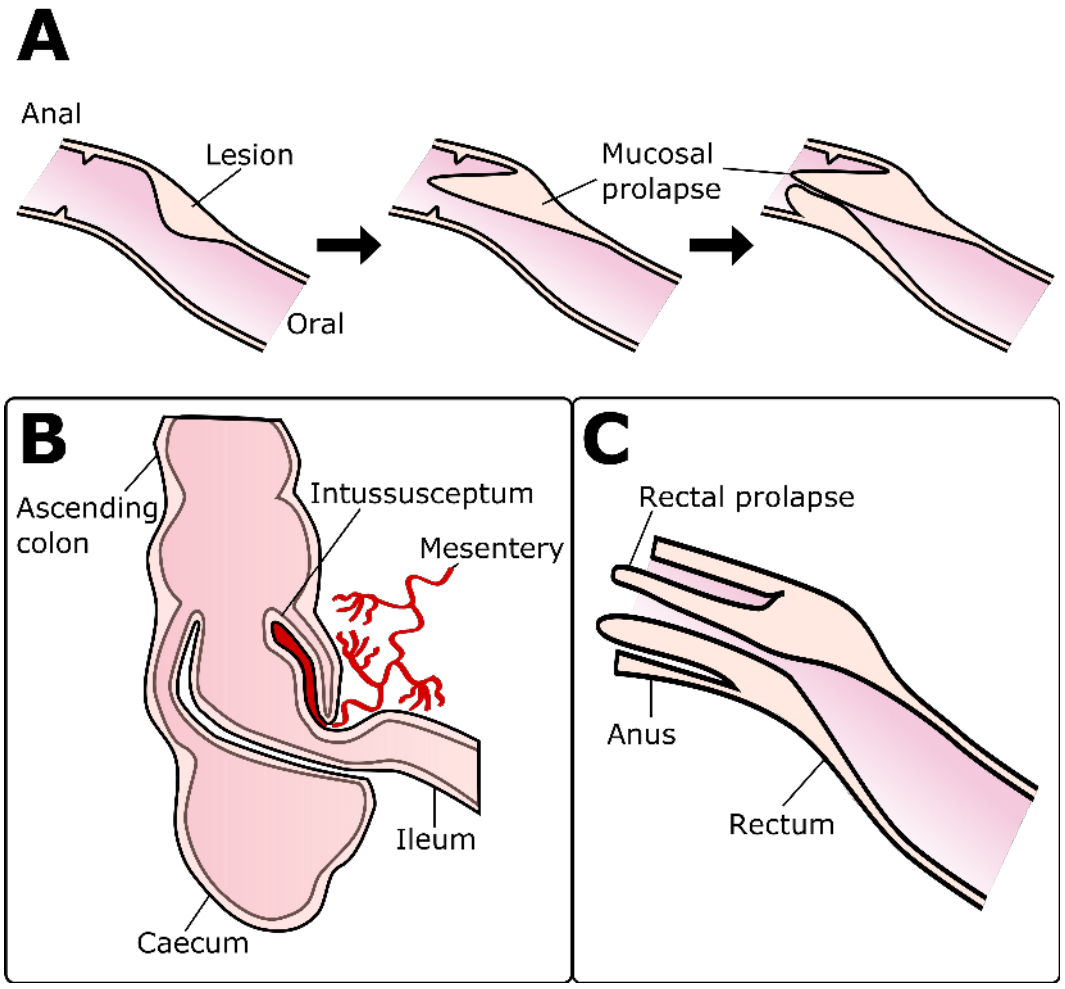

Figure 1.1: **Mucosal prolapse and intussusception of the lower gastro-intestinal tract.** Intussusception describes the ”telescopic” invagination of the intestine within itself, frequently involving the ileum of the small intestine. The invaginated ileum may advance aborally into the caecum and proximal colon, the compressed tissues impeding the normal transit of faecal matter. Mesenteric blood vessels supplying the intussuscepted tissue (intussusceptum) also become compressed by the surrounding intestine, obstructing venous return via mesenteric veins. Obstructed blood flow results in an ischaemia of the intussusceptum and engorged mesenteric blood vessels. Bleeding from the ischaemic intussceptum enters the intestinal lumen producing bloody stools.

Intussusception of the small intestine may be initiated by a range of lesions including inflammatory lesions, non-neoplastic polypoid lesions, diverticula, adhesions and strictures. Cancerous neoplasia, either primary or metastases, may serve as the lead-point for 18-48% of cases of enteric intussusception. In contrast, in 43%–100% of cases of colonic intussusception in adults, malignant neoplasia may be identified as a lead-point [51].

Rectal prolapse may be another complication associated with chronic ulcerative colitis [64]. Where most cases of rectal prolapse occur either in children or in the elderly, the incidence of rectal prolapse in adolescents and adults may be increased by chronic colorectal disease. Mucosal prolapse has been proposed as the likely cause of a set of similar disorders including rectal prolapse, haemorrhoids, solitary rectal ulcer syndrome and colitis cystica profunda [65]. Though the rectum seems particularly susceptible mucosal prolapse, polypoid mucosal prolapse has also been observed in the stomach and colon [66]. Mucosal prolapse may present endoscopically as ulcerative, polypoid, or erythematous lesions The key histological features of mucosal prolapse are a thickening and disruption of the muscularis mucosae. Mucosal crypts are mildly distorted and hyperplastic, occasionally displaying a serrated epithelium [67].

Whilst mechanistic evidence for is scant, it has been hypothesised that mucosal abnormality induced by colonisation of the colorectum by bacteria or helminths triggers rectal prolapse. Inflammatory responses to schistosomal infestation of the rectum are known to induce the formation of a polypoid lesion (bilharzioma) within the rectal mucosa, which co-incide with rectal prolapse [68]. Similarly infection with enterohepatic *Helicobacter* species in susceptible laboratory mouse strains co-incides with a higher incidence of rectal prolapse. Examination of murine rectal prolapse cases at Massachusetts Institute of Technology animal facilities revealed that the majority (52%) of cases arose in mice with colitic disease or known immunodeficiencies such as interleukin-10-deficient or recombination-activating gene-1 (Rag1)-deficient strains [69]. That a variety of colorectal pathogens are associated

with rectal prolapse would suggest that the inflammatory response to these pathogens is the underlying aetiology of rectal prolapse.

Prolapsed rectum often displays a flaccid and fibrotic appearance upon examination, with progressive degeneration of the pelvic and anorectal muscle and/or their innervating neurones suggested as an underlying aetiological factor [70]. Neuromuscular remodelling induced by chronic inflammation of the colon and rectum could explain the association of rectal prolapse with infection through the progressive remodelling of connective tissue and local neurones. Depletion of cholinergic motor neurones has been shown in prolapsed segments of rectum from mice with chronic colitis, suggesting that chronic colitis results in a progressive loss of rectal contractility [71]. However, it remains unclear whether a decline in neuromuscular dysfunction in colitic animals precipitates rectal prolapse or whether it is produced by additional stresses placed on the involved tissue following intussusception.

Notably a strain of lamellipodin-deficient mice displays a high incidence of rectal prolapse in the absence of a florid inflammation [72]. Further investigation of the prolapsed rectum revealed the existence of invasive adenocarcinoma within the involved tissue. The association between rectal carcinoma and prolapse suggests that the cancer-induced alteration to structure to the rectal wall may provide a lead point for intussusception of the rectal mucosa (incomplete prolapse) and eventually a circumferential (complete) prolapse of the rectum.

Thus it would appear that the structural alterations to the mucosal and submucosal connective tissues resulting from cancerous invasion render the affected rectal tissue liable to prolapse.

Most notable among these local complications is the association of UC with colorectal cancer.

1.2.4 Epidemiology of colitis-associated neoplasia

Numerous studies have addressed the issue of increased risk of intestinal carcinogenesis in patients with IBD. An association between an increased risk of developing CRC and colonic

CD is well known [73]. Meta-analysis of reports of CRC incidence among patients with CD has shown a 2.5–4.5-fold increase in risk relative to the general population [74]. Though far rarer than CRC, small bowel cancer may be up to 33 times more likely in patients with CD than in the general population. However, the majority of studies of CRC incidence among patients with IBD have been focussed on UC. Discrepancy exists between the risk of developing CRC in patients with UC between early and more recent studies. The degree of CRC risk reported by studies utilising patients with UC from tertiary care centres [75] is generally greater than that reported by population-based studies [76].

A population-based study of patients with IBD residing in Minnesota observed no difference in the incidence of CRC relative to US population census data [42]. Diagnosis of UC-associated CRC occurred at a relatively early age in the previous study, with a median age at diagnosis of 51 years. Subsequent studies of a Danish cohort identified an earlier onset of neoplasia in the chronically inflamed bowel of patients with UC relative to the non-IBD population. The median age at which patients were diagnosed with CRC of 64 years in patients with UC, compared to 71.6 years in non-IBD patients [76]. Recent population-based analysis performed in Denmark by Jess *et al.* [77] has suggested an overall decline in the risk of CRC development in patients with UC over a 30-year period. In contrast, Herrinton *et al.* [75] had observed a stable incidence rate of CRC development in patients with IBD over a 14.5-year time-frame. Differences in the trend of incidence rates may be partially explained by stratification of age groups. Based on the Danish study, patients diagnosed with UC between the ages of 0–39 years, are at greatly increased risk of developing CRC than the general population [77]. In contrast, patients $>$39 years of age were at no greater risk of developing CRC than non-IBD patients. Based on the associations already made between severity and duration of UC, it seems likely that the greater extent of disease typically exhibited by the paediatric UC subset at diagnosis and therefore longer duration of disease would explain the disparity in CRC incidence between the age groups.

Another explanation for discrepancies between the studies is due to changes in the management of IBD during this time. The declining use of 5-aminosalicylic acid and sulfasalazine coinciding with increased use of immunomodulators such as thiopurines (azathioprine, 6-mercaptopurine or methotrexate) and anti-tumour necrosis factor therapy (infliximab, etanercept), has become increasingly prevalent [75, 78]. In the case of the Danish study, endoscopic surveillance was minimal. Therefore improvements in chemopreventative therapy for IBD are likely to be at least partly responsible for the diminished incidence of CRC among patients with IBD. Cumulative incidence of CRC in patients with pan-colonic UC was estimated to be 2% after 10 years of disease, 8.5% after 20 years, and 17.8% after 30 years [79]. A more recent study presented a lower estimate of cumulative CRC incidence in pan-colonic UC; 2.5% after 20 years, 7.6% after 30 years and 10.8% after 40 years disease duration [80]. When the incidence of dysplasia with CRC, the predicted rates were closer to the estimates reported by Eaden *et al.* [79] 7.7% at 20 years and 15.8% at 30 years. Differences between studies may be explained by selection bias or differences in CRC surveillance and treatments after diagnosis with IBD.

Sixteen studies examining ten year intervals of UC duration included in the meta-analysis showed that 19% of patients developed CRC within the first ten years after diagnosis with UC [79]. Similarly, twenty-one percent of patients with UC-associated CRC involved in a retrospective analysis of Dutch hospital patients developed cancer in less than 8–15 years of disease duration [81]. Using the same clinical database as Lutgens *et al.* but with a larger patient cohort, Baars *et al.* observed CRC occurrence in 45% of patients less than ten years after diagnosis with UC [82]. Unlike Lutgens *et al.* however, Baars *et al.* excluded patients diagnosed simultaneously with CRC and IBD. Exclusion of patients presenting with IBD and CRC concomitantly may be expected to underestimate the incidence of early CRC, however the number of early CRC cases was higher in the latter study. The study by Baars *et al.* described an association between age of diagnosis and the interval between

CRC occurrence in patients with IBD. Patients diagnosed with UC at a later age were expected to develop cancer within 5–10 years. Sporadic CRC incidence is low in patients younger than 50 years old but increases sharply with age. The average age of diagnosis amongst Australians is 69 years old which is close to the median age for diagnosis in most industrialised countries [83, 84]. A similar relationship between incidence of colitis-associated cancer (CACC) and age may reasonably be expected in 50–60 year old patients with UC.

It is unlikely that the overall the risk of CRC occurrence in patients with IBD has been grossly overstated. Eaden *et al.* estimated a cumulative incidence of 2% 10 years post-diagnosis with IBD, a figure that has been confirmed by the results of studies published since [79]. An unanswered question in assessing the epidemiology of CACC involves the source of discrepancies in the reported CRC incidence obtained from studies performed in recent years between earlier studies. Whether the incidence of CRC in patients with UC has declined due to evolving medical and surgical practices, or has been produced by differences in study design and population may never be fully resolved. A largely unexplored aspect of CRC associated with IBD is the mechanisms by which chronic inflammation contributes to carcinogenesis in the colon.

1.3 Pathogenesis of UC

Understanding the origins of UC-associated neoplasia requires an understanding of the pathogenetic basis for UC itself. The aetiology of UC is considered to lie in multiple host and environmental factors. The culmination of these factors is suspected to produce an exaggerated immune response to luminal bacteria, permitted perhaps by a defect in intestinal barrier function.

1.3.1 Genetic factors for susceptibility to UC

Genetic factors pre-disposing individuals to the development of UC have been the subject of intense study in the last decade. Large genome-wide association studies have identified several genetic loci associated with a modified risk of developing UC. Among the strongest associations so far have been made between risk of UC and the genes encoding the human major histocompatibility complex (MHC). Certain gene variants in the MHC-II complex (human leukocyte antigen [*HLA*]) gene region have been associated with more extensive UC and an increased risk of colectomy [85, 86]. Shared HLA variants between extensive UC and primary sclerosing cholangitis (PSC) may also explain the shared associations between these diseases [85, 87]. Since MHC-II is crucial for the presentation of antigenic peptides by antigen-presenting cells, UC may arise as a result of inappropriate immune responses arising from genetic abnormalities in immunoregulatory genes. Less frequent risk variants for UC susceptibility can also be found in genes regulating mucosal inflammatory responses, particularly those characterised by IL-17-expressing T-helper lymphocytes (T_H17) such as the interleukin-23 receptor (*IL23R*) and C-C motif-containing chemokine receptor-6 (CCR6) [88]. Additional UC-associated variants have also been identified in loci enconding immunoregulatory interleukin-10 (*IL10*) and genes involved in the transduction of pro-inflammatory cytokine signalling via the caspase-recruitment domain family member-9 *CARD9* and Janus kinase-2 (JAK2), [88, 89].

Collectively these polymorphisms may represent a defect in pathogen recognition and clearance and aberrant immune responses to the intestinal microbiota. Interactions between defective immune responses and the microbes resident within the colon may thus be causative factors in the pathogenesis of IBD.

1.3.2 Colonic mucus

While the innate and adaptive arms of the immune system are normally capable of preventing and limiting infection, the overwhelming number of micro-organisms makes it highly advantageous to separate them from the host tissues as much as possible. An impermeable barrier would effectively segregate host tissue from microbes but would simultaneously impair the primary absorptive function of the gastro-intestinal tract. Mucus, however, presents a solution to this dilemma. In the colon, the secreted mucus forms two layers, an adherent inner layer approximately 200 μm thick in humans and 50 μm thick in the mouse and an easily removed outer layer [90]. The inner mucous layer is capable of excluding objects down to 50 μm in size thus preventing bacteria contact with the colonic epithelium, but still permitting the diffusion of water and small molecules. Clearly, the structure of the intestinal mucous layers is crucial to the prevention of intestinal disease.

Colonic mucus differs in its composition from the mucus produced in other mucosal tissues such as the lung, and even compared to other regions of the gastro-intestinal tract. The essential components of mucus are the mucin family of proteins. Intestinal mucins in the human are either secreted gel-forming mucins (MUC2, MUC5AC, MUC5B and MUC6) or cell-surface mucins (MUC1, MUC3, MUC4, MUC12, MUC13 and MUC17) [91]. Secretion of the Muc2 gel-forming mucin increases from the oral to the anal end, with mucin secretion in the distal colon limited to Muc2 alone [92,93]. Human *MUC2* encodes a 5,179 amino acid protein synthesised in the endoplasmic reticulum (ER) of the intestinal goblet cell. It is in the ER that MUC2 proteins dimerise via disulphide linkages of the CK domain of each MUC2 molecule [94]. Subsequent to dimerisation MUC2 is translocated to the Golgi apparatus where the protein undergoes heavy glycosylation of intramolecular domains enriched in proline, threonine and serine residues [95]. Further post-translational modification occurs trans-Golgi, where MUC2 dimers form disulphide linkages between the N-terminal D3 domains to form a MUC2 trimer [96]. Interactions between the N-terminal D1-D2-D'D3

domain-containing region of the MUC2 molecules to form hexagonal structures [97]. The ordered packing of the complex MUC2 molecules into the secretory vesicle requires an acidic environment (pH = 5) and abundant Ca^{2+}. Release from the secretory vesicle would therefore expose the folded MUC2 proteins to a neutral pH outside the cell and trigger an unfolding of the MUC2 structure. Experimentally increasing the pH or the addition of sodium bicarbonate has been demonstrated to dissolve the interactions between the MUC2 N-termini, permitting the unfolding of the MUC2 mucin into the extended net-like polymer observed during release from secretory vesicles [97]. Modelling of MUC2 N-terminal interactions has indicated the possibility that the MUC2 polymers may actually maintain the stratified network structure even after release from the secretory vesicle [98]. Being the primary secreted mucin in the distal colon, disruption of Muc2 function could be expected to allow a persistent microbial colonisation of the colonic mucosa. Genetic ablation of Muc2 in mice abolishes the stratified secreted mucous layer, resulting in a spontaneous, chronic colitis [99]. Abrogation of genes regulating synthesis, secretion and folding of the Muc2 mucin have also been demonstrated to permeabilise the inner mucous layer to the luminal microbiota [100]. Segments of actively inflamed mucosa from patients with UC have displayed a similar permeability to bacterial-sized material to that observed in genetically modified animals which spontaneously develop chronic colitis [100]. Interestingly, while the defect in the inner mucous layer was repaired when remission was achieved in patients with UC, a minority of patients with UC in remission displayed a persistent permeabilisation of the mucus barrier to bacterial-sized objects. Although it is unclear to what extent a primary defect in the colonic mucous barrier contributes to the initiation of UC pathogenesis, animals displaying defective mucin biosynthesis and secretion to produce chronic colitis remain an appealing model of UC.

1.3.3 Colonic microbiota

Interactions between the host immune system and the resident microbes within the intestine are believed to represent a key aetiological factor in the pathogenesis of ulcerative colitis. Variants of the genes encoding NOD2, ATG16L1 and MHC display strong associations with susceptibility to IBD [88]. Since NOD2, ATG16L1 and MHC proteins are crucial in the recognition and clearance of bacteria at mucosal surfaces, IBD-associated variants of these genes would likely pre-dispose individuals to aberrant interactions between the host immune system and the luminal microbiota [101]. Less clear is whether IBD-associated gene variants result in an 'intolerance' to non-pathogenic commensal microbes or whether IBD-associated genes instead permit pathogenic expansion of specific subsets of microbial families.

Structural defects in the inner colonic mucous layer would allow greater numbers of bacteria not just to colonise the mucus but also the epithelial surface. Quantification of the total bacterial burden associated with the colonic mucosa in patients with UC has revealed abnormally high levels of bacteria [102]. That the burden of mucosa-associated bacteria in patients with UC was similar between inflamed and non-inflamed colon suggested that the observed bacterial expansion is unlikely to occur secondary to inflammation. An increased bacterial burden associated with the mucosa raises the possibility of an opportunistic expansion of certain bacterial species. Profiling of the microbiota composition in IBD has repeatedly identified reductions in the Firmicutes and Bacteroidetes phyla that predominate in the non-IBD colon [103–105]. High proportions of Actinobacteria, particularly members of *Bacteroides* and *Prevotella* genera, or Proteobacteria, particularly Enterobacteriaceae members (*Shigella spp.* and *Escherichia spp.*) have been identified associated with UC in disease-discordant twins [106]. In addition to adherent and invasive *Escherichia coli* and *Shigella spp.*, *Fusobacterium varium* was frequently identified in the or adjacent to the colonic epithelium in patients with UC [107]. Alterations to the abundance of bacterial species could be considered an expansion of bacterial species better adapted to the metabolic

stresses imposed by ongoing inflammation in the colon. Mesalamine treatment, for example, co-incides with a reduction in the abundance of *Escherichia coli* and *Shigella spp.* [103]. Thus, although colonisation of the defective mucus may precede chronic colitis in UC, chronic inflammation seems to favour a microbiota favouring less diversity and a greater abundance of pathogenic bacteria.

Expansion of potentially pathogenic bacteria associated with the colonic mucosa in patients with UC could perhaps only occur at the expense of normal commensals. Reductions in the abundance of members of the Firmicutes and Bacteroidetes in the normal human colon are associated with active UC [103, 108]. Most notably, the Clostridales members *Faecalibacterium prausnitzii* and *Roseburia spp.* are reduced in UC relative to healthy patients [103, 109, 110]. While *F. prausnitzii* colonisation in the colon of patientws with UC is reduced during active disease, the abundance of this bacterium may increase again following the induction of remission [109]. Both *F. prausnitzii* and *Roseburia spp.* have been identified as colonic commensals with anti-inflammatory properties in experimental colitis, and may therefore protect against UC in uhumans [111, 112]. Part of the anti-inflammatory effects of *F. prausnitzii* can be attributed to the production of short-chain fatty acids (SCFA), particularly acetic, butyric and propionic acids. Production of SCFA may suppress the production of pro-inflammatory cytokines through the inhibition of nuclear factor-$\varkappa$B (NF-$\varkappa$B) and inducible nitric oxide synthase [113, 114]. Reduced faecal concentrations of acetate and propionate have been associated with UC, and though butyrate concentrations may be no different to the healthy colon, its metabolism by the colonic epithelium may be impaired [110, 115]. In the absence of an abundant commensal population in UC, PRR ligands such as lipopolysaccharide (LPS) from the bacteria colonising the colonic mucus may thus provoke exaggerated inflammatory reactions. Congruent with the structural abnormalities observed in the colonic mucous layer in patients with UC, an increased abundance of mucolytic and sulphate-reducing bacteria including *Ruminococcus gnavus*,

Ruminococcus torques and *Desulfovibrio desulfuricans*, *Bacteroides fragilis* and *Bacteroides vulgatus* [116]. An increase in mucolytic bacteria may provide other commensals and pathogenic bacteria with a source of nutrition. *Clostridium difficile*, *Salmonella typhimurium* and *Escherichia coli* for example, are capable of utilising mucin metabolites produced by mucolytic commensals. While a number of mucolytic bacteria increase in abundance in UC the common mucolytic commensal *Akkermansia muciniphila* has been reportedly decreases in UC [117]. Since *A. muciniphila* colonisation appears to be dependent on Muc2 either an intrinsic defect in synthesis of colonic mucus, or an expansion of a combination of mucolytic microbes may deprive *A. muciniphila* of suitable binding locations.

1.3.4 Aberrant immune responses in UC

Interaction between the luminal microbiota and the host immune system centres on the colonic epithelium. The underlying colonic mucosa is home to a range of immune cells which maintain an essential balance between pro-inflammatory responses to potential pathogens and maintaining tolerance to beneficial commensals. The identification of the aforementioned risk-variants such as *IL23R* and *NOD2* associated with immune function suggest that the recognition of, and responses to, microbial molecular patterns by the colonic epithelium and the underlying mucosal immune cells may contribute to the chronic inflammation associated with IBD. Concordant with the idea that microbial products trigger inflammation in IBD is the observation massive infiltration of neutrophils, macrophages and $CD4^+$ T-lymphocytes to the inflamed colonic mucosa in UC. Lamina propria mononuclear cells isolated from mucosal biopsies obtained from patients with UC and CD have shown increased reactivity to commensal bacteria normally tolerated in the intestine [118, 119]. Furthermore, leukocytes isolated from the inflamed mucosa of patients with CD have also been shown to produce higher levels of interleukin-6 (IL-6), interleukin-12 (IL-12), IL-23 and tumour-necrosis factor-α (TNF-α) in response to exposure to certain commensal bacterial species [120]. Hyper-reactivity of the innate immune system may favour the polarisation of T-lymphocytes

toward pro-inflammatory phenotypes and suppress the development of immunomodulatory regulatory T-lymphocytes, numbers of which are decreased in UC [121].

Consistent with the identification of the IL-23R as a risk factor associated with susceptibility to UC and CD, neutralisation of IL-23 has proven to ameliorate chronic colitis in both UC and mouse models of IBD [88, 122]. Since IL-23 is critical for the initiation, generation of mucosal immune responses characterised by production of pro-inflammatory T_H17 cytokines such as interleukin-17A (IL-17A), it would follow that IL-17-type cytokines would be among the key effectors of the tissue damage associated with chronic UC. Indeed, the mucosa of patients with UC exhibits increased production of IL-17 family members with concomitant expansion of IL-17A-producing $CD4^+$ T-lymphocytes and APCs [123, 124]. The overall effect of an IL-21/IL-23/IL-17-type inflammatory response would be expected to feature an augmentation of neutrophil recruitment and elevated production of degradative proteinases through production of granulocyte-colony stimulating factor (G-CSF) and IL-6.

IL-6 as an essential mediator that governs the early or acute phase of the immune response against pathogenic insults, may be produced by a wide range of cell types, including intestinal epithelial cells. The cytokine IL-6 is abundant in the colonic mucosa during the active phase of IBD-associated inflammation and is itself capable of polarising immune responses toward a T_H17 profile via the [125].

Notably chronic production of IL-17 and the IL-17-promoting cytokines IL-21, IL-23, have been shown to promote the growth of experimental colonic tumours in mice [126, 127]. Exactly how interleukin-17-type T-helper lymphocyte (T_H17) promote tumourigenesis in the colon is somewhat unclear. Several mediators of IL-17 responses, including IL-6, cyclooxygenase-2 (COX-2) and inducible nitric oxide synthase (iNOS) have also been implicated in colonic tumourigenesis [128–130]. Altogether, maintenance of the colonic mucous barrier would seem to be essential for preventing chronic inflammation and by extension, colonic cancer in the long-term.

1.4 Initiation of carcinogenesis in the chronically inflamed colon

Though connection between chronic inflammation and cancer is undisputed, the specific mechanisms linking the ongoing immune-microbial interactions and oxidative stress to the process of carcinogenesis is not yet fully understood. Carcinogenesis is a process generally considered to require 'initiation' through acquired or inherited genetic or epigenetic alterations [131]. The alteration of genes during the initiation stage leads into the promotion of tumourigenesis through the clonal expansion of the transformed cells by increased proliferation and reduced cell death. The final stage of carcinogenesis is the progression from a benign or precancerous lesion to invasive carcinoma. Progression is typified by an increase in the size of the tumour, invasion into deeper tissue layers and metastasis to other distant tissues.

Table 1.2: **The Vienna classification for gastrointestinal epithelial neoplasia**

Category 1	Negative for dysplasia/neoplasia
Category 2	Indefinite for dysplasia/neoplasia
Category 3	Non-invasive low-grade neoplasia (low-grade dysplasia/adenoma)
Category 4	Non-invasive high-grade neoplasia
	4.1 High-grade dysplasia/adenoma
	4.2 Non-invasive carcinoma (carcinoma in situ)
	4.3 Suspicion of invasive carcinoma
Category 5	Invasive neoplasia
	5.1 Intramucosal carcinoma
	5.2 Submucosal carcinoma or beyond

The overwhelming majority ($> 95\%$) of colonic neoplasia arises from transformed colonic epithelial cells [132]. In the sequence proposed by Fearon and Vogelstein, colonic adenocarcinoma arises from a benign, dysplastic precursor lesion (Fig. 1.2) [133]. Dysplasia

is by nature a broad term as it includes a range of architectural and cytological changes indicative of pre-cancerous change. The most commonly encountered dysplasia in the colon is the polypoid epithelial outgrowth often referred to as an 'adenoma' [132]. Dysplastic lesions display increasing complex architectural abnormalities as the constituent cells acquire additional oncogenic mutations. Grading the degree of architectural and cytological change therefore reflects the risk of progression to malignancy [134]. While the progression from non-dysplastic mucosa to dysplasia and onward to carcinoma, is preserved in UC, the morphology of colitis-associated dysplasia is more varied. While 80% of dysplastic lesions in patients with UC present as raised polypoid lesions, an additional 20% of display a "flat" non-polypoid morphology [135]. Raised, non-invasive polyps are readily detected during standard endoscopy, and removed via endoscopic mucosal resection with minimal risk of recurrence. Due to the lack of a raised lesion projecting into the lumen, flat dysplasia is difficult to detect reliably in the inflamed colon without the use of chromoendoscopy [136]. Additionally, patients with IBD are also more likely to present with multifocal dysplasia, a factor that when coupled with flat morphology suggests an exceptionally aggressive course of disease [136]. Given the propensity of flat dysplasia for rapid progression to carcinoma, a deeper understanding of the mechanisms that initiate or promote the early stages of colonic carcinogenesis would be advantageous for future management of IBD.

1.4.1 Oxidative stress

Chronic inflammation is associated with the production of a large volume of harmful reactive oxygen species (ROS) and reactive nitrogen species (RNS). Both of the terms ROS and RNS encompass a range of free radicals and their intermediates. The ROS include the radicals superoxide anion ($O_2^{\bullet -}$), hydroxyl ($^{\bullet}OH$), peroxyl ($RO_2^{\bullet}$) and alkoxyl ($RO^{\bullet}$) and oxygen-derived intermediates singlet oxygen (O_2), ozone (O_3), hydrogen peroxide (H_2O_2) and hypochlorous acid (HOCl) [138]. The RNS are predominantly derived nitric oxide (NO) and its nitrosyl radical (•NO and ions — nitroxyl (NO^-) and nitrosonium (NOS^+). From

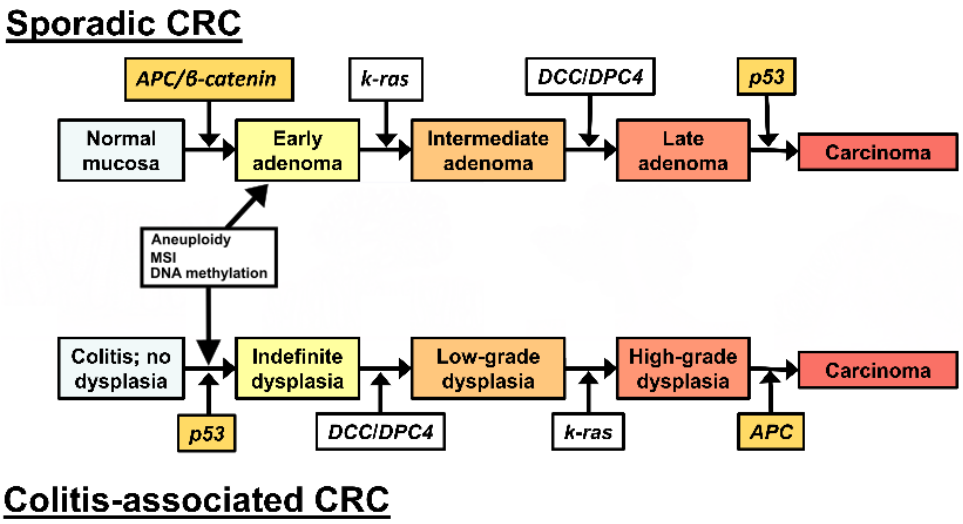

Figure 1.2: **Sequence of key genetic mutations in the pathogenesis of sporadic and colitis-associated neoplasia.** Sporadically occurring (top) and chronic colitis-associated (bottom) pathways share a similar progression through dysplastic precursors (predominantly adenoma in sporadic cases) to invasive carcinoma. Both pathways display differences in the timing and frequency of the key oncogenic gene mutations. In the sporadic pathway inactivating mutations in adenomatous polyposis coli (*APC*) alleles are associated with early adenomatous dysplasia. Mutations in the Kirsten rat sarcoma viral oncogene (*KRAS*), are associated with more intermediate stages of dysplasia, while deleted in colorectal carcinoma (*DCC*) and homozygously deleted in pancreatic cancer, locus 4 (*DPC4*) are more freqent in advanced adenoma. Transformation-related protein 53 (*TP53*, p53) mutations are also associated with progression to carcinoma. In contrast, mutations in the transformation-related protein 53 (*TP53*) frequent in the non-dysplastic, chronically inflamed epithelium in UC. DCC/DPC4 mutations also occur earlier, associated with early stages of dysplasia, whereas KRAS and APC mutations are rare comparative to the sporadic pathway and occur in advanced dysplasia/carcinoma. Chromosomal instability and aneuploidy or microsatellite instability (MSI) may occur at any time, potentially accelerating the acquisition of further genetic mutation. Methylation of gene promoter regions have been observed in sporadic dysplasia but are also active in the chronically inflamed colonic epithelium, suggesting that these may initiate colitis-associated colorectal carcinogenesis. Adapted from Ullman and Itzkowitz (2011) [137]

these nitrogen radicals intermediates including nitrite (NO_2^-), peroxynitrite ($OONO^-$) and nitrogen oxides ($\bullet NO_2$, N_2O_3, N_2O_4) may be generated through interactions between NO

and oxygen or its derivatives. Formation of ROS and RNS are primarily dependent on the activity of reduced nicotinamide diphosphate (NADPH) oxidases (collectively called NOX enzymes) and nitric oxide synthase (NOS) enzymes respectively. A number of NOX family members have been identified in wide range of human tissues and cell types [138]. Most widely distributed of the NOX family is NOX2, due to it being predominantly expressed by phagocytes, regardless of tissue compartment. While most NOX enzymes are found in phagocytes or neurones and endothelium, NOX1 is notable for its abundance in the colonic epithelium [139, 140]. The NOS enzymes can be divided into four isoforms based on their distribution — neuronal NOS (nNOS, NOS-1), iNOS (NOS-2), endothelial NOS (eNOS, NOS-3) and mitochondrial NOS [141]. The nNOS and eNOS isoforms are thought to be constitutively active and are restricted to certain cell types. Large increases in RNS production must therefore arise due to increased activity of the inducible isoform iNOS, which may be induced in most cell types provided with sufficient stimulus. While production of ROS and RNS may provide important cues for diverse processes such as cell proliferation, apoptosis and iron metabolism, these reactive species are crucial to inflammatory processes.

The ability to generate ROS and RNS is of considerable advantage to mucosal defence. Animals deficient in either ROS or RNS are susceptible to *Salmonella* infection under experimental conditions [142–144]. Inhibition of ROS/RNS production attenuates the mucosal damage induced by chemical agents in animal models of chronic colitis, suggesting that ROS/RNS generation is also crucial for perpetuating leukocyte recruitment and the resultant inflammation [145, 146]. Therefore ROS and RNS may either directly or indirectly limit the ability of bacterial pathogens to invade the intestinal mucosa. Both NADPH oxidase and iNOS are expressed intracellularly by phagocytes, though neutrophils show higher levels of ROS production than that observed in activated macrophages [141]. In contrast, macrophages display greater production of RNS than neutrophils. Production of superoxide and its derivatives from phagocytes may generally be elicited immediately the through

assembly of existent NOX subunits to form an active enzyme complex [147]. In contrast, RNS production via iNOS requires *de novo* synthesis of the enzyme. Increased transcription of iNOS may be induced by common pro-inflammatory triggers including bacterial LPS, interferon-γ (IFN-γ), TNF-α, interleukin-1β (IL-1β), presumably through the activation of mitogen-activated protein kinase (MAPK), JAK-STAT-IRF and NF-$\varkappa$B pathways [148, 149]. Within phagocytes the generated NO·, superoxide and hydrogen peroxide may readily diffuse through bacterial and fungal cell walls, where they inhibit normal microbial metabolism and cellular replication by damaging essential proteins and DNA [150–152]. Generation of both ROS and RNS by leukocytes and their release into the extracellular environment therefore forms an inflammatory process important for limiting microbial invasion into host tissues.

Besides their direct antimicrobial effects of ROS and RNS, these reactive species may also serve as key signalling events in the regulation of colonic mucosa. High levels of NOX1 expression in the colonic epithelium, particularly in the distal colon, co-incides with the high bacterial load in the lumen and mucous layer. Naturally, epithelial NOX1 is not constitutively active, and requires the ligation of PRRs like TLR5 to trigger its activation [153]. The function of ROS produced by the colonic epithelium may fulfill a second line of defence for microbes which manage to penetrate the inner colonic mucous layer. Production of ROS by NOX1 and dual oxidase (Duox; another NOX family member) may serve as a signal promoting the synthesis of serotonin from enterochromaffin cells thereby altering intestinal secretion and motility, perhaps promoting bacterial clearance [154]. Additionally, NOX/Duox-derived ROS in the colonic epithelium has been shown to precede activation of the NLRP6 inflammasome and Muc2 exocytosis, thereby maintaining the thickness of the mucous layer [155].

Conceivably, chronic exposure to microbial antigen could permit an accumulation of ROS and RNS from both phagocytes and the colonic epithelium, perhaps contributing to the pathogenesis of UC. Where ROS/RNS production overwhelms the ability of cells to limit

their damaging effects, a scenario referred to as ”oxidative stress” arises [156]. Consistent with chronic immune activation, the colonic mucosa of patients with active UC displays an increased synthesis of iNOS, higher even than that detected in CD and concomitant increases in peroxynitrite formation [157, 158]. Defective regulation of ROS or RNS may over time result in the accumulation of excessive amounts of intracellular damage, perhaps permitting genetic mutation and neoplastic transformation.

Given the broad range of metabolic processes that are disrupted by ROS/RNS produced in chronic colitis, it may be unsurprising that these radicals have also been associated with colitis-associated carcinogenesis. The inflammatory micro-environment features an abundance of NO and ROS, facilitating the formation of NO-derived oxides, particularly N_2O_3. Nitrogen oxides are capable of modifying a broad range of biological molecules. Cysteine and haem are both subject to nitrosylation or nitrosation. The sulphur groups common to cysteine and methionine are also vulnerable to oxidation. Both the peptidyl-ring carbons in tyrosine and tryptophan, and the carbon of fatty acids are targets for nitration. Nucleic acids may also be modified by oxidation or deamination by NO and intermediates

Hydroxyl and peroxynitrite radicals produced during inflammation attack deoxyguanosine within both chromosomal and mitochondrial DNA, forming 8-hydroxyldeoxyguanine (8-OHdG). Abnormal accumulation of nuclear 8-OHdG is detectable in the colonic epithelium is detectable in the chronically inflamed colon of patients with UC [159]. Failure to remove 8-OHdG prior to synthesis of the complementary DNA strand, potentially results in guanine (G) to thymine (T) G$\rightarrow$T transversion mutations in the position of the modified base [160]. Superoxide and NO-derived N_2O_3 causes deamination of nucleotides to uracil, xanthine and hypoxanthine [161, 162]. Peroxynitrite is also capable of introducing transversion mutations in vitro through nitration of guanine [163]. Furthermore, peroxynitrite is also capable of causing single-stranded DNA breakages [164]. Accumulation of ROS/RNS in the colonic

mucosa during active UC could therefore be expected to introduce the aforementioned DNA modifications, and eventually DNA mutation.

While DNA modifications induced by ROS/RNS may introduce mutations into the genome, these may be repaired through DNA repair mechanisms. Base-excision repair is perhaps the most important pathway for the repair of ROS/RNS-induced DNA damage [165]. Conceivably, inactivation of BER mechanisms would permit the accumulation of DNA mutation due to ROS/RNS present in chronic inflammation. The first step of BER requires the removal of inappropriate bases by lesion-specific DNA glycosylases [165]. The primary DNA glycosylase involved in the excision of 8-OHdG bases is the MutY human homologue (MutYH), mutations of which have been associated with inherited colon neoplasms [166]. Immunohistochemical analysis of MutYH and 8-OHdG in the colonic mucosa of patients with UC has indicated levels of MutYH are reduced as oxidative DNA damage increases during chronic inflammation [159]. The absence of MutYH mutations in the colonic mucosa of patients studied by Gushima *et al.* suggested an alternate mechanism for the inactivation of DNA repair. In addition to their effects on nucleic acids, ROS/RNS have a range of deleterious effects on proteins. Peroxynitrites are capable of oxidising sulfhydryl and thiol groups, inactivating catalytic domains of various enzymes. Importantly, ROS/RNS have been demonstrated to inhibit the removal of oxidative DNA lesions by BER mechanisms. The 8-oxoguanine-excising DNA glycosylase OGG1 and the O^6-methylguanine DNA methyltransferase which excises alkylated bases from chromosomal DNA, are both known to be inhibited by NO-derived species [167, 168]. Experimental evidence from genetic ablation of the murine Ogg1 DNA glycosylase supports the notion of a prolonged colitis-induced oxidative stress as an initiating factor in carcinogenesis. Long-term administration of a colitogen in Ogg1-deficient mice produced colonic tumours in over half of the exposed animals compared to 24% of wild-type animals [169].

1.4.2 TP53 mutation

Transformation-related protein-53 (often simply referred to as p53), encoded by human *TP53* and *Trp53* in mice, is a central regulator of cellular metabolism and an important tumour suppressor [170]. Loss of heterozygosity and p53-inactivating mutations are common in cancers arising from a variety of tissues, indicating that repression of p53 confers some survival advantage to the growth of neoplastic cells. Allelic deletion in the gene encoding p53 has been reported in approximately 50-85% of colitis-associated neoplasia [171, 172]. Mutations in *TP53* appear in the chronically inflamed mucosa of patients with UC preceding the appearance of dysplasia [173]. UC-associated dysplasia and UC-associated carcinoma displayed frequent mutations and loss of heterozygosity (76% and 83% respectively) [174]. Wild-type p53 may protect against DNA damage induced by ROS/RNS production by repressing iNOS transcription, thus preventing the accumulation of oncogenic mutations in the mucosa of patients with UC [175]. However, an over-abundance of the ROS/RNS in colitis may over time, inactivate p53 through direct DNA damage in the *TP53* locus. In support of this hypothesis, certain *TP53* mutations found in the colonic tumours in IBD patients are infrequent in sporadic neoplasms. Notably, G→T tranversions similar to those commonly induced by ROS have been reported in key tumour suppressor genes associated with colonic carcinoma, including *TP53* [173]. Higher frequencies of G→T and cytosine (C) to adenine (A) C→A mutations in *TP53* have also been observed in the inflamed UC mucosa when compared to paired uninflamed mucosa or to uninflamed non-IBD mucosa [173]. Mutation of *TP53* would therefore be expected to much more frequent in UC-associated carcinoma than the rate of *TP53* mutation in sporadic cancers. However, recent whole-exome profiling suggests that the rates of *TP53* mutation may be equivalent between the two pathologies. Studying invasive carcinoma alone indicated that approximately 60% of IBD-associated carcinoma possessed genetic mutation of the gene encoding p53, a rate similar to that observed in sporadic CRC [176].

1.4.3 Chromosomal instability

Genomic instability is thought to be a process involved early in the progression from chronic colitis to colonic neoplasia. Abnormally high rates of chromosomal mis-segregation arising due to defective chromosomal alignment during mitosis, are commonly found in tumour cells and may introduce point mutations such as nucleotide insertion, substitution and deletion mutations [177]. Translocation, inversion and loss of chromosomal segments may cause inactivation of tumour suppressor genes, permitting dysregulated cell growth. Conversely, over-expression of genes favouring cell survival may occur due to amplifications of chromosomal segments. Chromosomal alterations have been reported in the non-dysplastic mucosa of 36% of colectomy specimens obtained from patients with UC [178]. Furthermore, non-dysplastic tissue from two of the five patients displaying chromosomal instability and 43% of dysplastic tissue, also exhibited a loss of either the long arm of chromosome 18 (18q) or the entire chromosome 18. Loss of chromosome 18 or the 18q locus would abolish transcription of the genes encoding DCC, SMAD2 and SMAD4 (DPC4), all of which suppress tumour development [179]. Loss of chromosomal segments would therefore be thought to result in a loss of heterozygosity in the 18q tumour suppressor genes. Despite the reported frequency of abnormalities in this region, mutations in DCC and SMAD4 appear to be relatively rare in early in IBD-associated tumourigenesis [180–182]. Chromosomal instability may be a cause of DNA aneuploidy, i.e. an imbalance in chromosome number. Aneuploidy is observed in 60–70% of sporadic CRC cells, with most aneuploidy involving chromosomes 20q and 18q [183]. Cytometric assessment in UC-associated neoplasia has associated frequent aneuploidy with dysplasia and carcinoma [184, 185] increases in aneuploidy. DNA aneuploidy appears to be strongly associated with neoplasia, with little aneuploidy detectable in non-dysplastic mucosa, but $>$80% of UC-associated dysplasia and carcinomata also displayed aneuploidy [184]. Abnormal shortening of telomeres reportedly co-incides with chromosomal instability and DNA aneuploidy in the colonic epithelium in

patients with UC [186, 187]. Accelerated shortening of telomeres in UC may permit losses of chromosomal segments and thus initiate neoplasia in long-standing chronic colitis [188]. However, chromosomal instability can only arise if DNA damage checkpoints or repair mechanisms are inhibited. Excessively short telomeres will induce replicative senescence through activation of wild-type p53 [189]. Mutation within *TP53* however, may therefore permit colonic epithelial cells in UC to proliferate despite excessive telomere shortening, resulting the accumulation of chromosomal abnormalities and further genetic mutations, thereby initiating neoplasia

1.4.4 Microsatellite instability

Microsatellite instability (MSI) describes small deletions or expansions of short (mononucleotide to tetranucleotide) tandem repeats in the DNA. Microsatellites are prone to replication errors and have the potential to introduce frame-shift mutations if they are not repaired prior to replication [190]. Repair of the incorrectly paired bases is performed primarily by DNA mismatch repair (MMR) enzymes and thus high levels of MSI are considered diagnostic of defective MMR mechanisms. Silencing of gene transcription or inactivating mutations within the MMR genes *MLH1* and *MSH2* produce the high-level MSI (MSI-H) phenotype associated with the hereditary non-polyposis CRC syndrome [191]. Neoplasms arising in the distal colon of patients with UC seldom display high levels of MSI (MSI-H). Analysis of MSI in colectomy specimens from 14 UC patients identified MSI-H dysplasia and carcinoma from two patients [178]. A MSI-H phenotype has been reported at frequencies between 0.7–17% in UC-associated neoplasia [192–195]. More recent analysis of MSI in the laser-dissected colonic epithelium obtained from patients with UC revealed that the majority of samples displayed low-level MSI (MSI-L) [196]. However, expression of *MLH1*, *MSH2* and *MSH6* was not impaired in the MSI-L colonic epithelium in the UC mucosa, suggesting that if MMR activity is impaired, then this may occur through post-translational modification of repair enzymes by ROS/RNS.

1.4.5 Gene promoter methylation

In addition to genetic alterations described in this review, changes at the ”epigenetic” level may also influence the transition from chronic colitis to neoplasia in IBD. Epigenetics, here is used to refer to both inerited and non-inherited modifications to the DNA molecule including DNA methylation, non-coding RNA and histone modification. Promoter regions of many genes display enrichment of C-phosphodiester-G (CpG) DNA sequences. CpG islands can be defined as 500–2000 bp long fragments of DNA within which CpG make up more than 50% of the base pairings with an observed:expected CpG ratio of greater than 60% [191]. Methylation of the cytosine residues may therefore negatively affect the binding of transcriptional enhancers and polymerases to suppress transcription of genes downstream of the promoter region. Hypermethylation of tumour suppressor gene promoter regions may therefore act as a substitute for genetic mutation in the same gene, thus promoting carcinogenesis. Study of the rectal mucosa of patients with predominantly pan-colitic UC has previously revealed a 10-fold higher amount of unmethylated CpGs than that observed in the non-IBD rectal mucosa [197]. Although DNA hypomethylation increased as inflammation increased in severity, the amount of hypomethylation remained almost 8-fold higher in inactive disease relative to non-IBD controls. Global hypomethylation is similarly reported in sporadic CRC suggesting that this feature may may be involved in the progression of colitis to neoplasia [198]. Cytosine methylation is maintained by the DNA cytosine-5-methyltransferase-1 (DNMT1), whose expression positively correlates with the progression to dysplasia and carcinoma in UC [199,200]. Despite an reduction in methylation overall, hypermethylation of specific promoter regions may predispose individuals with long-standing UC to colonic cancer. A positive relationship between p16 and p14 promoter hypermethylation and the progression of UC-associated neoplasia [201, 202]. Additionally, the promoter of the gene encoding E-cadherin (*CDH1*) displayed methylation in 93% of dysplasia specimens obtained from long-standing UC as opposed to just 6% of non-

dysplastic mucosa and 0% of non-IBD controls [203]. Comparison of promoter methylation between UC-associated neoplasia and sporadic cancers has indicated lower methylation of the O^6-methylguanine-DNA-methyltransferase (*MGMT*), *MLH1*, both *CDKN2A* p16 and p14, oestrogen receptor-α and *SFRP1* promoters in UC-associated carcinoma relative to sporadic CRC [204, 205]. UC-associated neoplasms seem unlikely to possess the 'CpG island-methylator phenotype' characterised by frequent methylation of MMR genes such as *MLH1* and the tumour suppressor *CDKN2A* [206]. DNA methylation in UC is therefore a potential mechanism by which neoplasia is initiated and/or promoted in the absence of key oncogenic genetic mutations.

1.4.6 Wnt signalling pathway

The structure of the colonic crypt is organised such that the rates of cell division and cell death are tightly regulated. Proliferation of colonic epithelial cells is determined by a number of signalling pathways involving interactions with the surrounding epithelium and basement membrane. The Wingless/int-1 (Wnt) pathway is a critical signalling pathway that directs proliferation and differentiation of the colonic crypt cells within the crypt structure. Since dysplasia are identifiable due to their abnormal crypt morphology, where perhaps an uncontrolled proliferation produces outgrowth of the crypt structure, subversion of the Wnt pathway may precede carcinoma. The adenomatous polyposis coli gene (*APC*) earns its name from the familial adenomatous polyposis disorder (FAP) a disorder in which patients inherit a germ-line *APC* inactivation mutation, and as a result, are predisposed to the development of large numbers of benign colonic adenomata. Although the majority of dysplastic lesions arising from the un-inflamed colon display *APC* mutations, colitis-associated dysplasia and even the resultant carcinomata display comparatively fewer *APC* mutations [207]. The relatively high frequency of *APC* mutation in sporadic dysplasia may be explained by the essential negative regulation on cell-cell contact-dependent cell proliferation that *APC* provides. The cell-surface protein E-cadherin is an essential mediator

of epithelial cell polarity and proliferation [208]. Homotypic interactions between E-cadherin molecules on adjacent epithelial cells determine the activity of several proteins associated with the cytoplasmic terminal of E-cadherin. One such protein is β-catenin, which in the absence of E-cadherin binding the E-cadherin of neighbouring cells, is released into the cytoplasm and relocates to the cell nucleus, where it acts as a transcription factor. The *APC* gene product, together with axin and GSK-3β, forms a protein complex capable of phosphorylating the N-terminal serine/threonine residues of β-catenin [209]. Rapid phosphorylation, ubiquitinylation and subsequent proteasomal degradation limits the amount of active β-catenin that may be transported to the nucleus. Nuclear β-catenin activates TCF/LEF transcription factors and enhanced transcription of cyclin-D1 (*CCND1*) and myelocytomatosis oncogene c-Myc (*MYC*) which in turn increases cellular proliferation [210, 211]. Mutation of *APC* would thus assist in the acquisition of the ability for epithelial cells to proliferate irrespective to adjacent cell contact, and could conceivably account for the exophytic pattern of growth in sporadic colonic dysplasia. Alteration to the Wnt-β-catenin pathway is thought to occur early in adenoma formation and is thus believed to be an important initiating step in colonic carcinogenesis, allowing accelerated accumulation of further mutations. Despite the lack of *APC* mutations in IBD-associated neoplasia, mutations elsewhere in the Wnt pathway are not absent entirely. Indeed, mutations in genes elsewhere in the Wnt/β-catenin signalling pathway such as *SOX9*, *FZD8*, *AXIN1* and *TCF7L2*, may account for the lack of APC mutations IBD-associated cancers [176]. Alternatively, transient cytokine signalling via (NF-κB or STAT3) may increase β-catenin may instead circumvent the need for APC or Wnt/β-catenin mutations [212, 213].

Similarly to sporadic CRC, IBD-associated colorectal cancers are mostly adenocarcinomata [132]. Mucinous carcinomas compose a large proportion of the carcinoma phenotypes arising from IBD, up to 50% estimated by some studies. Signet-ring cell carcinomas are

more numerous, perhaps ten-fold more common in patients with IBD compared to the general population.

1.4.7 SMAD4

Mutation or deletion of SMAD4 (DPC4) has been associated with sporadic colorectal carcinoma [214] The role of the SMAD4 mutation in the progression of sporadic colorectal carcinoma appears to be significant in advanced neoplasms. Immunohistochemical analysis of SMAD4 expression indicated that decreased or complete loss of SMAD4 expression was frequent in sporadic CRC but rare in normal mucosa [215]. Stratification of colorectal neoplasms into adenoma and invasive carcinoma (stage I-IV) has revealed the timing of SMAD4 loss of heterozygosity or deletion in the sporadic carcinogenesis. Analysis of 115 sporadic colorectal neoplasms indicated that SMAD4 mutation was absent in sporadically-occurring colorectal adenomata and early stage invasive carcinoma [216, 217]. SMAD4 mutations became more common as cancer progressed to metastasis, with 31% of tumours with distant metastases exhibiting SMAD4 mutations [216]. These findings suggest that loss of SMAD4 expression may promote metastasis in colorectal adenocarcinomata. SMAD4 is a transcription factor involved in the transduction of TGF-β signalling via the TGF-β receptor. Loss of SMAD4 expression in colorectal neoplasms has been correlated with a loss of E-cadherin expression, potentially facilitating detachment from neighbouring epithelial cells and metastasis to other sites [218, 219]. Of particular interest is the occurrence of SMAD4 mutations in colorectal neoplasms exhibiting MSI. Primary colorectal carcinomas and CRC cell lines displaying MSI rarely show evidence of abnormal SMAD4 expression [215, 220]. Lei *et al.* did not observe SMAD4 mutation in a series of ten colitis-associated carcinomas [181]. Similarly Hoque *et al.* did not observe SMAD4 mutation in a series of five carcinomas resected from patients with UC- or CD-associated carcinomas [221]. In contrast to the results from carcinomas one specimen of HGD was also analysed which was positive for SMAD4 mutation. Hoque *et al.* included neoplasms from various locations

in the colon and rectum. Therefore SMAD4 mutations are unlikely to active in the early tumourigenesis in the IBD-associated neoplasia.

1.5 Animal models of UC

Replication of carcinogenesis in patients with UC would ideally involve the spontaneous onset of a relapsing and remitting chronic colitis and an increased rate of colonic neoplasia. Chemicals such as dextran sodium sulphate (DSS), and the hapten, 2,4,6-trinitrobenzene sulphonic acid (TNBS), are commonly used to induce acute and chronic colitis. Colitis induced by either DSS or TNBS differs in their induced immunopathology and histopathology. DSS is considered to produce an inflammation more reminiscent of human UC, where tissue damage is mostly restricted to the colonic mucosa, whereas TNBS will often induce transmural damage.

1.5.1 Dextran sulphate sodium

Colitis induced by dextran sodium sulphate (DSS) is perhaps, at present, the most widely used experimental model of chemically-induced colitis. Similar to heparin, DSS is composed of heavily sulphated polysaccharide polymers of varying lengths, and may be separated into high and low molecular weight fractions. Analysis of the colitogenic properties of three different molecular weights of DSS; 5 kDa, 40 kDa and 500 kDa showed that the resultant inflammation differed according to their weights [222]. Polymers were of 40 kDa mass produced the more severe inflammation of the distal colon while distal colonic inflammation was mild or absent in the other fractions studied. DSS is conveniently administered through the drinking water, typical for a period of 5–7 days to simulate acute inflammation, or administered in a cyclic fashion to instead simulate chronic colitis [223]. Chronic colitis is typically induced through administration of a cyclic regimen of 5–7 days oral DSS challenge, followed by a longer 5–14 day recovery period. Similar to UC, DSS-induced

colitis is most severe in the distal colon, which displays extensive crypt and epithelial cell damage accompanied by infiltration of numerous neutrophils among other leukocytes into the intestinal mucosa, tissue oedema and severe ulceration [224]. Concordant with DSS-induced injury in the colon mice undergoing prolonged DSS challenge will exhibit weight loss, loose stools and diarrhoea, and rectal bleeding. Cessation of DSS administration will however, permit a gradual repair of mucosal damage and result in a remission of symptoms. Whether complete recovery from repeated bouts of DSS-induced colitis is achieved in every case is questionable. Since duration and severity of chronic colitis in human patients with UC is associated with an increased risk of colonic neoplasia, it would stand to reason that mouse models of colitis would be similarly predisposed. Epithelial dysplasia in the inflamed colon of mice exposed to repeated bouts of DSS administration over an extended period induce [225, 226].

It has been suggested that DSS has a direct cytotoxic effect on intestinal epithelial cells, effectively abrogating intestinal barrier function and thereby facilitating exposure to commensal microbes [227, 228]. Although some evidence for a direct toxic effect exists [229], DSS-induced inflammation is likely initiated by penetration of the normally sterile colonic inner mucous layer in mice has been demonstrated to precede colonic inflammation [100]. Through as yet unknown mechanisms, DSS is capable of rapidly altering the structure of the inner colonic mucous layer, thereby allowing the passage of beads of 0.5 μm and 2 μm in diameter through the inner mucous layer and into intimate contact with the colonic epithelium [230]. That DSS-induced inflammation is concentrated in the distal colon where the dependence on Muc2 for formation of the colonic mucus is highest would suggest that DSS may interact directly with Muc2. Luminal commensals and pathogenic bacteria resident in the outer colonic mucus thus come into contact with the colonic epithelium and mucosal immune cells thereby stimulating pro-inflammatory immune responses. The ability for DSS to permeabilise the inner colonic mucous layer to the luminal microflora would explain the

lack of a requirement for the adaptive immune involvement in DSS-induced colitis. While T-lymphocytes are deemed critical to the colonic pathology in IBD, injury induced by DSS has been shown to occur independent of functional T and B lymphocytes [231, 232]. Since deficiency in either B-lymphocytes or T-lymphocytes still permits the induction of colitis by DSS, it seems likely that DSS-induced injury is primarily derived from the mucosal innate immune system in response to increased bacterial products within the mucosa [233].

Dependence on the non-specific luminal microflora is perhaps the accounts for the the necessity to optimise the concentration of DSS administered different mouse strains. For example C57BL/6 mice are more susceptible to chronic inflammation induced after 3–5 cycles of DSS recovery as opposed to BALB/c mice [234]. As a result variable concentrations of DSS are reported in the literature, as are the length and number of DSS cycles employed.

Table 1.3: **Colitis-associated neoplasia in DSS-induced murine models**

Strain	Mutation	Treatment	Duration	References
SWR	WT	5%	7 days of DSS, 14 days recovery, variable timepoints	[225]
C57BL/6J	WT	4%	4 cycles of 4 days DSS, 12 days recovery	[235]
CBA/J	WT	3%	9 cycles of 7 days DSS followed by 14 days recovery	[226]
C57BL/6J	WT	2.5%	12 cycles of 7 days DSS followed by 10 days recovery	[236]
C57BL/6J	WT	0.7%	15 cycles of 7 days DSS followed by 10 days recovery	[237]
C57BL/6J	WT	0.1%-0.4%	60 days	[238]

1.5.2 Interleukin-10

IL-10 is a key cytokine that is responsible for immune tolerance in the intestinal mucosa. IL-10 is produced by T-lymphocytes, macrophages, some B-lymphocytes, dendritic cells and

thymocytes. IL-10 is a cytokine that regulates both innate and adaptive immune functions by inhibiting macrophage function and also inhibiting T_H1 responses. IL-10-deficient mice spontaneously develop an inflammation involving both the colon and small intestine by the age of two months [239]. Histological features of the *Il10*$^{-/-}$-associated colitis included epithelial hyperplasia with crypt abcesses accompanied by leukocytic infiltrates in the mucosa and submucosa [239]. Notably, inflammation in *Il10*$^{-/-}$ mice occurred despite being maintained in specific pathogen-free conditions. Although avoidance of specific pathogens was unsuccessful in preventing intestinal inflammation associated in *Il10*$^{-/-}$ animals, the ability of antibiotics to ameliorate the disease suggested that inflammation was likely triggered by an abnormal reaction to commensal microbes [240]. The notion that an Il10-deficiency triggers a non-specific immune response against the resident microbiota is supported by the permeability of the colonic mucus to bacteria-sized material in *Il10*$^{-/-}$ mice [100]. Though IL-10 is an immunoregulatory cytokine, recent evidence suggests that it has an essential function in mucus production and secretion directly through IL-10R1 expression by colonic goblet cells [241]. Therefore, the *Il10*$^{-/-}$ mouse likely represents a model of IBD where a defect in mucus biosynthesis precipitates a chronic immune response directed against luminal commensals. Considering that *Il10*$^{-/-}$ produces extensive colitis, it may be expected that these mice are susceptible to colonic cancer. Twenty-five percent of *Il10*$^{-/-}$ mice from a C57BL6 ×129OLa background developed adenocarcinoma after three months of age [239]. The incidence of adenocarcinoma in *Il10*$^{-/-}$ animals increased with age, with 60% of animals presenting with adenocarcinoma after six months.

1.5.3 Mdr1a

The multi-drug resistance protein gene Mdr1a (*ABCB1* in the human, the murine orthologues being *Abcb1a* and *Abcb1b*) encodes an ATP-binding efflux transporter protein with a possible role in the regulation of luminal bacteria in IBD. Mdr1a expression in the murine intestine is limited primarily to the apical surfaces of differentiated intestinal epithelial

cells, and a population of mucosal leukocytes [242]. Pharmacological inhibition of Mdr1a function has been shown to permit emhanced bacterial attachments to the apical surface of immortalised colonic epithelial cell monolayers *in vitro* [243]. When housed in specific pathogen-free conditions, mice with homozygous Mdr1a ablation spontaneously developed a severe pan-colonic inflammation by the average age of 20 weeks [242]. The colitis induced by Mdr1a deficiency resembled the histopathology of UC, featuring enlarged crypts, leukocytic infiltration, crypt abscesses and ulceration. Consistent with the function of Mdr1a in inhibiting bacterial colonisation of the colonic epithelium, colitis induced by Mdr1a deficiency is ameliorated by antibiotic therapy [242]. Providing still further evidence for increased exposure to commensal bacteria, cells isolated from colonic lymphoid tissue of the Mdr1a-deficient animals displayed a heightened proliferative response to bacterial antigens. Supporting a possible role for Mdr1a dysfunction in human IBD, the abundance of human Mdr1a transporter has been shown to decrease as disease severity increases in UC [244]. Despite the correlation between Mdr1a expression and active inflammation in UC, it remains unclear whether down-regulation occurs primary to colitis or whether is Mdr1a down-regulated by the inflammation. Of particular relevance is the observation that Mdr1a deficiency in the $Apc^{Min/+}$ mouse has been shown to reduce the formation of intestinal polyps [245]. Homozygous *Abcb1* gene deletion reduced tumour multiplicity by up to 50% in the small intestine and colon of $Apc^{Min/+}$ mice. This result runs counter to the reasoning that chronic inflammation predisposes the inflamed tissue to neoplasia. Given the broad range of substrates which utilise the Mdr1a efflux transporter, further exploration of these substrates may explain the apparent paradox in the induction of colitis and subsequent neoplasia.

1.5.4 $G\alpha_{i2}$

The α subunit of the inhibitory GTP-binding protein Gi2 ($G\alpha_{i2}$) protein is expressed in many cell types including intestinal epithelial cells and intestinal lymphocytes. Deficiency of $G\alpha_{i2}$

in 129SvEv genetic background mice produces a progressive chronic inflammation in the intestine by the age of 8–12 weeks [246]. The disease associated with $G\alpha_{i2}$-deficiency is characterised by mucosal ulceration, crypt abscesses and mucin depletion, with the most severe symptoms in the distal colon. Interestingly, $G\alpha_{i2}$-deficiency exhibit an abnormal adaptive immune response to the luminal microbiota and a greater resistance to suppression by regulatory T-lymphocytes [247, 248]. Consistent with the chronic, progressive colitis, approximately 30% of $G\alpha_{i2}$-deficient mice develop non-polypoid, colonic adenocarcinoma by the age of twelve weeks, with colonic dysplasia visible in 50% of mice as early nine weeks [246, 248].

1.5.5 Muc2

Velcich *et al.*. described a truncating mutation in Muc2 (C57BL6/J ×129SvOla background) that produced a total abrogation in Muc2 synthesis [99]. Associated with the abolition of Muc2 was the disappearance of the characteristic acidic polysaccharide-containing granules that identify the goblet cell. While heterozygous Muc2 mutants (*Muc2*$^{-/-}$) displayed normal weight gain, but displayed occult bleeding indicative of erosive intestinal disease. Homozygous gene deletion of the gene encoding mucin-2 *Muc2* produces a spontaneously occurring phenotype characterised by weight loss, diarrhoea, intestinal bleeding [249]. Histological examination of *Muc2*$^{-/-}$ reveals immune cell infiltration, loss of goblet cells, crypt elongation and superficial ulceration of the mucosa [249]. Ectopic expression of the Muc6 gastric mucin was reported in the colon of mice with homozygous *Muc2*$^{-/-}$.

Unlike wild-type mice, *Muc2*$^{-/-}$ mice displayed a crypt hyperplasia and infrequent exophytic epithelial tumours, some invasive, throughout the small and large intestine. Notably, tumours arising in the colon in *Muc2*$^{-/-}$ mice were infrequent relative to those of the small intestine. Of the 21% of Muc2 mutants that had developed colonic tumours by the age of 12 months, only one mouse was reported to have multiple colonic tumours.

1.5.6 Winnie

Of particular interest for the study of UC is Winnie strain of mice which harbour a single-nucleotide, missense mutation in the *Muc2* gene that encodes a full-length protein. Missense mutation in the *Muc2* D3 domain of *Muc2* inhibits oligomerisation of Muc2 and would therefore reduce the effectiveness of the secreted colonic mucus in excluding the luminal microbiota from the colonic epithelium [250]. Misfolded Muc2 also accumulates within the secretory goblet cells of the colonic epithelium and subsequently leads to activation of the unfolded protein response (UPR) and endoplasmic reticulum (ER) stress [250]. The combination of ER stress and a defective secreted mucus in Winnie is associated with a colitis affecting the middle and distal colon, producing diarrhoea. The colitis in Winnie mice shares some of the same histological features of UC with mucin depletion, crypt branching and elongation and focal neutrophilic crypt inflammation and the formation of crypt abscesses [250]. Likewise, the immunopathology in the Winnie colon is characterised by expansion of $CD11c^+$ APCs and activated DCs ($CD11c^+$ MHC-II^{hi}) with T_H17 polarisation of mucosal immune responses [251]. Mucosal barrier dysfunction in the Winnie mouse results in a complex colitis involving both an innate immune element and a T_H17-mediated adaptive immune response similar to the cytokine profile observed in patients with IBD [123]. While Muc2-deficient animals are prone to intestinal neoplasia, the susceptibility of Winnie mice to colonic neoplasia remains unclear.

1.6 Aims and hypothesis

Evidence for the tumour-promoting effects of various pro-inflammatory mediators is constantly accumulating. Less is known about the transition from a normal mucosa to the early pre-cancerous mucosa. It is advantageous therefore to replicate such a transition *in vivo* in order to better characterise molecular events and trial interventions in colitis-associated colonic tumourigenesis.

Therefore the aim of this project was to investigate the potential for colonic carcinogenesis in an experimental model of chronic spontaneous colitis initiated by a goblet cell defect:

i) Examine the effect of repeated bouts of severe colitis on pro-cancerous change in a model of a colitis initiated by defective Muc2 synthesis.

ii) To identify potential mechanisms by which colitis initiates pro-cancerous changes in the colonic epithelium.

CHAPTER 2

MATERIALS AND METHODS

2.1 Prepared solutions

Phosphate-buffered saline (PBS) (1×, pH 7.3)

Compound	Quantity	Manufacturer
Phosphate-buffered saline (20×)	50mL	Amresco, Solon, OH, USA
Distilled water	950mL	

Diluted pre-prepared stock solution of PBS (20×) in distilled water. Stored at RT.

10% Neutral buffered formalin (NBF)

Compound	Quantity	Manufacturer
Formalin (37%)	50mL	VWR International, Brisbane, Australia
PBS (1×, pH 7.3)	450mL	

Formalin solution diluted in PBS, mixed and stored at room temperature.

Sodium citrate buffer (10mM, 0.05% Tween-20, pH 6.0)

Compound	Quantity	Manufacturer
Trisodium citrate, dihydrate	2.94g	Amresco, Solon, OH, USA
Tween-20	0.5mL	Amresco, Solon, OH, USA
Distilled water	up to 1L	

Prepared as a 1× solution, pH adjusted to 6.0 and stored at 4°C.

Sodium acetate solution (0.1M)

Compound	Quantity	Manufacturer
Sodium acetate	8.2g	Amresco, Solon OH, USA
Distilled water	up to 1L	

Sodium acetate added to distilled water and mechanically agitated to ensure complete dissolution. Stored at room temperature.

Acetic acid solution (0.1M)

Compound	Quantity	Manufacturer
Glacial acetic acid (99.7%)	5.74mL	VWR International, Brisbane, Australia
Distilled water	up to 1L	

Glacial acetic acid diluted in distilled water and mixed. Stored at room temperature.

Acetate buffer (pH 5.5)

Compound	Quantity	Manufacturer
Sodium acetate (0.1M)	180mL	
Acetic acid (0.1M)	20mL	

Combined acetic acid and sodium acetate solutions. Adjust pH to 5.5 if necessary. Stored at room temperature.

Aqueous glycerol solution (1%)

Compound	Quantity	Manufacturer
Glycerol	10mL	Amresco, Solon, OH, USA
Distilled water	up to 1L	

Glycerol added to distilled water and agitated to dissolve.

Sodium periodate solution (1mM)

Compound	Quantity	Manufacturer
Sodium metaperiodate	2.0g	Sigma-Aldrich, Sydney, Australia
Acetate buffer (0.1M, pH 5.5)	200mL	

Periodate dissolved in acetate buffer (pH 5.5) with mechanical agitation. Kept at room temperature.

Potassium metabisulphite solution (0.5%)

Compound	Quantity	Manufacturer
Potassium metabisulphite	1g	Ajax, Melbourne, Australia
Hydrochloric acid (0.15M)	100mL	
Distilled water	100mL	

Hydrochloric acid diluted in distilled water. Metabisulphite dissolved in the hydrochloric solution.

Alcian Blue solution, pH 1.0

Compound	Quantity	Manufacturer
Alcian blue 8GX	1%	Gurr Scientific, Oxford, UK
Hydrochloric acid (0.1M)	100mL	

Mixed mechanically for 1 hour. Stored at room temperature and filtered through Whatman paper immediately prior to use.

Schiff's reagent (Mowry's variant)

Compound	Quantity	Manufacturer
Pararosaniline	0.5g	Gurr Scientific, Oxford, UK
Sodium metabisulphite	5g	Ajax, Melbourne, Australia
Hydrochloric acid (37%)	3mL	VWR International, Brisbane, Australia
Distilled water	up to 200 mL	

Mixed mechanically for 2 hours, filtered through Whatman paper and volume adjusted to 200mL with distilled water. Stored at 4°C before use.

Antibody diluent (2% Bovine serum albumin (BSA), 0.05% Tween-20)

Compound	Quantity	Manufacturer
BSA (2%)	10g	Bovogen Biologicals, Melbourne, Australia
Tween-20	0.25mL	Amresco, Solon, OH, USA
Thiomersal	0.25mL	BDH, Poole, UK
PBS (1×, pH 7.3)	up to 500mL	

BSA dissolved in PBS, added thiomersal and mixed mechanically until completely dissolved. Adjusted pH to 7.2–7.4 with hydrochloric acid. Volume of Tween-20 added and resulting solution stored at 4°C.

3,3'-diaminobenzidine (DAB) solution

Compound	Quantity	Manufacturer
DAB solution	0.16mL	Biocare Medical, Concord, CA, USA
DAB buffer	3.2mL	Biocare Medical, Concord, CA, USA

Volume of the pre-prepared DAB reagent is mixed into the chromagen substrate buffer solution. Filtered immediately prior to use.

Haematoxylin (Carrazzi)

Compound	Quantity	Manufacturer
Haematoxylin	2g	Gurr Scientific, Oxford, UK
Glycerol	200mL	Amresco, Solon, OH, USA
Potassium metaperiodate	0.2g	Ajax, Melbourne, Australia
Aluminium potassium sulphate	50g	Ajax, Melbourne, Australia

Haematoxylin dissolved in glycerol, potassium periodate is dissolved in 300mL of the distilled water with agitation overnight. Diluted periodate is added to the haematoxylin solution, mixing well after every addition. Potassium metaperiodate dissolved in remaining distilled water with warming. Potassium periodate is added to the haematoxylin-alum sulphate-glycerol mixture. The final mixture is shaken well and is ready for use immediately.

2.2 Animal Procedures

2.2.1 Ethics statement

All animal procedures were performed in accordance with the Australian Code of Practice for the Care and Use of Animals for Scientific Purposes of the National Health and Medical Research Council. The study was approved by the Animal Ethics Committee of the University of Tasmania (protocol #13329).

2.2.2 Animal care and housing

Winnie mice (homozygous *Muc2* mutant; C57BL6/J background) were re-derived from stock maintained by the Monash Animal Services (Monash University, Melbourne, Australia) into the specific pathogen-free Cambridge Farm Facility (University of Tasmania Animal Services, Tasmania, Australia) for breeding purposes. Eleven to twelve week-old inbred Winnie and C57BL6/J mice of both sexes were sourced from the University of Tasmania Animal Services and transferred to the laboratory at the University of Tasmania School of Health Sciences. After transferral to individual cages animals were acclimatised to their holding environment for at least seven days before commencing experiments.

Animals were held in a room at the University of Tasmania School of Health Sciences. where temperature was maintained at 21°C$\pm$ 4°C, with unregulated humidity and artificially lit for 12 hours each day. Presence of specific pathogens within animals was not monitored, however animals were housed within a individually ventilated Maxi-Miser caging unit (Thoren Caging Systems Inc., Hazleton, PA, USA). Although caging provided animals with high-efficiency particulate-absorbing (HEPA) filtered air (HEPA), the room in which animals were housed was supplied by unfiltered air. Mice would therefore be exposed to a non-sterile environment when animals were weighed, food and water changed. Protocols to limit microbiological contamination were therefore used in housing and monitoring mice. Every week mice were transferred to a clean cage containing autoclave-sterilised

corncob bedding (Andersons, Maumee, OH, USA) and were permitted *ad libitum* access to γ-irradiated and autoclaved rodent feed (Barastoc Rat & Mouse, Ridley AgProducts, Australia) and autoclave-sterilised, tap-water. All surfaces and equipment used to handle mice were disinfected prior to coming into contact with animals to limit exposure to any additional microbes and pathogens.

Based on a small number of available mice, dysplasia-like mucosal lesions were observed in 2/3 Winnie mice and submucosal crypt extension in 1/3 Winnie mice following three cycles of 1% DSS. In contrast none of the untreated Winnie mice displayed histological features indicative of anything more than mild inflammation. Based on crude proportions, as few as 4 Winnie mice per treatment group may be used to identify a difference in dysplasia Sample sizes sufficient to identify a large effect size, assuming a power of 0.8 and a significance level of 0.05, could be achieved with as few as 7 animals per group if a factorial analysis of variance (ANOVA) was used.

2.2.3 Exacerbation of colitis with dextran sulphate sodium

In order to exacerbate colitis in Winnie, a solution of DSS was administered in a cyclic regimen. Each cycle of the experimental DSS regimen consisted of the administration of DSS for seven days before substitution of 1% DSS for water for an additional seven days. Winnie and C57BL6/J littermates were randomly allocated to one of two groups. A group of twelve Winnie and six C57BL6/J mice received a 1% w/v DSS (40,000–50,000 Da; USB, Affymetrix Inc., Cleveland, OH, USA) diluted in the sterile tap water. Alternatively a DSS 'vehicle' control group of six Winnie and four C57BL6/J animals, were administered sterile drinking water only. Mice in the experimental group received DSS in a total of three cycles over 42 days, with a single Winnie mouse euthanased prior to the conclusion of the DSS regimen. Mouse body weight and disease symptoms (e.g. diarrhoea, rectal bleeding) were monitored daily during the experiment. Euthanasia, defined as humane killing to relieve

pain and distress as per the Australian Code of Practice for the Care and Use of Animals for Scientific Purposes, was necessary in a single case of excessive morbidity and weight loss following the first DSS cycle. In the case of both euthanasia and experimental termination (day 42), mice were humanely killed via CO_2 asphyxiation and cervical dislocation, in accordance with the Australian Code of Practice for the Care and Use of Animals for Scientific Purposes, before the abdomen was dissected and colon removed.

2.3 Histopathology

2.3.1 Tissue processing

The length of the colon from ileo-caecal junction to the rectum was recorded. The colon was subsequently opened along its longitudinal axis and the luminal contents were removed prior to weighing the organ. The colon was bisected longitudinally and one half was prepared using the Swiss roll technique [252]. The remaining colonic tissue was dissected and snap-frozen for molecular analyses. Swiss rolls underwent 24-hour fixation in 10% (v/v) NBF at room temperature before being transferred to 70% ethanol. Intestinal rolls were processed by first dehydrating tissue through progressively increasing concentrations of ethanol (2$\times$ changes of 95% ethanol, followed by 4$\times$ 100% ethanol), then cleared of alcohol through 2$\times$ changes of xylene and finally infiltration with 2$\times$ changes of molten Histo-Prep paraffin wax (Fisher Scientific, Philadelphia, PA, USA) at 60°C. All processing steps were automated using a Citadel 1000 tissue processor (Shandon Scientific, Runcorn, UK). Swiss rolls were immediately transferred to an embedding station (HistoCentre 2; Shandon Scientifcc) and embedded in Histo-Prep paraffin wax. Sections were cut at 5μm with at least three levels 50 μm apart obtained using a rotary microtome (Leica 1512). Sections were stained with Gill's haematoxylin and eosin Y (H&E; HD Scientific, Sydney, Australia). Slides stained with H&E were evaluated for inflammatory features and neoplasia.

2.3.2 Histpathological evaluation

Histological inflammation was graded in a blinded fashion by a single observer based on previously used criteria (refer to Fig. A2) [251]. Briefly, crypt architectural distortion was graded 0-5, frequency of crypt abscesses graded 0-3, crypt hyperplasia graded 0–4, extent of mucosal damage graded 0–4, goblet cell depletion graded 0–4, extent of inflammatory infiltration graded 0–4 and frequency of lamina propria polymorphonuclear (PMN) leukocytes graded 0–3. The inflammation score for each individual region (distal, middle and proximal colon) was derived from the sum of the score for each of the aforementioned criteria. Assessment of dysplasia was performed independently by two pathologists (RF and TB) blinded to experimental groupings. Crypts involved in glandular profunda were classified as non-dysplastic lesions. Dysplastic change and submucosal invasion were graded as no change (0), low-grade dysplasia (1), high-grade dysplasia (2) and invasive carcinoma (3). Overall inter-observer agreement on the classification of dysplastic change was estimated to be moderate ($\varkappa = 0.41$, $P = 0.005$). In cases of disagreement, the highest grade of either observer was adopted.

2.3.3 Mucin histochemistry

Paraffin-embedded tissue sections (3 μm thickness) were de-waxed and washed in 0.1 M sodium acetate buffer (pH 5.5) at 2°C for 5 min. Sections were then oxidised using 1 mM sodium periodate diluted in 0.1M acetate buffer (pH 5.5) for 10 min. Periodate solution was rinsed off with 1% aqueous glycerol followed by distilled water each for 5 min. Sections were subsequently treated with Schiff's reagent (prepared the previous week) at room temperature for 15 min. Sections were rinsed in three changes of 0.5% potassium metabisulphite in 0.05 M hydrochloric acid for 5 min. Sections were thoroughly rinsed with running water for 5 min, rinsed in distilled water then stained with acidic Alcian blue (pH 1.0) for 15 min. Sections were rinsed, stained with Gill's haematoxylin, dehydrated and mounted using DPX.

2.4 Immunohistochemistry

Slides were dewaxed and exposed to heat-induced epitope retrieval (4 min at 121°C) in a sodium citrate buffer (pH 6.0) in a decloaking chamber (Biocare Medical, Concord, CA, USA). Slides were cooled to room temperature in running tap water and washed in 1× Tris-buffered saline (TBS) 2 min/wash. Endogenous peroxidase activity was blocked by incubating slides in 3% H_2O_2 in methanol for 20 min, followed by 3 × 2 min washes (twice with distilled water, followed by one wash with 1× TBS). To reduce signal from endogenous IgG Background Sniper (Biocare Medical) was applied to the slides for 20 min and washed off with 3 × 2 min washes with TBS. Rabbit anti-human beta-catenin (clone E247; Abcam, Cambridge, UK), applied at a 1:500 dilution or rabbit anti-human Ki67 (clone SP6; Abcam), applied at a dilution of 1:100 was incubated with the slides for 1 h. Anti-vimentin (Cell Signalling Technology, Danvers, MA, USA) and anti-N-cadherin (Cell Signalling Technology) were used at 1:250 and 1:400 dilutions respectively. Excess primary antibody was removed with 3 × 2 min washes with TBS prior to application of HRP-conjugated anti-rabbit secondary polymerised antibody (Biocare Medical) for 30 min. Slides were thoroughly rinsed with 1× TBS for 3×2 min washes before the addition of a proprietary 3,3'-diaminobenzidine (DAB) chromagen solution (Biocare Medical) for 4 min. Tissue was subsequently counterstained with Corrazzi's haematoxylin, dehydrated and mounted with dibutyl pthalate in xylene (DPX; Sigma-Aldrich, Sydney, Australia).

2.4.1 Assessment of epithelial cell proliferation

In order to evaluate cellular proliferation within the colonic crypts, nuclei labelled by anti-Ki67 within the crypt epithelium were quantified. From each animal, multiple fields of view were evaluated with at least 15 well-oriented crypts assessed by dividing them along their longitudinal axis, approximately into thirds: apical (top), middle and base. Both Ki67-expressing cells and unlabelled epithelial cells within each of the assessed crypts were

Table 2.1: **List of antibodies**

Antigen	Clone	Reactivity	Origin	Product No.	Supplier
β-catenin	Monoclonal (E247)	Mouse	Rabbit	32572	Abcam
Cxcl5	Polyclonal	Mouse	Rabbit	2549R	Bioss
Ki67	Monoclonal (SP5)	Mouse	Rabbit	16667	Abcam
N-cadherin	Monoclonal (D4R1H)	Human, Mouse	Rabbit	13116	Cell Signalling Technology
Vimentin	Monoclonal (D21H3)	Human, Mouse	Rabbit	5741	Cell Signalling Technology

counted and were expressed as a percentage of Ki67-positive cells of the total number of cells within the epithelium. The proportion of Ki67-expressing cells was also expressed relative to the total cell count for the either the top, middle and basal crypt regions.

2.4.2 Assessment of β-catenin

Images of the colonic mucosa were collected using the 40× objective on a IX71 microscope (Olympus, Tokyo, Japan) and the attached DP21 microscope camera (Olympus, Tokyo, Japan). Ten random fields were selected for the segment of colon and the image was de-convoluted using ImageJ v1.60 [253] and the colour de-convolution extension based on the algorithm designed by Ruifrok and Johnston to separate [254]. The colour channel containing DAB staining was used to determine the percentage of the area of the visual stained using the primary antibody.

2.5 RNA purification

Whole-thickness colonic tissue was homogenised using rotor-stator generator probes (Omni International, Marietta, GA, USA) and RNA extracted using the RNeasy Mini spin column

kit (Qiagen, Melbourne, Australia) according to the manufacturer's instructions. To minimise genomic DNA contamination DNAse I (Qiagen) digestion was performed "on-column" during the RNA extraction protocol. Integrity and concentration of extracted RNA was assessed using the Experion Eukaryotic Total RNA electrophoretic system (Bio-Rad Laboratories). Samples with an RNA integrity number (RIN) > 7 were deemed suitable for RT-qPCR. Complementary DNA (cDNA) was synthesised from RNA samples using the iScript Reverse Transcription enzyme and reagents (Bio-Rad) using reaction conditions suggested by the manufacturer.

2.6 Real-time quantitative polymerase chain reaction

Screening for potential markers of colonic carcinogenesis was performed using pre-designed 96-well Tier I RT-qPCR array plates containing lyophilised primers for 91 genes, refer to Table A.1. Fifty picograms of cDNA was added to each well of a 96-well plate and mixed with a SYBR Green master mix (Bio-Rad) prior to thermal cycling using a StepOnePlus RT-qPCR system (Applied Biosystems, Foster City, California, USA). Gene expression was quantified using the comparative $\Delta\Delta C_T$ method [255] where the threshold cycle (C_T) for each gene was normalised to the average of three reference genes (Actb, Gapdh, Hprt). Relative gene expression in the DSS-treated animals was compared to control animals and presented as $2^{-\Delta\Delta C_T}$. To confirm the results from the intial RT-qPCR array, differentially expressed genes were amplified using TaqMan probe/primer sets. Two-hundred nanograms of cDNA from each sample was added to a a PCR reaction including the Taq polymerase enzyme mix supplied within the TaqMan Fast Master Mix (Applied Biosystems, Foster City, CA) and a single TaqMan probe/primer mix. Identities of the primers used are listed in Table A.2. Relative gene expression was quantified using *Gapdh* as a reference gene.

2.7 DNA purification and bisulphite conversion

Segments of distal colon were minced prior to lysis with proteinase K using the DNA Tissue lysis kit (Kurabo Bio-Medical, Osaka, Japan). DNA lysates were purified using the colum-based QuickGene 810 system (Kurabo) and eluted in nuclease-free water. Extracted DNA was quantified using the Qubit 3.0 fluorometric system (Qiagen). Unmethylated cytosines in genomic DNA were converted to thymine using the bisulphite treatment supplied with the EpiTect Bisulfite conversion kit (Qiagen) according to the manufacturer's instructions. Three microlitres of bisulphite-converted DNA was used as the template for a 20 μL PCR amplification containing a mixture of MyTaq high-sensitivity DNA polymerase (0.5 U; Bioline Australia Pty, Sydney, Australia), forward and reverse primers (0.2 μM) and 1 mM dNTPs, 3 mM $MgCl_2$. Forward and reverse primers designed to amplify bisulphite-converted DNA were predicted using the PyroMark Assay Design software v2.0 (Qiagen), refer to Table A.3 for sequences). Reverse primers with 5'-biotinylation were synthesised and subsequently purified through HPLC to remove free biotin (Geneworks, Adelaide, Australia). Thermal cycling was performed using a C-1000 thermal cycler (Bio-Rad) with a single polymerase activation at 95°Cfor 60 sec, followed by a sequence of DNA denaturation at 95°C for 15 sec, annealing at 55°Cfor 15 sec and extension at 72°C for 10 sec, for a total of 40 cycles.

2.8 CpG methylation sequencing

Added PCR-amplified DNA (10 μL) to each pyrosequencing reaction with sequencing primer at 2 μM concentration. Pyrosequencing was performed using the PyroMark Gold (Qiagen) nucleotides, enzymes and substrate, with sequencing performed using the QSeq pyrosequencing system (Bio Molecular Systems, Coomera, Australia).

2.9 Statistical analysis

Change in body weight over time was compared using repeated-measures analysis of variance (ANOVA). Incidences of graded histological lesions were compared between treatment groups stratified within genotype using the Mantel-Haenszel χ^2 statistic. Comparisons between means of each unique combination of genotype and treatment were performed using a two-way ANOVA model. Differences in histological scores between anatomical regions were tested post-ANOVA using Tukey's multiple pairwise comparisons test. To determine differences in the calculated survival curves for time to rectal prolapse between DSS and untreated Winnie mice, a Mantel-Cox analysis was performed using GraphPad Prism v5.03 (GraphPad Software, San Diego, CA, USA). Non-parametric Spearman's rank correlation was used to test for monotonic relationships between relative transcript abundance and dysplasia scores (non-dysplastic = 1, low-grade = 2, high-grade = 3, dysplasia with submucosal component = 4). In all cases, a P-value less than 0.05 was deemed to be statistically significant.

CHAPTER 3

HISTOPATHOLOGICAL CHARACTERISATION OF DSS-INDUCED INJURY IN THE WINNIE COLON

3.1 Introduction

The association of genes involved in the maintenance of mucosal integrity with susceptibility of UC and the development of a spontaneous chronic colitis in mice with defects in mucin synthesis have implicated these defects in the causation of UC. Key to our understanding of UC pathogenesis was the generation of the *Muc2*$^{-/-}$ mouse. Genetic abrogation of murine Muc2 abolishes the sterile, inner colonic mucous layer, rendering Muc2-deficient animals susceptible to colitis caused by colonisation of the colonic mucosa by the luminal microbiota [90, 249]. *Muc2*$^{-/-}$ mice develop a chronic colitis characterised by a mucosal neutrophilic infiltrate, crypt damage, reparative hyperplasia and depletion of goblet cell mucin [99, 249]. While the *Muc2*$^{-/-}$ mouse model has proven to be useful for understanding the pathogenesis of UC, Muc2 expression, although decreased, is not totally absent from the colonic epithelium [256, 257]. Furthermore, compensatory increases in the synthesis of the secreted mucin-6 (Muc6) are also observed in *Muc2*$^{-/-}$ mice, but not seen in UC [249]. Extrapolation from models of a primary mucous defect where Muc2 is somewhat intact, may

therefore be more reliable when applied to human UC. The differences between UC and *Muc2*$^{-/-}$ mice may stem from a primary defect in the secretory goblet cells. However, the pathology produced by total Muc2 abrogation displays several discrepancies when compared to human UC.

Similarly to aforementioned *Muc2*$^{-/-}$ mouse strain, the Winnie strain of mice develop a spontaneous colitis due to homozygous missense point mutations in *Muc2*. The Winnie Muc2 mutation results in a single amino acid substitution in the N-terminal D3 domain in the Muc2 protein, which adversely affects the oligomerisation of Muc2 [250]. Theoretically, prevention of Muc2 oligomerisation could prevent the formation of the mesh-like Muc2 polymers which form the basic structure of the inner mucous layer essential for the size-dependent exclusion of the luminal microbes [90,98]. The misfolding of Muc2 interferes with its secretion from the ER and Golgi of the colonic goblet cells, triggering the unfolded protein response in the colonic goblet cells of Winnie mice [250]. Increased ER stress corresponds to an increased epithelial apoptosis similar to that in patients with UC, supporting the concept of a primary secretory cell defect as an aetiologic factor in UC.

A significant gap in our understanding of the disease process in UC is how the theoretical secretory defect contributes to neoplastic transformation of the colonic epithelium. The highly organised structure formed by polymerisation secreted Muc2 mucin is essential to preventing contact between the luminal microbiota and the host immune response thereby preventing chronic colitis in animal models. Maintenance of the colonic mucus is therefore essential for both the prevention of colitis and appears to be protective against colonic tumourigenesis. Concordant with the persistent exposure to the luminal bacteria and chronic inflammation, *Muc2*$^{-/-}$ display an increased incidence of colonic neoplasia. Homozygous Muc2 deletion in mice of C57BL6/J $\times$ 129SvOla background was associated with increased incidence of tumours in the small intestine, colon and rectum relative to animals with wild-type *Muc2* [99]. Whereas colonic adenocarcinomata have been reported in the *Muc2*$^{-/-}$ and

Il10$^{-/-}$ models, no incident of colonic neoplasia has yet been reported in Winnie mice, even at twelve months of age [99, 239, 250]. Induction of a secretory cell ER-stress response and a defective Muc2-dependent mucous layer therefore makes the Winnie mouse an potential model for the pathogenesis of UC-associated neoplasia.

3.2 Aims/Hypothesis

Since total abrogation of colonic Muc2 produces adenocarcinoma of the colon within 12 months, it was hypothesised that Winnie mice would display an increased incidence of adenocarcinoma compared to mice with wild-type *Muc2*. The length of time needed to observe pre-cancerous changes in the colon of *Muc2*$^{-/-}$ animals limits the usefulness of this model for studying neoplasia resulting from an impaired mucous barrier. Since Winnie mice display a subtotal depletion of the colonic mucus we anticipated that colonic neoplasia would require at least 6–12 months to develop, we intended to exacerbate the existing chronic colitis to accelerate tumourigenesis.

3.3 Results

3.3.1 Clinical observations following three cycles of DSS

Twelve week-old mice of both C57BL/6J (*Muc2* wild-type) and Winnie (*Muc2* mutant) were monitored throughout the experiment for the clinical symptoms indicative of disease severity. Wild-type mice (n = 4) displayed no clinical signs of disease and gained weight normally when they received drinking water only for 42 days (Fig. 3.1A). While extended exposure to 1% DSS produced a mild diarrhoea in C57BL/6J mice with wild-type *Muc2* (n = 6), 1% DSS did not appear to exert an appreciable effect on the trend toward a increased body weight over the course of the experiment. Individual Winnie mice were clinically asymptomatic apart from recurrent episodes of a mild, non-watery diarrhoea. Bouts of diarrhoea were

typically accompanied by slight but reversible losses in body weights of individual Winnie mice (Fig. 3.1B).

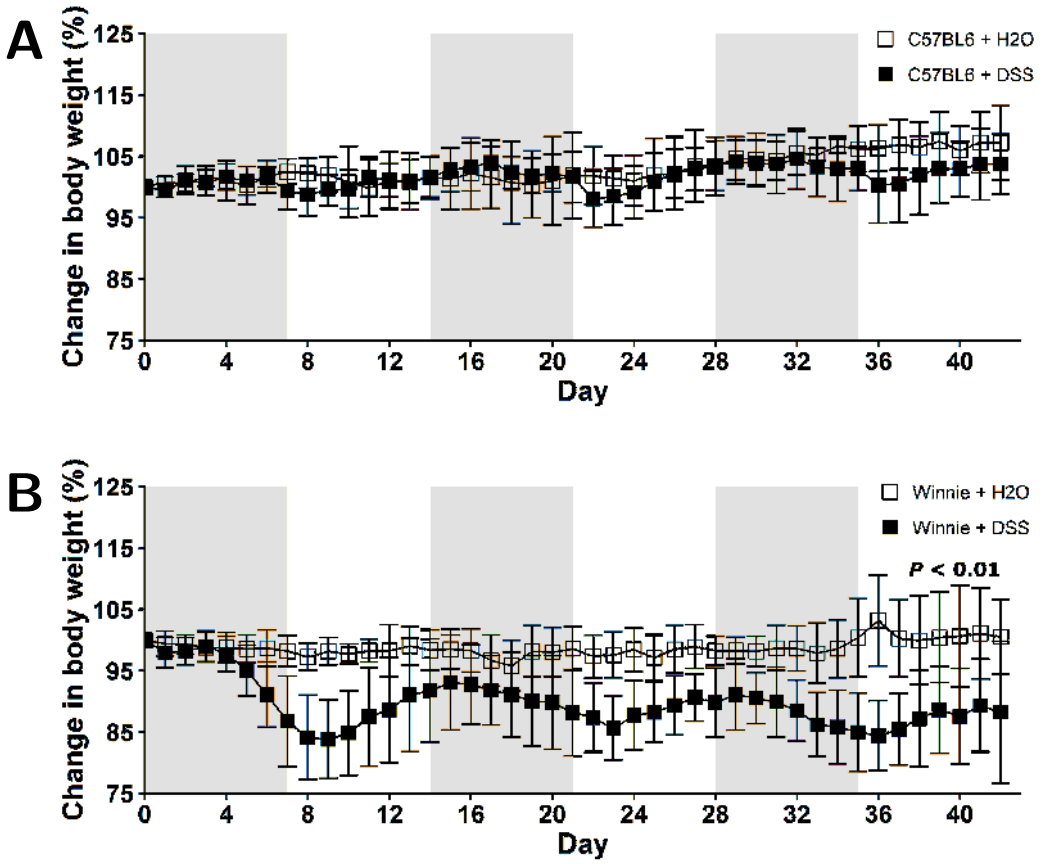

Figure 3.1: **Daily change in body weight of mice during the three cycle DSS regimen.** Twelve week-old Winnie mice (*Muc2* mutant) and age-matched C57BL/6J mice (wild-type *Muc2*) receiving drinking water only, or three cycles of 1% DSS. Body weight was recorded each day and recorded as percentage change from the starting body weight prior to commencement of the experiment (day 0). **A.** Comparison of average body weight change between untreated C57BL/6J mice, which received drinking water only for 42 days, and C57BL6/J mice exposed to three cycles of 1% DSS. **B.** Average body weight change between untreated Winnie mice, which received drinking water only for 42 days, and Winnie mice exposed to three cycles of 1% DSS. Each point represents the mean percentage change in body weight relative to the initial body weight. Error bars depict standard deviation (SD) from the mean. Grey bars represent days during which mice were administered DSS.

However, the average body weight of control Winnie mice (n = 6) during the experiment remained relatively stable over the 42 days of the experiment. Compared to the wild-type C57BL6/J, Winnie mice displayed a higher sensitivity to the administration of DSS in the drinking water (n = 11). Oral administration of DSS at 1% w/v for 7 days induced a bloody, watery diarrhoea co-inciding acute with weight loss which continued 1-2 days after cessation of DSS administration. The only mortality during the experiment occurred when one Winnie mouse receiving the first DSS cycle developed disease and excessive weight loss necessitating euthanasia. The overall trend in body weight change in Winnie was attenuated by three cycles of 1% DSS administration.

Upon termination of the experiment, when mice had reached an age of approximately 18 weeks, mice were killed and the colon dissected for further examination. Colon length measured from the caecum to the rectum, and the wet colon weight were measured as gross indicators of disease severity. The absolute length of the colon in Winnie mice exposed to the DSS regimen was decreased by an average of 24% compared to Winnie mice receiving drinking water alone (Fig. 3.2A). In contrast, the weight of the whole colon from Winnie mice administered DSS was, when standardised to body weight, no heavier than Winnies receiving only drinking water (Fig. 3.2B). Colons of Winnie mice administered 1% DSS, despite being the same weight on average as untreated Winnie, displayed visible features indicative of chronic inflammation. The colon from Winnie following three cycles of 1% DSS was noticeably whitened in colour with apparent thickening of the colonic wall relative to untreated animals, and displayed enlargement of mesenteric lymph nodes compared to control Winnie mice (Fig. 3.2C).

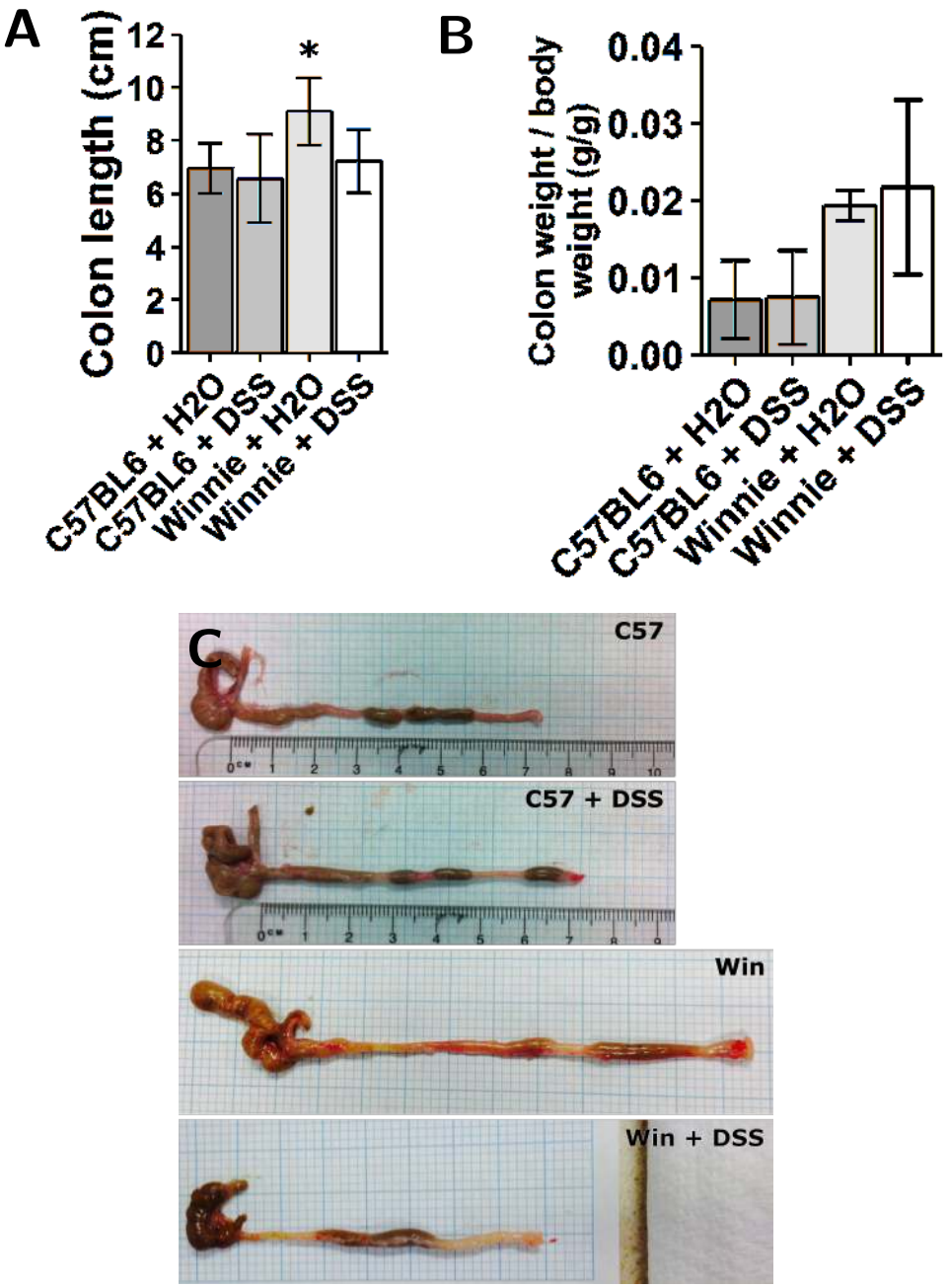

Figure 3.2: **Clinical features of DSS-induced colitis in Winnie.** **A**. Mean colon length at termination. **B**. Mean colon weight relative to body weight at termination. **C**. Gross appearance of the Winnie colon at termination. Representative images of Winnie colon after receiving three cycles of water only (top) and the colon of Winnie receiving three cycles of DSS (bottom). Error bars depict SD from the mean. *, mean significantly different (P <0.05) in Winnie + H_2O compared to all other groups.

3.3.2 Histopathology

Histological examination of the colon was undertaken to characterise the pathology induced by three cycles of 1% DSS in the Winnie colon. Compared to the wild-type C57BL6 (Fig. 3.3A) and wild-type exposed to three DSS cycles (Fig. 3.3B), diffuse leukocytic infiltration into the mucosa, and to a lesser extent the submucosa, was common in the distal and mid-colon of Winnie mice (Fig. 3.3C & 3.3D). In these mice, crypt architecture in the distal colon was occasionally irregular and frequently elongated, with infrequent crypt abscesses observed in both the mid-colon and distal colon.

At the time of termination (day 42), severe damage to the distal and mid-colon of Winnie mice exposed to DSS remained evident (Fig. 3.3D). DSS administration in Winnie resulted in an increased influx of leukocytes into the mucosa and submucosa. Large mucosal aggregates of mononuclear leukocytes were frequent, and often extended into the expanded submucosal compartment. Glandular profunda was identified in the distal colon involving the larger lymphoid aggregates, which expanded beyond the muscularis mucosae. Areas of superficial mucosal erosion and crypt loss were observed, frequently with foci of crypt fission adjacent the erosion (Fig. 3.3D). Generally, the mucosa of the Winnie distal colon was extensively thickened and contained hyperplastic crypts following repeated DSS exposure. In addition to the typical inflammatory effects observed in Winnie, we assessed the colon for early neoplastic changes. Crypt hyperplasia within the distal and mid-colon of Winnie mice exposed to DSS was often accompanied by foci of abnormal crypt architecture resembling dysplasia.

Forty-five percent of Winnie mice displayed crypt abnormalities consistent with a low-grade dysplasia after administration of DSS (Table 3.8), whereas aberrant crypts were only observed in one untreated Winnie. Low-grade lesions displayed marked architectural distortion, with subtle cytological features such as crowding of epithelial nuclei and increased

ratio of nucleus-to-cytoplasm (Fig 3D). Low-grade lesions were absent from all wild-type animals except for one of six C57BL6/J mice exposed to DSS (Table 1).

Changes to crypt architecture, frequency of crypt abscesses, crypt hyperplasia, the extent of mucosal damage, mucin depletion, extent of inflammatory infiltration and frequency of lamina propria neutrophils were graded in a blinded fashion. Examination of the colon was divided into three segments: proximal colon (PC) , mid-colon (MC) and distal colon (DC).

Crypt abscesses were defined as crypts containing an intra-luminal accumulation of cellular debris and neutrophils. The number of crypt abscesses observed in each segment of colon was counted for each level of section. Crypt abscesses were not observed in the untreated wild-type C57BL6 or those administered 1% DSS, in any of the three intestinal segments (PC, MC and DC) (Fig. 3.4). Winnie mice however, displayed a median crypt abscess score of 1.5 and 1 for the mid-colon and distal colon respectively, while the proximal colon was unaffected. Exposure to three cycles of 1% DSS seemingly increased the frequency of crypt abscesses in the distal colon but not the proximal and mid-colon.

Loss of normal crypt architecture was graded for each intestinal segment for each of the genotypes and treatment groups. Normal crypt architecture was found throughout the entire colon of untreated C57BL6 mice (median of 0). Median scores for all intestinal segments in C57BL6 mice following exposure to 1% DSS were also at baseline, though 1/6 mice displayed a mild glandular irregularity (grade 1) in the distal colon. For crypt length a median score of 1 (150–199 μm) was recorded for crypt length in the proximal colon of untreated C57BL6 mice, but a median of 0 for all other segments ($<$250 μm and $<$200 μm for middle colon and distal colon respectively).

While crypt length was within the baseline range following 1% DSS in C57BL6 mice for proximal colon and distal colon, the median score for the distal colon was 0.5 suggesting a heterogeneous increase in crypt length. Crypt length was markedly increased in DSS-treated and untreated Winnie mice (median scores were $>$2) throughout the colon. Crypt elongation

in Winnie was most pronounced in the distal colon segment, with 50% of animals displaying crypts longer than 350 μm in both untreated and DSS groups.

Depletion of goblet cell morphology was completely absent in both untreated and DSS-treated C57BL6 mice. Winnie on the other hand displayed a reduction (median scores $\geq$ 1) in identifiable goblet cells primarily in the mid-colon and distal colon in both untreated and DSS-treated animals. Goblet cell numbers appeared largely unaffected by the Winnie mutation or 1% DSS with median scores of 0.5 and 0 respectively.

Untreated C57BL6 mice displayed a diffuse non-neutrophilic leukocytic infiltrate, with occasional small follicles, consistently throughout the colonic mucosa regardless of segment (median score = 0). The median score for inflammatory infiltrate remained low even after the administration of 1% DSS although a increased scores were more likely in the distal colon (median score of 0.5) of mice following 1% DSS administration. One of these animals in particular, displayed a marked leukocytic infiltration in both the submucosa and mucosa of both mid-colon and distal colon. Neutrophils in the mucosa of the colon were infrequent in the colon of C57BL6 mice, with or without exposure to three cycles of 1%DSS, with an average of $<$5 PMN cells per high-power field (40$\times$ objective). Although average numbers of PMN cells per field were similar to C57BL6 mice in untreated and DSS-treated Winnie mice, Winnie exhibited foci of neutrophilic crypt abscesses and mucosal leukocytic aggregates containing relatively high numbers of neutrophils.

Neutrophilic infiltrates were prominent in mucosal aggregates in mucosa where crypts were attenuated or absent. Tissue damage was generally absent in untreated and DSS-treated C57BL6 mice, however the three-cycle DSS regimen induced infrequent, focal attenuation of the surface epithelium in the distal colon in 2/6 mice and the mid-colon in 1/6 mice. Tissue damage was more frequent in the mid-colon and distal colon of Winnie compared to C57Bl6 mice. Five of the six untreated Winnie mice displayed at least focal attenuation of the surface epithelium, and dilation of the colonic crypts in the distal colon, with a median

score of 1. Following three cycles of 1% DSS the median score was 2, with 8/11 (72%) of mice displaying extensive attenuation of the surface epithelium and glandular dilation. Three of the eleven mice also displayed prominent mucosal erosion due to necrosis of the glandular epithelium in the distal colon. Proximal colonic mucosal damage was in contrast, low, with median scores of 0 for both Winnie and DSS-treated Winnie mice.

Overall, the histopathological changes observed in Winnie differed significantly from that observed in the C57BL6 genotype control groups when the histopathological parameter scores were summed (Fig. 3.5). Cyclic DSS exacerbated the severity of inflammation in both middle and distal segments of Winnie mice relative to untreated Winnie mice, while DSS had only a minor influence on inflammation in the proximal colon (Fig. 3.5).

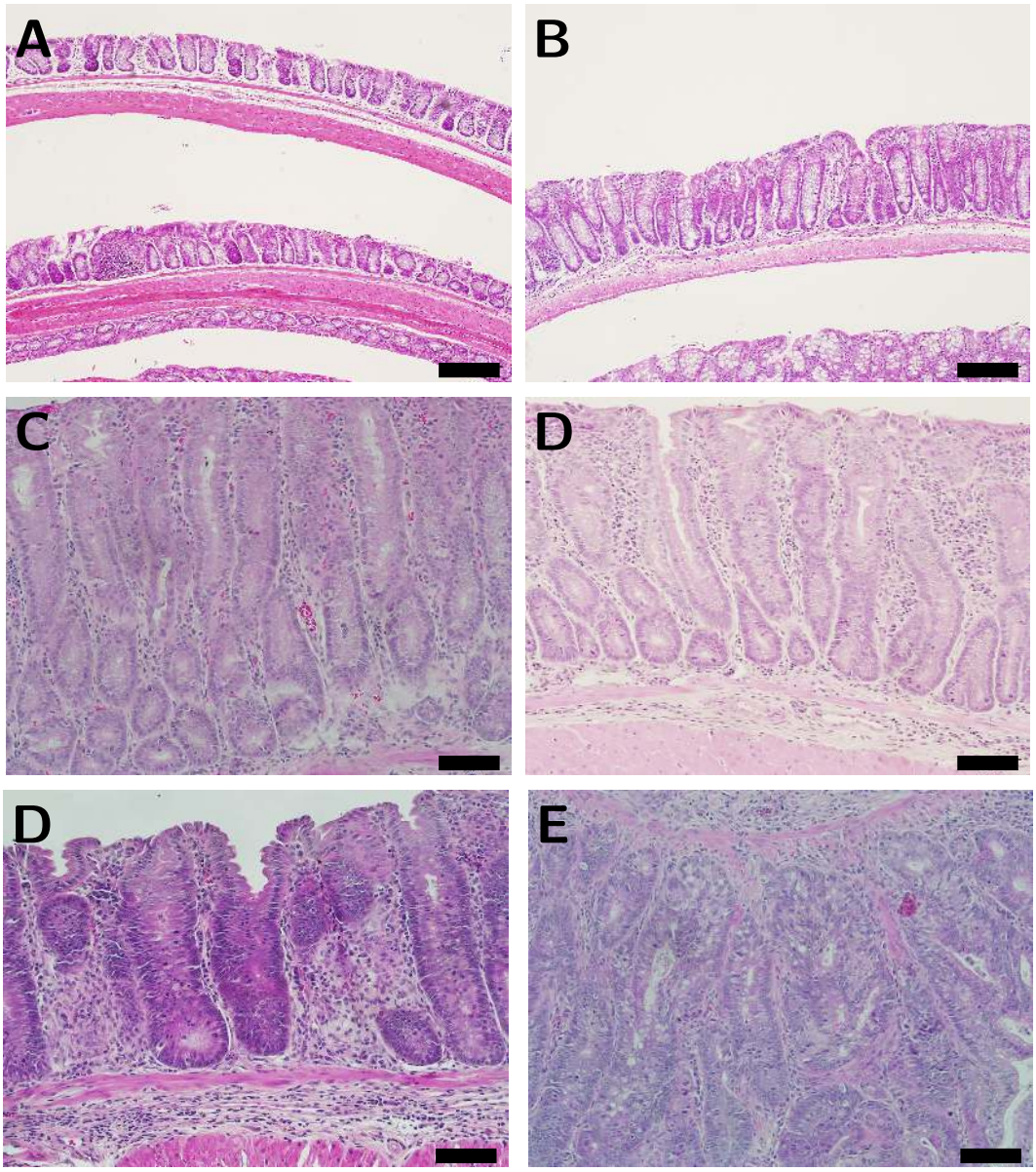

Figure 3.3: **Distal colonic mucosal alterations induced by three cycles of dextran sulphate sodium.** **A**. Representative image of the distal colon obtained from one of four untreated C57BL6 mouse. **B**. C57BL6 distal colon exposed to dextran sulphate sodium (DSS). Image representative of six eighteen week-old C57BL6 mice exposed to three cycles of 1% DSS. **C**. Distal colon of Winnie mouse without exposure to DSS. Crypts are hyperplastic and the mucosa displays an active mucosal inflammation, indicated by the presence of neutrophils among an influx of other leukocytes. **D**. Distal colon representative of Winnie mouse without exposure to DSS. Crypts are hyperplastic and mucosa displays a marked infiltration of leukocytes, including neutrophils. Image representative of six untreated Winnie mice examined. **E**. Distal colon of Winnie mouse displaying colonic hyperplasia and mild focal dysplasia following three cycles of 1% DSS. Mucosa displays features of an active chronic inflammation, with prominent submucosal leukocytic infiltrate. Extensive crypt hyperplasia is visible with a focus of atypical glandular architecture (asterisk). Note the loss of surface epithelium. Numerous mitotic figures are evident. Image representative of the hyperplasia and dysplastic foci total of eleven Winnie mice exposed to three cycles of 1% DSS. All sections stained with H&E, scale bar is equivalent to 100 μm in **A** and **B** and 50 μm in **C**–**E**.

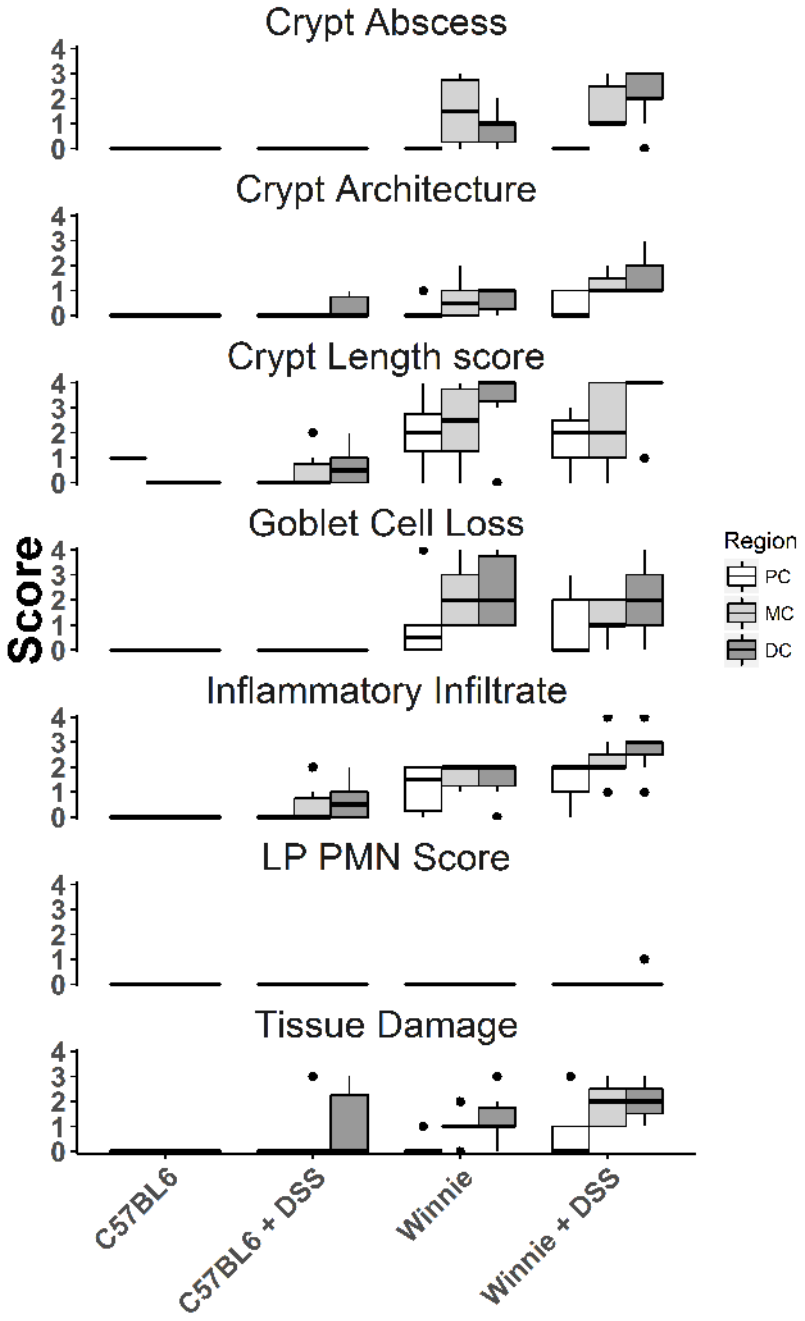

Figure 3.4: **Characteristics of histological inflammation in Winnie following three cycles of 1% DSS** Microscopic changes in the mucosae of both WT and Winnie mice (aged 18 weeks) either untreated, or exposed to three cycles of 1% DSS, were examined.. The number of crypt abscesses, severity of crypt distortion, degree of crypt elongation, extent of goblet cell loss, severity of inflammatory infiltration, numbers of lamina propria (LP) PMN cells and severity of mucosal tissue damage were graded in at least three levels from each animal. Horizontal bars represent median score for each of the groups analysed: untreated C57BL6 (n = 4), C57BL/6 + DSS (n = 6), Winnie (n = 6), Winnie + DSS (n = 11) Boxes represent upper (75th) and lower (25th) percentiles of the data. Whiskers represent (1.58 $\times$ interquartile range).

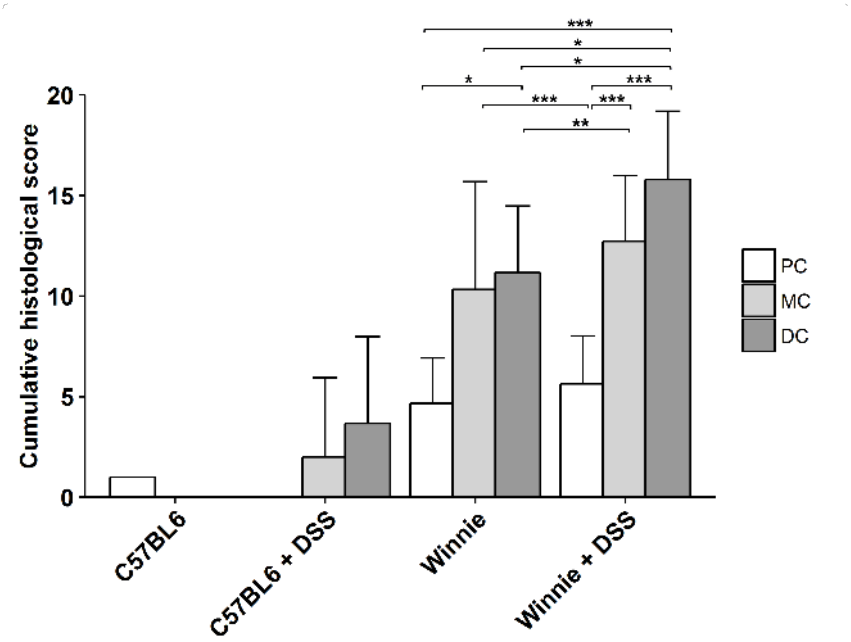

Figure 3.5: **Severity of inflammatory damage in the colon following three cycles of 1% DSS in Winnie.** Histological sections obtained from eighteen week-old mice were scored for inflammatory features in a blinded fashion at three levels at least 50 μm apart for colonic segments (proximal, middle and distal colon). Scores for individual mice at each level were were summed for both control Winnie mice (n = 6) and Winnie mice receiving DSS (n = 11) for each anatomical division of proximal (PC), middle (MC) and distal (DC) colon. Horizontal line indicates median. Summary of summed histological scores presented in Fig. 3.4. Bars represent mean score for each grouping in the experiment. Error bars represent standard deviation (SD). *, P $<$0.05, **, P $<$0.01, ***, P $<$0.001.

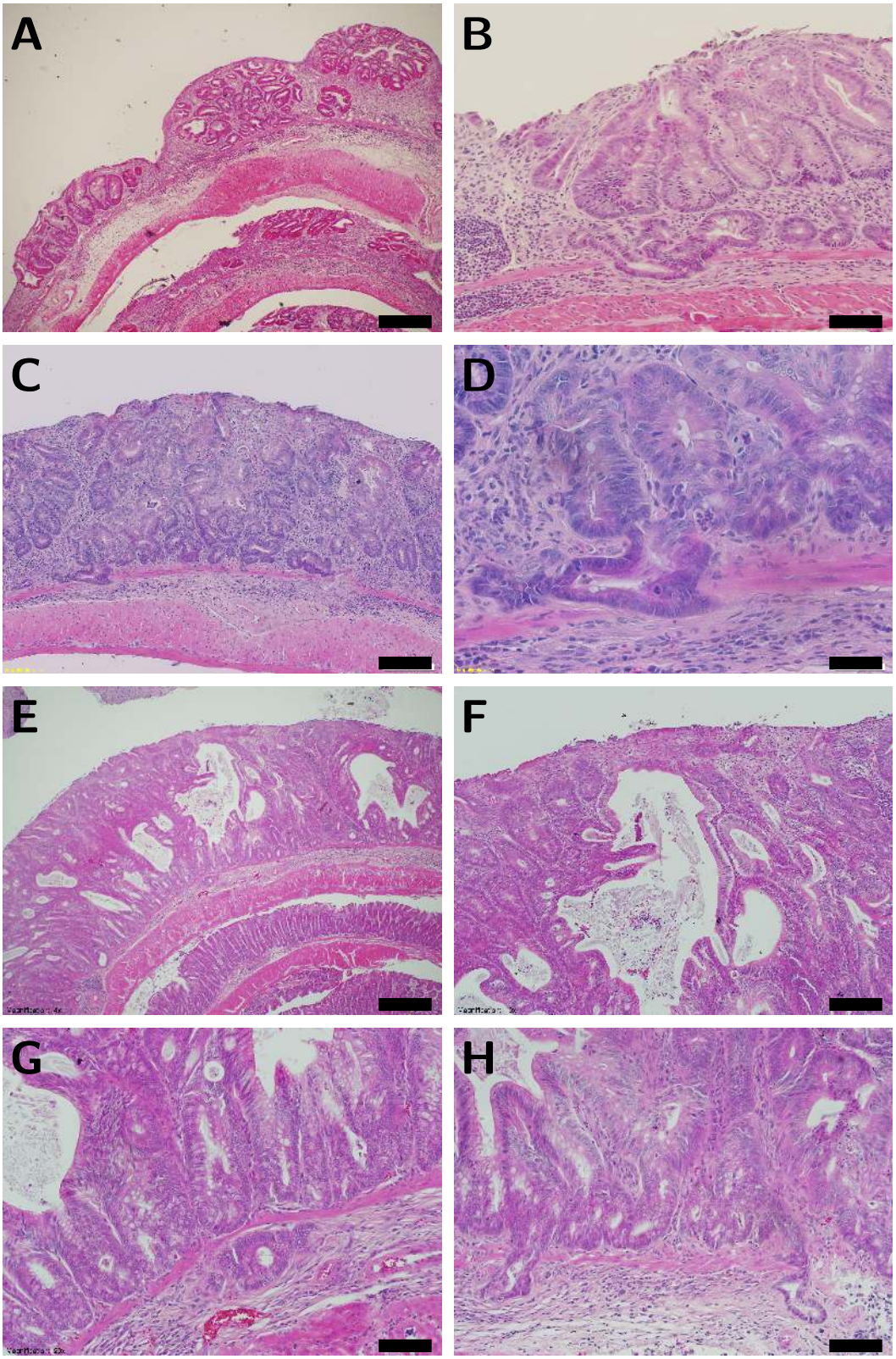
A
B
C
D
E
F
G
H

Figure 3.7: **High-grade dysplasia and submucosal penetration in Winnie.** **A**. Distal colon of Winnie following three cycles of 1% DSS. Mucosa ulceration persists with the mucosa featuring a prominent leukocytic infiltrate with focal extension into the submucosa. Crypts frequently displayed branching, dilation and distortion from the normal straight tubular structure. Instances of distorted glands interconnected the base are visible above crypts misplaced within the submucosa separated by an intact muscularis mucosae.
B. Distal colon displaying branching crypts within inflamed mucosa. A neutrophilic infiltrate is prominent in the mucosal erosion to the left of the regenerating crypts. Mildly distorted, laterally branching gland was visible penetrating a seemingly deformed muscularis mucosae, entering the submucosa. **C**. Winnie distal colonic mucosa after DSS exposure. Distorted and atypical hyperplastic glands (asterisk), with focal infiltration into underlying submucosa through an otherwise intact muscularis mucosae (arrowhead). **D**. Higher magnification of **A**. Atypical mucosal and submucosal glands display relatively bland cytology; nuclear polarity mostly intact, though nucleus:cytoplasm ratio is increased. Mitotic figures are common beyond the crypt base. Region of crypt epithelium displaying loss of nuclear polarity (arrowheads). Note the stroma associated with submucosal glands. **E**. Low magnification image of the mid–distal colon of Winnie with severe mucosal hypertrophy following three cycles of 1% DSS. **F**. Higher magnification of **E** distal colonic mucosa featuring abnormal hyperplastic crypts. Multiple large mucus-containing cysts have formed (M), apparently formed by confluent dilated crypts lined with hyperplastic goblet cells. **G**. Higher magnification of **E**. Crypts displayed back-to-back arrangement associated with high-grade dysplasia. Multi-focal penetration of the muscularis mucosae by the overlying abnormal crypts (arrowheads). **H**. Instance of submucosal crypt penetration in greater detail. Focal penetration of the submucosa by atypical mucosal crypt. Stained with H&E, scale bar represents 100 μm in **B** and **C**, 50 μm in **G** & **H**, 20 μm in **D**. Images obtained from 4/11 Winnie mice exposed to three cycles of 1% DSS.

High-grade lesions were observed in the distal half of the colon in 55% of Winnie mice exposed to DSS but were absent from the colon of untreated Winnie and all wild-type mice (Table 3.8). High-grade crypt lesions displayed the severe architectural distortions such as cribriform (Fig. 3.7A–C) or back-to-back (Fig. 3.7E–H) glandular arrangements associated with colonic dysplasia. In 27% of Winnie mice exposed to DSS, crypt epithelium could be observed within the submucosa underlying apparently dysplastic lesions separated by an intact muscularis mucosae (Table 3.8). Submucosal glands were lined with columnar or flattened cuboidal enterocytes but displayed minimal nuclear atypia (Fig. 3.7). Serial sections demonstrated continuity between abnormal mucosal glands and those in the submucosa. No obvious stromal reaction was associated with the submucosal glands. Notably, submucosal

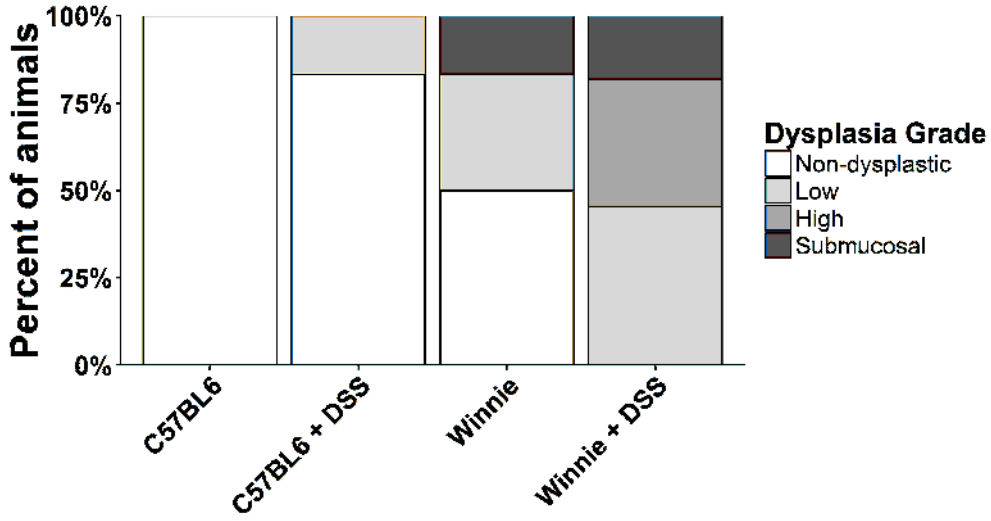

Figure 3.8: **Incidence and severity of dysplasia-like atypia.** The colon of Winnie mice exposed to three cycles of 1% DSS (n = 11) and untreated Winnie (n = 6) was examined for dysplastic change. Untreated C57BL6 mice (n = 4) C57BL6 exposed to three cycles of 1% DSS (n = 6) were included as genotype controls. Lesions were graded as either non-dysplastic, low-grade or high-grade dysplasia and dysplasia with submucosal extension. The maximum grade of lesions observed was recorded for each mouse and the percentage of mice for each combination of treatment and genotype displayed animals The incidence of dysplasia-like lesions in Winnie mice was markedly increased by administration of DSS (Mantel-Haenszel $\chi^2 = 6.667$, $P < 0.01$).

glands were usually observed in close proximity to the submucosal vasculature and mirrored the laterally spreading growth pattern seen in the mucosa.

3.3.3 Mucus staining in the Winnie colon

Alcian blue staining was present in the crypt epithelium of Winnie mice in a vesicular form or external to the cell adjacent to the apical surface of the epithelium, indicating the presence of sulphomucins. Staining with Alcian blue was frequently observed in the absence of staining with the Schiff's-positive material in the epithelial cells of the Winnie distal colon (Fig. 3.9A). Increased co-mingling of sulphomucin and sialic acid/neutral hexose staining occurred in cells appeared to co-incide with a position in the crypt epithelium closer to the surface epithelium. In the inflamed mucosa of the Winnie distal colon however, vesicular staining of the epithelium was markedly reduced (Fig. 3.9B). No obvious shift in the pattern of mucus O-acetylation was observed in Winnie mice regardless of DSS treatment. Following repeated DSS-induced injury, the inflamed mucosa also showed a general depletion of mucosubstances from within the epithelium and the cell surface (Fig. 3.9A).

Crypts penetrating the muscularis mucosae also displayed a visible absence of vesicular staining in the epithelium (Fig. 3.9C-D). In a single case, an abundance of secretory cells, containing mostly vesicles of mixed staining, was apparent within hyperplastic colonic crypts (Fig. 3.9D.

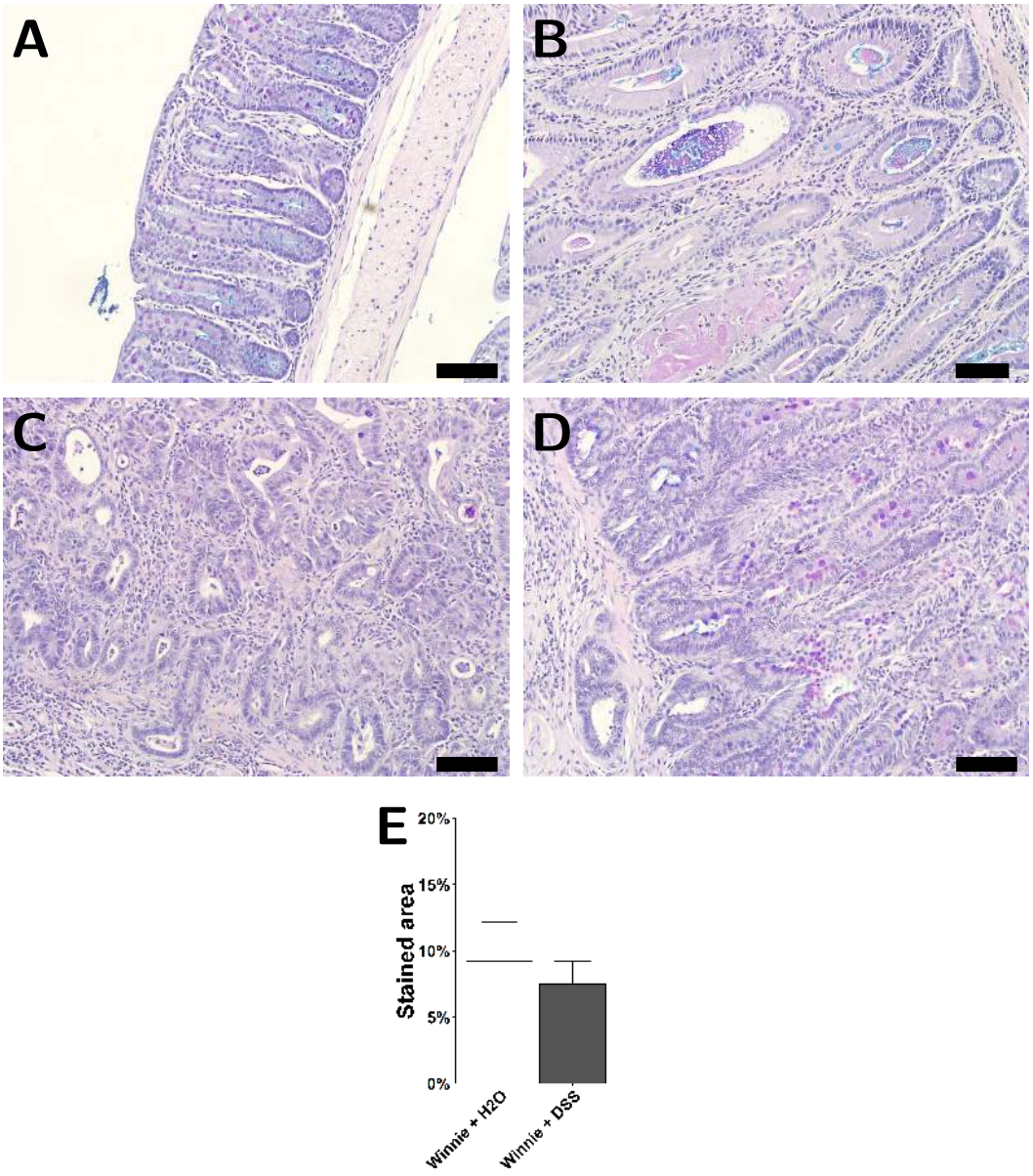

Figure 3.9: **Pattern of mucus in the distal colon of Winnie mice following exposure to three cycles of DSS.** Winnie mice were allowed access to water only or exposed to three cycles of DSS. Sections of colon were stained with Alcian blue and Schiff's reagent following oxidation with periodic acid. **A**. Distal colon of Winnie having received only water for six weeks. **B**. Distal colon of Winnie having received water only. Crypt abcesses are visible. Note the mucus depletion in the involved crypts. **C**. High-grade lesion in distal colon of Winnie having received three cycles of DSS. Note the mucin depletion in the distorted crypts, including those penetrating into the submucosa. While cellular debris can be observed in the crypt lumen, little secreted mucosubstance is visible. **D**. High-grade lesion arising in the distal colon of Winnie exposed to three cycles of DSS. Note the hyperplastic goblet cells containing an increased proportion of sialylated mucin. **E**. Percent of mucosal area (high-power field from 40$\times$ objective) occupied by stained sulphomucins in the distal colon of Winnie. Images obtained from n = 3 for untreated and treated Winnie respectively. Plotted bars represent mean, error bars represent 1 SD from the mean. Scale bar represents a distance of 50 μm.

3.4 Discussion

Due to the absence of colonic tumours reported in Winnie mice of up to 12 months of age, and the relatively low incidence of colonic neoplasia in a similar time-frame, even in the more permissive mixed 129Sv background, we anticipated the need to accelerate carcinogenesis. Further insult to the colon was therefore provided to exacerbate the pre-existing inflammation in the Winnie colon. The distal colon of Winnie mice proved sensitive to exacerbation with a relatively mild insult of 1% DSS and resulted in the loss of only a single animal.

Histological examination of the colon of Winnie mice following repeated exposure of 1% DSS revealed florid reparative lesions with features resembling colonic dysplasia. Consistent with the ability of DSS to permeabilise the inner colonic mucous layer, the distal colon in Winnie mice displayed more severe tissue damage after three cycles of 1% DSS than the same concentration *Muc2* wild-type C57BL6/J mice. Acute administration of 1% DSS produced a colitis characterised by superficial erosion and prominent mucosal inflammatory infiltrates, accompanied by neutrophils, all indicative of an active mucosal inflammation. Much of the DSS-induced tissue damage in Winnie mice remained at the end of the three DSS cycles with areas of mucosal erosion interspersed between regions of hypertrophic mucosa in the distal half of the colon. Therefore 1% DSS was suitable for the induction of extensive distal colonic mucosal damage and repair with only a single mortality. Similar to *Muc2*$^{-/-}$ mice, crypt hyperplasia was frequent in the distal colon of Winnie following three cycles of 1% DSS. The distal colon of Winnie mice that received DSS also displayed foci of abnormal crypt architecture resembling the dysplasia reported after repeated administration of DSS [225, 226]. While DSS appeared to rapidly produce foci of non-polypoid dysplasia in the distal colon of 100% Winnie mice under our experimental conditions, the neoplastic potential of these lesions remains uncertain. The time-frame used in the present study was

considerably shorter than the 120+ days used by Cooper *et al.* and any incident dysplasia in Winnie might therefore be expected to be comparatively less advanced [225].

Penetration of crypt epithelium into the submucosa was observed in 27% of Winnie mice exposed to DSS as opposed to 17% and 0% in the control Winnie group and both C57BL/6 groups respectively. Minimal fibrosis was observed surrounding the laterally spreading submucosal glands and were frequently associated with small breaches of the muscularis mucosae. The close proximity of glands entering the submucosa to blood and lymphatic vessels perhaps suggests that crypts may infiltrate the submucosa through weak points in the muscularis mucosae through which these vessels pass. The penetration of apparently dysplastic crypts into the submucosa raises the possibility of an early invasive carcinoma. A fraction of the abnormal crypts, including those penetrating the submucosa, displayed a lateral branching of the epithelium at the crypt base, extending parallel to the muscularis mucosae. Horizontal growth resulting in ”L” or ”inverted T” shaped crypts, accompanied by bland cytologic morphology, are histological features frequently associated with the pre-cancerous sessile serrated adenomata [258]. Dysregulated epithelial cell growth may contribute to the abnormal crypt architecture associated with the serrated adenomatous lesions. Simultaneously increased proliferation and inhibition of apoptosis has been offered as a mechanism underlying the abnormal crypt morphology within serrated adenomatous lesions [259]. Chronic inflammation of the colon may also promote a comparable dysregulation of epithelial homeostasis in UC [260]. Elongated laterally growing crypts may therefore arise in response to colitis, their branching perhaps permitting the re-population of the glandular mucosa after crypt loss. If however, oncogenic mutations such as those in *Trp53* exist within the regenerative epithelium this lateral spread may permit the rapid expansion of dysplastic or cancerous cells, an effect termed ”field cancerisation” [261].

Identification of early invasive carcinoma in the context of a chronic colitis is complicated by the co-existence of similar morphological characteristics in non-neoplastic epithelium. Repeated insult using DSS produced the florid inflammatory hyperplasia, some of which

displayed dysplasia and infiltration into the submucosa. Diverticular penetration of colonic crypts, such as that occurring in colitis cystica profunda, although uncommon, is observed at a higher frequency in patients with UC. Allen *et al.* reported that in patients with IBD who exhibited no evidence of dysplasia, the misplaced colonic crypts were composed of non-dysplastic epithelium [262]. Conversely, misplaced epithelium was dysplastic in 82% of patients with neoplasia arising from UC. Thus, penetration of crypts into the submucosa even when dysplastic crypts are involved, may occur independent of any neoplastic process. Mechanisms explaining the occurrence of the glandular profunda in colitis are not well-understood. It is possible that during tissue repair following acute inflammation, the regenerative epithelium either expands into an ulcerated submucosa, or is forced through the muscularis at points where lymphatics or by infolding of a hyperplastic polyp. Deep ulceration and abscesses may also permit access of dysplastic glandular epithelium into the submucosa which may persist while the dysplastic mucosa above regresses. Occasionally herniation of colonic crypts into submucosal lymphoid tissue was observed in animals exposed to DSS, which we labelled glandular profunda. Glandular profunda, despite their dysplastic appearance and the discontinuity of the overlying muscularis mucosae, have no recognised neoplastic potential and are thus discounted from any diagnosis of invasive carcinoma [263].

Several characteristics of invasive carcinoma have been identified that distinguish carcinomas from glandular profunda/diverticula/herniation [263]. To classify a suspect lesion in animal models of intestinal cancer as carcinoma, the presence of several histological features should be examined. The first is a higher grade of nuclear atypia than the overlying mucosa, i.e. an invasive gland with high-grade dysplasia beneath a low-grade dysplastic mucosa [263]. Mucosal herniation is not typically associated with a desmoplastic reaction, especially one without a prominent inflammatory cell infiltrate [263]. Non-neoplastic epithelium penetrating into lymphoid tissue also displays a dysplastic morphology, and therefore it is easier to distinguish herniation from invasion in the absence of prominent inflammatory cell

infiltration. In keeping with their dysplastic phenotype, invasive glands are more likely to be of a sharp angular or irregular shape. Significant cell loss and the presence of cellular debris exudate in the crypt lumen may also suggest the presence of carcinoma. In the case of mucosal herniation the gland is displaced into the submucosa along with the lining basement membrane whereas invasive glands do not. While the abnormal glands in Winnie following three cycles of DSS display dysplasia-like architecture, occasionally luminal debris, the nature of the surrounding connective tissue was not easily discerned.

Mucus production in the colonic epithelium is altered in both inflammation and in colonic tumours. Colonic goblet cells in Winnie mice displayed focal reduction in intracellular mucins stained by either Alcian blue or PAS. Severe mucin depletion was observed more frequently in the distal colon Winnie mice following three cycles of 1% DSS in crypts displaying a dysplastic morphology. Mucin-depleted crypt foci have been offered as a very early precursor to colonic adenocarcinoma initiated by azoxymethane [264]. While mucin depletion may be indicative of a neoplastic transformation in the azoxymethane model where the colon is uninflamed and mutations in β-catenin are frequent, the significance of mucin depletion in the abnormal crypts in the chronically inflamed Winnie colon is less certain. Besides mucin depletion, mucin production in the neoplastic colonic epithelium appears to shift from the secretion of heavily O-acetylated mucus to non-O-acetylated mucus [265]. Changes in O-acetylated sialomucins may be detected using the mPAS method, which in Winnie labelled crypt foci where non-O-acetylated sialomucins were increased while sulphomucins decreased. While the mucosa in most Winnie mice displayed a general reduction in mucus-containing cells, goblet cell hyperplasia was observed in a single animal. In addition to the aforementioned mucus alterations in Winnie, goblet cell hyperplasia was also on display in the colon of a single animal after exposure to three cycles of DSS. Observation of a goblet cell hyperplasia is in agreement with the resistance of the colonic goblet cells to apoptosis in the Winnie colon [250]. Goblet cell hyperplasia has similarly been reported in patients with UC and CD, and also adjacent to neoplasia in patients with

either UC or CD [266, 267]. Due to the unusual morphology of goblet cell hyperplasia, their potential as neoplastic precursors has been investigated. Total colectomy specimens studied by Lee *et al*. identified goblet cell hyperplasia adjacent to the colonic adenocarcinoma in 80% of cases [268]. Goblet cell hyperplasia in CD were frequently shown to display p53 over-expression when adjacent to carcinoma [267]. Since excessive p53 protein is associated with dysplasia and carcinoma, it is plausible that goblet cell hyperplasia may precede dysplasia and carcinoma in the chronically inflamed colon.

3.5 Conclusion

Exacerbation of colitis over three cycles of 1% DSS in Winnie mice with impaired colonic mucin secretion produced extensive mucosal hypertrophy in response to inflammation. Abnormal, dysplasia-like crypt foci were present within the hyperplastic mucosa and in several instances penetrated into the submucosa. Study of later time-points post-DSS administration would provide evidence as to whether laterally spreading crypts infiltrating the submucosa underlie the rapid progression of colitis-associated neoplasms. Additionally, markers of abnormal cellular proliferation or apoptosis may be useful in determining the neoplastic potential of these lesions.

CHAPTER 4

EFFECT OF EXTENDED DSS ON THE INDUCTION OF COLONIC NEOPLASIA IN WINNIE

4.1 Introduction

At present the most reliable model for simulating neoplasia arising from the chronically inflamed colon involves the administration of azoxymethane (AOM) and subsequent dextran sulphate sodium (DSS) [269]. While the AOM-DSS protocol provides a model for studying colonic neoplasia driven by colonic inflammation, it relies upon the induction of carcinogenesis primarily through specific mutations in the β-catenin and Kras pathways [270, 271]. In contrast, the Winnie mutation provides a potentially unique starting point for the initiation of neoplasia. How the presence of ongoing goblet cell ER-stress in addition to the primary defect in the colonic mucous barrier influences carcinogenesis in the large intestine is a question that is largely unexplored.

Carcinogenesis is a time-dependent process and is thus sporadically occurring carcinoma is most typically observed in elderly animals. Inflammation appears to accelerate carcinogenesis associated with mutations acquired subsequent to exposure to potent genotoxic carcinogen such as AOM [272, 273]. A single injection of AOM (10mg/kg) followed by oral administration of 2% DSS for seven days has been shown to be sufficient to produce colonic, adenomatous neoplasia in 100% of animals (outbred, male ICR mice), within 20 weeks [272].

While such a protocol induced a rapid onset of colonic neoplasia with high incidence in ICR mice, C57BL6/N mice proved less susceptible to colonic neoplasia, correlating with their increased resistance to DSS-induced colitis [273]. The comparative resistance of C57BL6 to colonic neoplasia may be overcome by simply increasing the number of DSS cycles thereby increasing the incidence of neoplasia to 100% [269]. Similarly, when using DSS alone, incidence and time until onset of neoplasia will likely be dependent on the duration of colitis, i.e. the number of DSS cycles, and the interval between DSS administration and examination.

Administration of DSS alone appears to be capable of inducing colonic dysplasia, producing a varied morphology reminiscent of the colitis-associated dysplasia observed in patients with UC [225]. Duration of colitic disease would thus be expected to increase the incidence of neoplasia in Winnie. However, the incidence and time required for any colonic neoplasia in Winnie is unknown. The incidence of dysplasia or neoplasia naturally within the colon of Winnie mice has yet to be reported in mice up to one year-old [250]. While three cycles of 1% DSS appeared to induce epithelial dysplasia in the distal colon of all Winnie mice, submucosal crypts were uncommon and if genuinely invasive, in the early stages of growth. Definitive invasive carcinoma however, was not observed and thus additional cycles of 1% DSS may allow for further neoplastic progression in the colon. In addition to the number of DSS cycles, the time allowed until the colon is examined is another factor which will determine incidence and severity of any detected neoplasms. For example the incidence of cancer in outbred Swiss-Webster following four cycles DSS was increased by 15% if post-mortem examination was delayed by 120 days [225].

Under our conditions, three cycles of DSS were tolerated by Winnie mice with minimal mortality. It was assumed that additional cycles (seven days DSS, plus 7 days H_2O) may be similarly tolerated without significant mortality. Extending the duration of both the severe DSS-induced insult, and allowing a longer period of time following DSS administration should therefore allow colonic dysplasia in Winnie to progress to a more advanced stage.

The decision was made to increase the DSS regimen from Chapter 3 by another two DSS cycles (seven days of 1% DSS, seven days of drinking water), an additional month of DSS administration to exacerbate the damage to the colonic epithelium.

4.1.1 Hypothesis

We hypothesised that five cycles of 1% DSS administration would increase the incidence of carcinoma in the distal colon of Winnie mice, relative to three cycles of DSS.

4.2 Results

4.2.1 Clinical observations

To test the ability of DSS to induce neoplasia in the colon of Winnie mice, a group of twelve week-old Winnie mice were exposed to a cyclic 1% (w/v) DSS regimen of five cycles length (n = 8), whereas a control group of mice (n = 7) received only autoclaved tap water (Fig. 4.1).

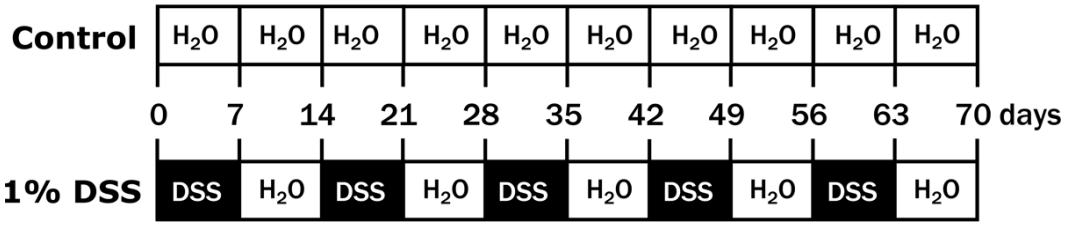

Figure 4.1: **Protocol for exacerbation of colitis using dextran sulphate sodium.** All mice were approximately twelve weeks of age at the beginning of the experimental procedure. A solution of 1% (w/v) DSS dissolved in autoclaved tap water was administered through the drinking water for a period of seven days. A period of seven days of DSS administration followed by seven days recovery period where mice received drinking water only, was considered to constitute a single cycle. Five cycle DSS regimen where Winnie mice (n = 8) were exposed to a DSS regimen of three cycles length, while a control group of mice (n = 7) received only autoclaved tap water. Mice were killed at various time-points during and up until 190 days had passed since the beginning of the first DSS cycle.

Mice were monitored throughout the experimental protocol for the external manifestations of colitis and general morbidity. Individual Winnie mice displayed recurrent episodes of a mild, non-watery diarrhoea consistent with a mild colitis. Winnie mice displayed the more

severe symptoms of rectal bleeding, weight loss and diarrhoea after the commencement of each DSS cycle, persisting until DSS administration ceased. Individual Winnie mice from both the control group and DSS-treatment group developed visible rectal prolapse throughout the course of the experiment, necessitating their euthanasia. Four of seven (57%) Winnie mice from the control group were euthanased within 56 days after the commencement of DSS administration. Two of three cage-mates allocated to the control group were euthanased due to excessive weight loss within 24 hours. Necropsy of these two animals revealed intussusception involving the terminal ileum, proximal colon and part of the caecum (Fig. 4.2A). The intussusception in both cases resulted in total occlusion of the colon and was associated with an expansion in the size of the caecum (Fig. 4.2B).

Since such a large number of intussusception/prolapse cases occurred in the control group, we conducted a Mantel-Cox analysis to determine if DSS was associated with protection from intestinal intussusception or rectal prolapse. When cases of euthanasia due to intussusception and prolapse in Winnie mice were considered together, survival analysis indicated that there was no difference in survival between treatment groups ($\chi^2 = 3.30$, $P = 0.069$; Fig. 4.3).

The unexpected mortality in the control group made comparisons between untreated Winnie mice with Winnie mice receiving the five cycles of 1% DSS. Only Winnie mice receiving drinking water displayed a trend toward increased weight gain with age (Fig. 4.4). Coinciding with symptoms of severe colitis, e.g. rectal bleeding, Winnie mice receiving five cycles of DSS displayed a similar pattern of weight loss recorded in mice receiving three cycles of DSS. Weight loss occurred approximately 1–2 days after commencement of DSS administration and persisted for several days afterward before weight gain was observed again.

4.2.2 Histopathology

To determine the extent of histomorphological changes in the colon of Winnie mice following repeated DSS-induced inflammation, sections of H&E-stained colon were examined

Figure 4.2: **Intussusception of the caecum, small intestine and colon in Winnie. A**. Gross morphology of the undissected colon from a euthanased Winnie mouse. Note the "ballooning" of the oral end of the colon and the discolouration of the caecum and anal end of the enlarged proximal section. **B**. Partially dissected colon from **A**. demonstrating the total obstruction of the colon caused by telescoping of the proximal colon and ileum within the distal colon.

microscopically. Histological analysis of the two cases of intestinal intussusception revealed an ischaemic inflammation was present in the mucosa and submucosa consistent with the restricted blood flow to the in-folded intestine (Fig. 4.5A-B).

Histological analysis of the colon immediately after repeated administration of 1% DSS for a total of four cycles revealed an abnormal regenerative crypt morphology in the single animal examined. Consistent with an ongoing active inflammation, neutrophilic infiltration was visible and often accompanied by crypt branching, distortion and hyperplasia in the distal and middle colonic segments (Fig. 4.6A). Dysplasia-like lesions in the distal half of the colon were not detected. The single animal killed 14 days after the end of the fifth DSS

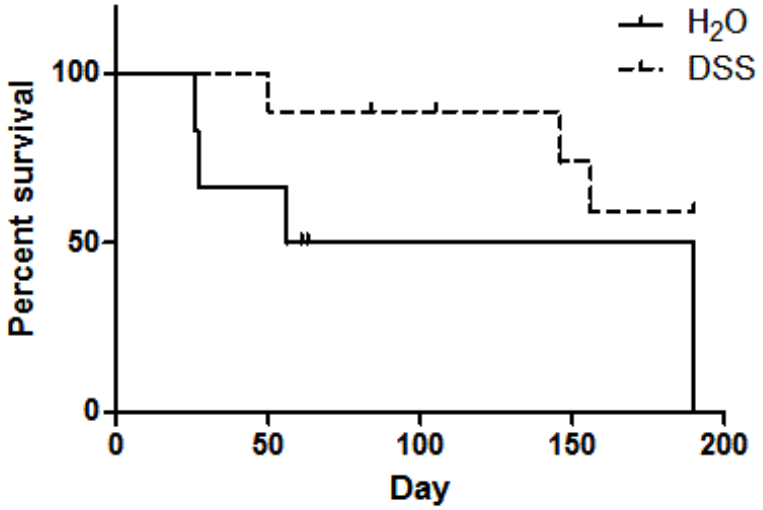

Figure 4.3: **Survival of Winnie mice from intussusception/prolapse of the colorectum.** Survival analysis of euthanasia due to rectal prolapse or colonic intussusception in Winnie mice. Winnie mice from the control group (H_2O; n = 7) were compared to Winnie mice receiving cyclic administration of 1% DSS (n = 8). Vertical bars represent censored events (deaths due to other causes).

cycle still displayed the characteristic crypt hyperplasia in the background of a prominent mucosal leukocytic infiltrate (Fig. 4.6B). Mild crypt distortion was evident along with crypt fission in the inflamed distal and middle colonic mucosa. Analysis of a single animal after the five cycles of 1% DSS displayed only mild distortions of the glandular architecture and a modest crypt hyperplasia in the distal colon indicative of a return to the mild colitic Winnie phenotype (Fig. 4.6C). By the age of 38 weeks (120 days since cessation of the fifth DSS cycle), mice displayed the histological features of a mild colitis similar to that observed in Winnie without repeated exposure to 1% DSS (Fig. 4.6D). The mucosa displayed a moderate level of leukocytic infiltration into the mucosa of the distal and middle colonic regions. Crypt architecture appeared mostly normal, with only occasional distortion and mild elongations.

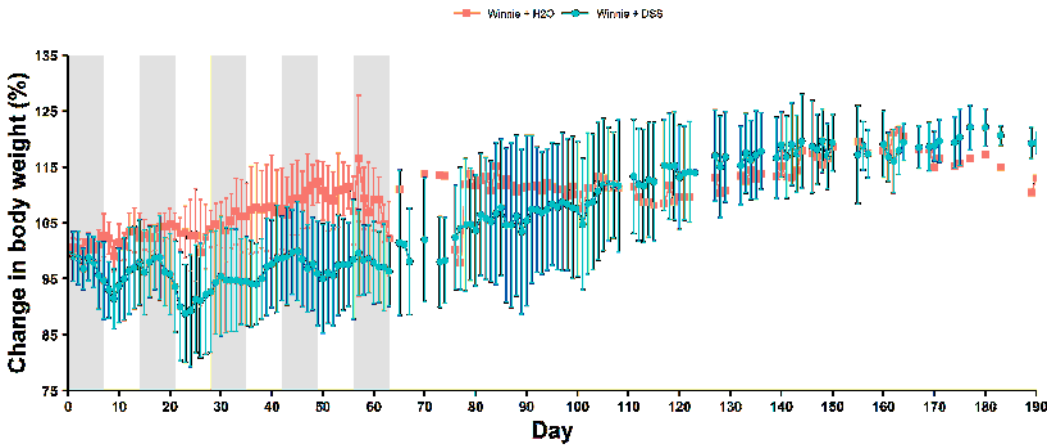

Figure 4.4: **Body weight change in DSS-induced colitis Winnie mouse.** Daily change in body weight of Winnie mice during the five cycle DSS regimen. Body weight was recorded each day and recorded as percentage change from the starting body weight prior to commencement of the experiment (day 0). Each point represents the mean percentage change in body weight relative to the initial body weight. Error bars depict standard deviation (SD) from the mean. Grey vertical bars identify the seven day period during which DSS solution was administered.

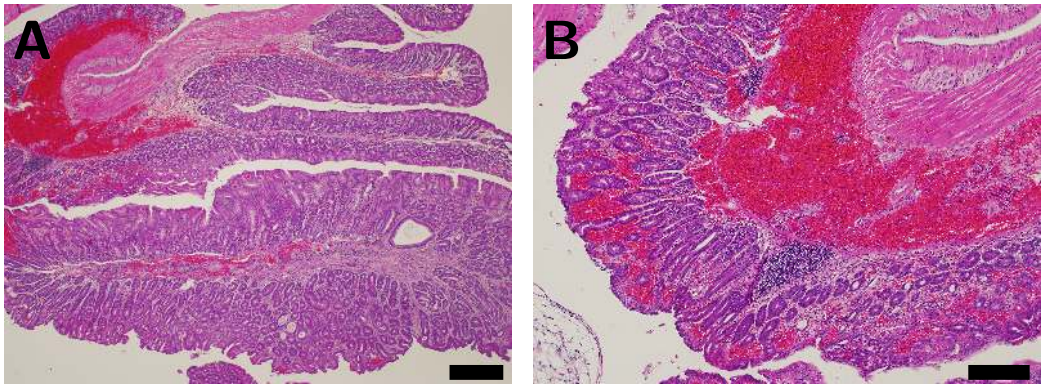

Figure 4.5: **Representative histopathology of intestinal intussusception in untreated Winnie mice. A**. Low-magnification field showing invagination of the villous ileum (top of the image) within the colon (bottom of the image). Ischaemia is present in both small and large intestine, but most prominent in the compressed segment of the intusscepted ileum. **B**. Higher magnification of **A** showing detail of the in-folded small intestine/caecum. Lymphocytic aggregates and neutrophils have accumulated in the mucosa and crypts show a mild structural distortion. Submucosa is expansive with high volume of bleeding visible. Stained with H&E. Scale bar represents 100 μm in **A** and 50 μm in **B**.

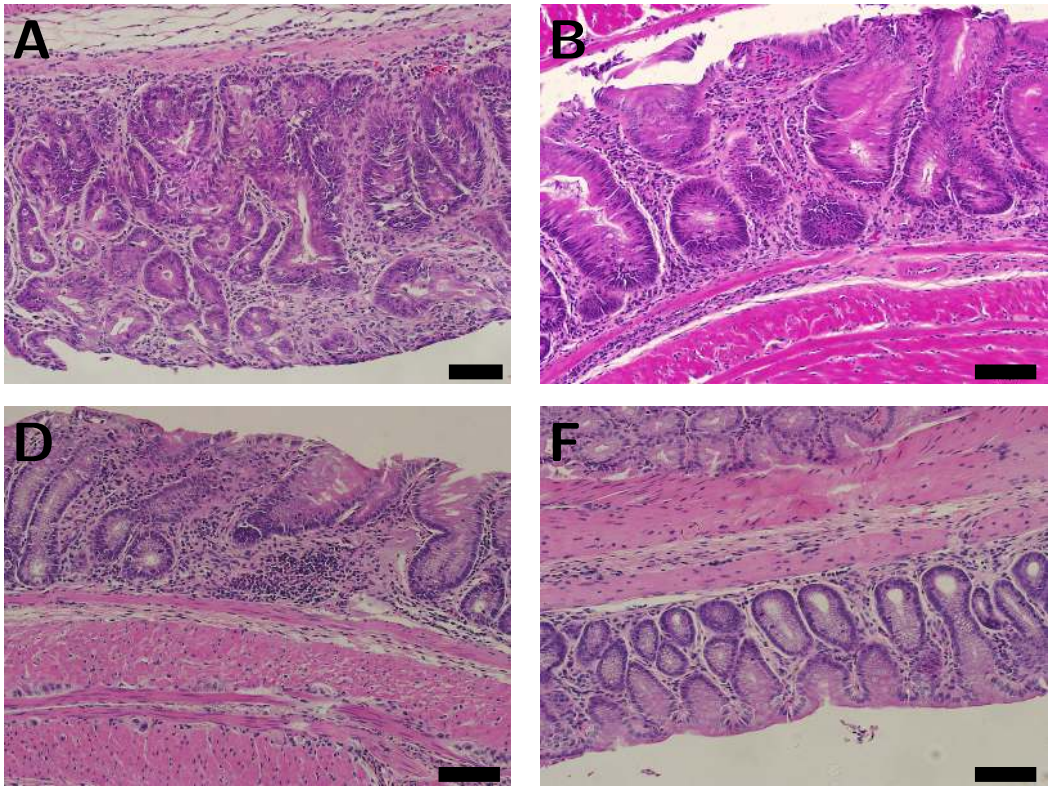

Figure 4.6: **Histological changes in the colon of Winnie after extended cycles of DSS.** **A**. Histology of the Winnie colon aged 20 weeks, immediately after the end of the fourth DSS cycle. Note the hypertrophic mucosa containing distorted crypts. **B**. Distal colon from Winnie at the age of 24 weeks, 14 days after cessation of the five-cycle DSS regimen. Crypt epithelium displays marked distortion of the normal glandular architecture, reduced mucin production and displays elongated basal nuclei with frequent mitotic figures. **C**. Histology representative of the distal colon from Winnie mouse aged approximately 24 weeks, 86 days after cessation of the five-cycle DSS regimen. Marked inflammatory infiltrate present with crypt distortion and elongation. Dysplastic-like lesions were absent from the colonic mucosa. **D**. Distal colon from Winnie mouse aged approximately 38 weeks, 120 days after cessation of five-cycle DSS regimen. Colonic mucosa approaching normal crypt length and architecture with only a mild inflammatory infiltrate in the mucosa and submucosa. Stained with H&E. Scale bars represent a distance of 50 μm.

4.3 Discussion

Since we observed an increased incidence of dysplasia-like crypt foci in the Winnie distal colon following three cycles of 1% DSS, we planned on a five cycle-long DSS regimen with the aim of producing more advanced dysplasia. Here we describe the histopathological effects observed in the colon of Winnie twelve week-old Winnie mice over the course of

190 days. Histologically, the pathology induced in the distal colon by five cycles of 1% DSS was not remarkably different from that induced by three cycles of 1% DSS.

Occurrence of rectal prolapse is a relatively uncommon complication arising in mice due to inflammation of the colorectum, such as in enterohepatic *Helicobacter* or *Campylobacter* infection [69, 274]. Increased incidence of rectal prolapse is observed in *Il10*$^{-/-}$ and lamellipodin-deficient mice, suggesting that rectal prolapse occurs secondary to an immune defect permitting bacterial colonisation [69]. Subsequently, lamellipodin-deficient mice have been shown to be prone to carcinoma of the rectum and the affected segment appears vulnerable to prolapse [72]. Adenocarcinoma of the distal colon induced by AOM and DSS similarly increased the incidence of prolapse in outbred ICR mice [272]. Similar to *Il10*$^{-/-}$, Winnie mice are prone to the development of rectal prolapse, with up to 25% of animals developing rectal prolapse after reaching 12 months of age [250]. Similar initiating factors to those involved in intestinal intussusception have been suggested to precipitate rectal prolapse. Intestinal intussusception of the human adult intestine is a rare event when compared to the number of juvenile cases [51]. While the majority of paediatric intussusception cases are considered idiopathic, though some cases may be induced by rotaviral or bacterial infection [52], adult intestinal intussusception typically occurs secondary to pre-existing pathology [51]. Benign and malignant polyps, carcinomata, strictures and diverticula, may all serve as lead points for invagination of a proximal segment of the bowel into the lumen of the distal bowel [51]. Through the induction of inflammation through the intraperitoneal injection of bacterial LPS, Nissan *et al.* were able to induce intussusception involving either small or large intestines in 26% of adult BALB/c mice [275]. Supporting the theory that inflammation precipitates intussusception in the adult intestine, blocking the effects of TNF-α or NO reduced the incidence of intussusception, while increasing available NO precursors increased the incidence of intussusception. Notably, strain effects modify the incidence of intussusception induced by LPS in mice. The C57BL/6 strain demonstrate considerably higher resistance to LPS-induced intussusception than the BALB/c strain and

the outbred ICR strain [276]. Both BALB/c and C57BL/6 mice were shown to produce similar levels of pro-inflammatory TNF-α, IL-6 and NO in response to LPS suggesting that the basis of susceptibility to intussusception may not be due to differences in immunological responses to LPS [276]. Given that inflammatory, and a variety of other non-neoplastic and neoplastic lesions increase the incidence of intestinal intussusception, it might be expected that exacerbation of chronic inflammation in Winnie using DSS would promote intussusception. Unexpectedly, all cases of intussusception in Winnie mice occurred in co-housed litter-mates which were assigned to the control group and thus never received DSS at all. While an inflammation of the distal colon would still have been present in untreated Winnie, no obvious lesions that could be considered to act as a lead-point for the intussusception could be identified histologically.

The occurrence of complicating intestinal intussusception in Winnie, involving either ileum-proximal colon or prolapse of the rectum, may arise as a consequence of neuromuscular perturbation. A hypothesised neuromuscular defect preceding the occurrence of intestinal intussusception is supported by animal models [275]. Inhibition of smooth muscle contraction by $MnCl_2$ co-incided with an increased incidence of intussusception regardless of the employed mouse strain [276]. The relative resistance of C57BL/6 mice to LPS-induced intussusception may therefore be explained by the co-inciding hyper-contractile response when compared to BALB/c mice. The occurrence of intestinal intussusception and prolapse in Winnie could also be attributed to defects in the intestinal motility of these animals. Study of the colonic innervation in the chronically inflamed Winnie colon has identified reductions in cholinergic, noradrenergic and sensory neuronal nerve fibres relative to wild-type C57BL/6 [277]. The prolapsed rectal mucosa in Winnie displays further reduction still in smooth muscle innervation. Decreases in inhibitory motor neurones and cholinergic nerve fibres in particular were associated with rectal prolapse [71]. Investigation into the contractile activity of the distal colon in Winnie has explained some of the functional effects of the neurological damage previously reported in Winnie. Decline in the density of intact

colonic cholinergic nerve fibres corresponds with a decreased amplitude of colonic excitatory junction potential and reduced smooth muscle contraction in response to cholinergic stimulation [278]. Simultaneously, inhibitory neurotransmission into the smooth muscle of the distal colon in Winnie was diminished. Purinergic neurotransmission was decreased, particularly the fast component of the inhibitory junction potential in the smooth muscle of the Winnie distal colon relative to C57BL/6 [278]. Additionally, distal colonic smooth muscle in Winnie mice was resistant to NO-induced relaxation relative to C57BL/6 mice, despite equivalent numbers of nNOS-expressing inhibitory motor neurones present in both Winnie and the wild-type [277, 278]. Some of these changes in neurotransmission within the distal colon can be explained the presence of a local inflammation. For example, purinergic transmission is impaired in the colon of mice following administration of DSS, likely due to an inflammation-induced inhibition of purine synthesis and transport [279]. Similarly, the distal colonic smooth muscle in *Il10*$^{-/-}$ mice displayed an absence of a relaxation in response to nitrergic signalling [280]. The source of the defect in nitrergic neurotransmission in Winnie however requires further investigation. Though they were not analysed in the present study, changes to the musculature of the distal colon and rectum have also been observed in Winnie. Hyperplastic thickening of the muscularis externa in the distal colon of 12–16 week-old Winnie is likely consistent with the ongoing inflammation [278]. Further thickening of the rectal muscularis externa by approximately four-fold has been observed in Winnie with rectal prolapse relative to Winnie without prolapse [71]. However, the presence of exacerbated histological damage associated with the prolapse makes it uncertain as to whether the thickening occurs as a result of inflammation secondary to the prolapsed tissue. Generation of ROS/RNS may produce dysfunction in DNA repair enzymes, and induce genetic mutation in the DNA of epithelial cells may explain the relationship between duration and severity of colitis. Studies utilising cyclic administration of DSS in mice have demonstrated that the incidence of dysplasia and cancer is related to the severity of inflammation. Cooper *et al.* reported an association between dysplasia and carcinoma and

high grades of histologic inflammation [225]. If animals were killed immediately after the end of the four cycles of 5% DSS the incidence was approximately double that observed if mice were examined 120 days after the four DSS cycles (204 days in total). Winnie mice exposed to five cycles of 1% DSS displayed the dysplasia-like phenomenon in the distal colon similar to that observed after three cycles. However, the histological examination of Winnie mice killed at time-points up until 120 days after the end of the five-cycle experiment, revealed a regression in the complexity of the abnormal crypts. At 120 days after the end of the five-cycle experiment, when mice were approximately 39 weeks-old the incidence of dysplasia-like lesions was low. Considering that the morphology of dysplasia-like lesions appeared to be less severe in animals which had experienced the longest period of recovery post-DSS, it is possible that these lesions are of non-neoplastic origin. It should be noted however, that colonic tumours initiated by DSS alone occur at a low frequency. Although an tumour incidence of 37.5% was reported in outbred Swiss-Webster mice 120 days after four cycles of DSS, a similar DSS regimen produced an incidence of 12.5% C57BL/6 mice [225, 235]. While DSS alone, or the resulting colitis, has been shown to initiate neoplasia in the absence of tumourigenic genetic mutations, long-term exposure is required and the incidence of neoplasia is relatively low.

The addition of AOM to the DSS-induced colitis provides a reproducible model of colitis-driven colonic neoplasia with a short duration from administration to tumour onset. One advantage to using the AOM-DSS model is that the progressive, pre-neoplastic change in the histology of the colonic mucosa has been studied in detail.

In a time-course study of AOM-DSS in ICR mice, adenomatous tumours could be identified in 40% of mice as early as the third week after AOM administration [273]. Tumour incidence increased rapidly, increasing to 100% of mice by the sixth week from AOM administration. Adenocarcinoma was identifiable early, detectable within the colons of 40% of animals. Similar incidences of neoplasia are also observed in BALB/c mice, though the incidence of neoplasia in C57BL/6 mice is considerably decreased despite using the same

protocol [273]. Considering that the C57BL/6 strain are among the mouse strains known to display resistance to colonic carcinogenesis, use of AOM-DSS or even AOM alone, in Winnie would be informative [263].

The earliest observed lesion preceding AOM-induced adenomatous tumours is the ”aberrant crypt focus” (ACF). Expansion of the ACF is thought to occur through crypt fission, by which clusters of abnormal crypts are formed. Expansion of ACF via the process of crypt fission is likely to be facilitated by the mucosal ulceration induced by DSS. Regenerating mucosa adjacent to ACF may allow abnormal crypts to rapidly spread laterally through the mucosa. Identification of ACF may be performed by examination following staining with methylene blue, however this was not performed.

Under the assumption that the *Muc2* mutation in Winnie had no effect on colonic tumourigenesis, and given the small number of mice which survived to 38 weeks, it might be reasonable to see few Winnie animals displaying neoplasia. While the C57BL/6 strain is relatively resistant to the induction of colonic inflammation and neoplasia by DSS, defective Muc2 secretion was expected to render Winnie mice susceptible to colonic neoplasia similar to total Muc2 abrogation [99]. Since an increased number of DSS cycles has been shown repeatedly to accelerate the onset of neoplasia, we assumed that the duration required to observe the incidences of neoplasia (68% by twelve months) reported by Velcich *et al.* was due to the low-level of inflammation present in *Muc2*$^{-/-}$ animals [99]. While further experiments utilising larger cohorts of mice are necessary to obtain more accurate evidence for the rate of neoplastic progression in the severely inflamed Winnie colon, this experiment raises the possibility that the Winnie *Muc2* mutation suppresses tumourigenesis.

4.4 Conclusions

While prolapse of the rectum is a known complication of the Winnie mutation, intestinal intussusception has to our knowledge, not previously been reported in Winnie. Despite the association between rectal prolapse and the Winnie phenotype, more severe colitis

induced by repeated DSS administration did not appear to influence the rate of prolapse and intussusception. Foci of abnormal crypts were observed within the distal half of the colon in Winnie after repeated administration of 1% DSS but were absent from control Winnie mice. Crypt derangement however, may be a transient phenomenon, with mice displaying little evidence of dysplasia-like crypts 120 days post-cessation of the cyclic DSS protocol.

CHAPTER 5

INVESTIGATION OF MOLECULAR PATHWAYS REGULATING TRANSITION FROM COLITIS TO DYSPLASIA

5.1 Introduction

Detection of early dysplasia within the chronically inflamed colon, is difficult due to the morphological similarities between dysplastic and regenerative epithelium. Since certain molecular changes in neoplastic precursor cells are likely to precede the manifestation of obvious morphological abnormalities, detection of these changes may aid in the identification of early dysplasia in IBD.

The most obvious feature common to both regenerative and dysplastic epithelium is that of abnormal proliferation of the crypt epithelium. Several investigators have assessed the validity of discrimination between regenerative changes and genuinely neoplastic transformations using the pattern of cellular proliferation in the colonic epithelium. Two markers of cell proliferation in particular have been studied in colorectal neoplasia, the nuclear proteins Ki67 and proliferating cell nuclear antigen (PCNA). The monoclonal anti-human Ki67 antibody (clone MIB-1) used extensively in a diagnostic setting to visualise cell proliferation in humans has limited reactivity to the homologous mouse Ki67 (Mki67). Monoclonal anti-mouse Mki67 (TEC-3 clone) antibodies however, have been reported to replicate the

effectiveness of the anti-human Ki-67 antibodies in detecting cellular proliferation in FFPE murine intestinal specimens [281]. The form of Ki67 detected by the MIB-1 antibody is observed in cycling cells, present in G_1, S, G_2 and M phases, but is absent in the G_0 phase [282]. Immunoreactivity with anti-Ki67 antibodies therefore corresponds to proliferative status of the labelled cell. In the normal human colonic mucosa the strongest labelling with Ki67 is for the most part, confined to the basal third of the crypt epithelium, the so-called proliferative zone. Under active inflammation and regeneration the crypt epithelium exhibits an apparent expansion of the $Ki67^+$ proliferative zone toward the luminal surface [283].

Invasiveness and metastasis of epithelial cancers has been associated with a phenotypic conversion from a differentiated epithelial cell to a motile cell type resembling mesenchymal cells during embryogenesis [284]. The so-called epithelial-mesenchymal transition (EMT) could conceivably permit a transformed cell to detach from the surrounding tissue and migrate into separate tissue compartments thus facilitating invasion and metastasis of tumours. Attachment of epithelial cells to the neighbouring epithelial cells is mediated by several families of cell-surface proteins which form the adherens junctions. A key membrane-spanning protein critical for the maintenance of epithelial integrity and polarity in the colon is the epithelial cadherin (E-cadherin) through its signalling via β-catenin [208]. Absence of homotypic interaction between E-cadherin on adjacent epithelial cells results in the activation of the associated β-catenin, which then shuttles to the nucleus to form a transcriptional regulation complex with lymphoid enhancer-binding factor (LEF). Excessive levels of active β-catenin, due to genetic mutations in *APC* or the gene encoding β-catenin (*CTNNB1*) are thought to promote neoplasia through their contribution to the up-regulation of genes encoding Myc and cyclin-D1. While oncogenic β-catenin signalling appears to correspond to the altered proliferation and differentiation of epithelial dysplasia, it may also be involved in the EMT. be less useful for the escape from the adjacent stroma seen in advanced neoplasia. Loss of E-cadherin may also amplify the effect of oncogenic β-catenin on transformation of the colonic epithelium [285]. Silencing of E-cadherin (*Cdh2*) transcription by promoter

methylation has also been suggested as a possible risk factor for neoplasia in patients with UC [202]. Changes in adhesion molecules such as E-cadherin is associated with a transition to a mesenchyme-like phenotype in epithelial cells [286]. Cadherin switching, such as a reduction of functional E-cadherin co-inciding with an increased cell-surface expression of the neuronal cadherin (N-cadherin) has been proposed as a marker of EMT, and is one characteristic observed in cancers [287]. Ectopic expression of the vimentin intermediate filament in epithelial cells also corresponds with increased potential for invasiveness and metastasis in colonic adenocarcinoma cells [288]. Detection of these features in the colonic epithelium in the colonic epithelium of Winnie may thus indicate the transition to a neoplastic phenotype.

5.2 Aims/Hypothesis

Since a number of molecular pathways have been identified that may predispose the chronically inflamed colonic epithelium to neoplasia, we intended to first analyse the gene expression within the distal colon of DSS-treated and untreated Winnie and wild-type mice. Increased cellular proliferation and nuclear localisation of β-catenin in the distal colonic epithelium of abnormal crypts in Winnie after three cycles of inflammation were expected. Since E-cadherin is frequently lost in IBD-associated neoplasia it would be expected that the abnormal distal colon in Winnie would display a molecular signature indicative of EMT.

5.3 Results

5.3.1 Epithelial cell proliferation in the Winnie colon

Aberrant patterns of crypt epithelial cell proliferation have been identified in precursors to colonic neoplasia. Immunoreactivity for Ki67 protein was therefore employed as a means to identify proliferative cells within the colonic epithelium. Normal Ki67 labelling in untreated C57BL6 mice extended uniformly for approximately a third of the crypt's total length (Fig. 5.1A). Examination of the intracryptal distribution of Ki67-expressing epithelial cells

revealed $< 20\%$ of the total cells were labelled by the anti-Ki67 antibody in the apical portion of the crypts in the distal colon C57BL6 mice (Fig. 5.1A). Higher proportions of labelled cells were visible within the middle and basal regions of crypts in the C57BL6 distal colon, approximately 52% and 68% respectively (Fig. 5.1B & C). Three cycles of 1% DSS in C57BL6 mice produced an apparent expansion of the proliferative zone in the crypts of the distal colon (Fig. 5.1B). While the proportion of Ki67-positive cells in the top (Fig. 5.1A) and middle (Fig. 5.1B) crypt divisions was similar to untreated C57BL6 mice, the DSS-treated animals displayed an increased proportion of Ki67-positive cells in the crypt base (90%). In Winnie the proliferative zone of the colonic crypt appeared to frequently extend to approximately half to two-thirds of the total crypt length in the distal colon (Fig. 5.1C). Despite an apparent shift in the distribution of Ki67-expressing epithelial cells, the proportion of labelled cells was not markedly different in the top (25%), middle (60%) and basal (67%) crypt divisions when compared to both untreated and treated C57BL6 (Fig 5.1A–C). Most cells within the crypt base in Winnie expressed Ki67 (Fig. 5.1C) and like in C57BL6 mice, the proportion of Ki67-positive cells decreased progressively from the middle (Fig. 5.1B) and upper (Fig. 5.1C) portions of the crypt. Chronic exacerbation of colitis in Winnie using three cycles of DSS extended the Ki67-reactive proliferative zone toward the surface epithelium further than that typically seen in Winnie (Fig. 5.1D). Crypts with dysplasia-like architectural distortion in Winnie displayed more diffuse Ki67 labelling throughout the crypt length. The diffuse labelling was also retained as a feature of glands penetrating into the submucosa. Despite the diffuse pattern of Ki67 expression, the proportion of Ki67-expressing cells in the top and middle crypt divisions were not markedly different from the distal colon of untreated Winnie or either untreated or treated C57BL6 mice (Fig. 5.1A–5.1C). When the whole crypt length was considered, the proportion of Ki67-expressing cells was overall not markedly different between any of the combinations of genotype and treatment (Fig. 5.1D). Thus, potential alterations to proliferative cell localisation are likely to co-incide with an increase in the total cell number within the crypt.

5.3.2 β-catenin localisation in the Winnie colon

To assess whether oncogenic perturbations in epithelial Wnt/β-catenin signalling were present in the chronically inflamed mucosa, we analysed the intracellular distribution of β-catenin immunohistochemically. Localisation of β-catenin in the colonic mucosa of untreated Winnie mice was restricted to the cell membrane of polarised cell types, specifically the colonic epithelial cells, endothelial cells and the glial cells of the myenteric plexus (Fig. 5.2A). Expression of β-catenin in the colonic epithelium was strongest at the lateral membranes between adjacent epithelial cells. Distribution of β-catenin in the colonic epithelium of Winnie mice remained largely unchanged after three cycles of DSS (Fig. 5.2B & 5.2C). Weaker cytoplasmic labelling may also be observed in the apical epithelium and epithelial cells of the crypt base in both untreated and DSS-treated Winnie mice. However, no nuclear translocation of β-catenin was evident in normal or any of the dysplasia-like lesions in Winnie mice after three cycles of DSS administration.

5.3.3 Gene expression analysis

To identify potential molecular pathways resulting in an abnormal epithelial regenerative or dysplastic response, we employed an pre-designed, commercially available qPCR array of targets associated with gastro-intestinal neoplasms (identity of genes covered are listed in Table A.1. Gene expression was compared between the distal colon of an untreated Winnie animal and a Winnie animal with severe distal colonic disease (shown in Fig. 3.7E-H) after three cycles of DSS. Transcript amplified by 13 primer sets displayed greater than a two-fold difference between untreated and DSS-treated animals (Fig. 5.3).

Differences in genes thought to influence neoplastic processes in the distal colon were subsequently assessed in Winnie following three cycles of DSS (primer information listed in Table A.2). Three cycles of 1% DSS increased expression of caveolin-1 (*Cav1* in the wild-type colon (Fig. 5.4). In the Winnie colon however *Cav1* expression was no different between untreated and DSS treatment. Three cycles of DSS induced an increase in C-C-

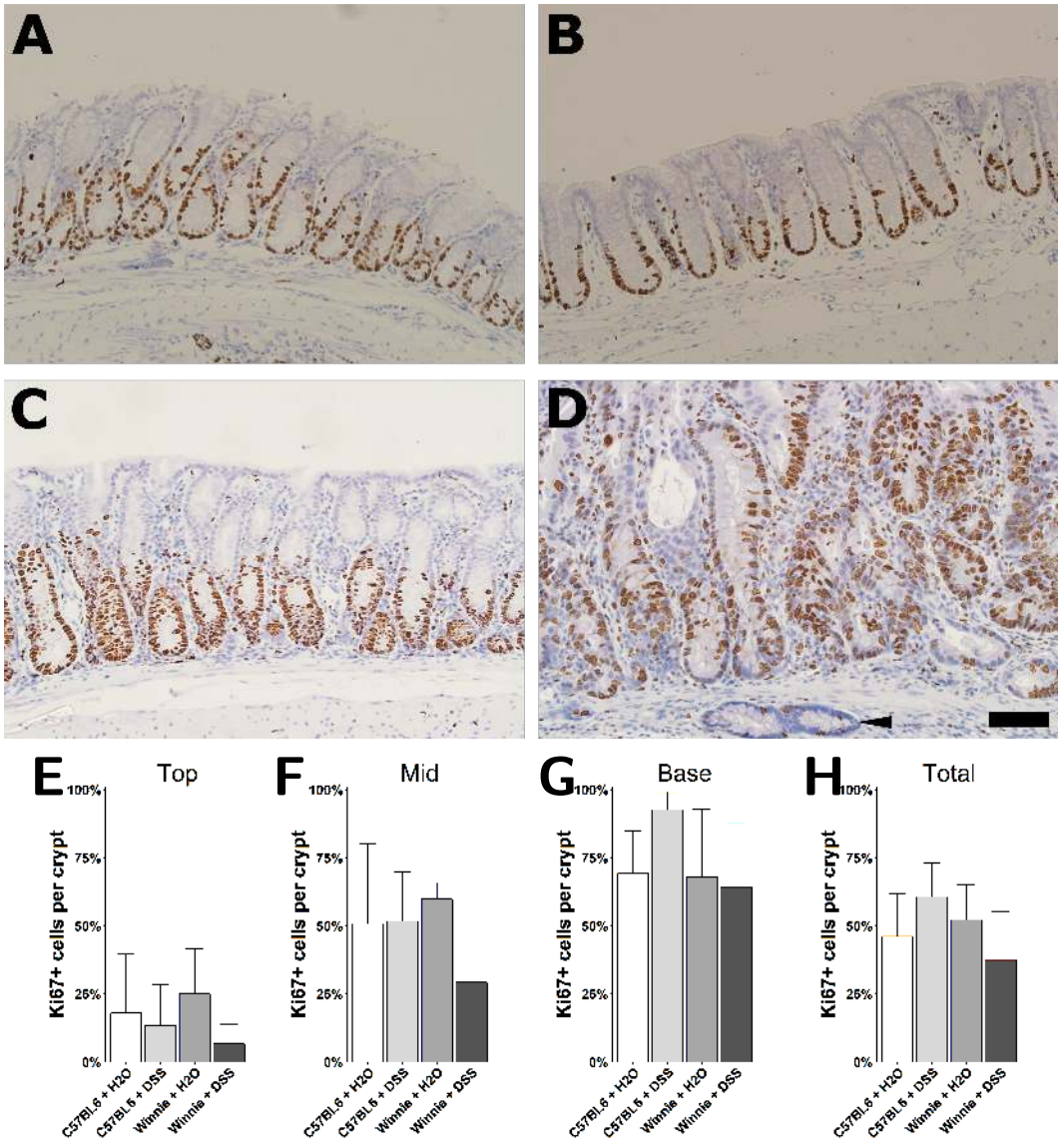

Figure 5.1: **Immunohistochemical detection of Ki67 in Winnie distal colonic mucosa A**. Immunostaining of Ki67 in the distal colon of untreated C57BL6 mice. Image representative of Ki67 localisation in the distal colon of the four C57BL6 mice examined. **B**. Distal colonic Ki67 localisation representative of six C57BL6 mice exposed to three cycles of 1% dextran sulphate sodium (DSS). **C**. Distal colon of Winnie mouse without exposure to three cycles of DSS. Ki67-labelling in the epithelium is visible apically approximately half the crypt length. **D**. Ki67 immunolabelling of the Winnie distal colon exposed to three cycles of DSS. Crypt base proliferative zone extends approximately two-thirds of the crypt length. Submucosal gland (arrowhead) displays few positive nuclei. **E-G**. Proportion of cells labelled by anti-Ki67 antibodies of the total cells in the apical (**E**), middle (**F**) and basal (**G**) region of crypts in the distal colon. **H**. Proportion of Ki67-expressing cells of the total number of cells within the full crypt length. All images were drawn from untreated wild-type (n=3), wild-type + DSS (n=4), untreated Winnie (n=3) and Winnie + DSS (n=4). Differences between means for which $P < 0.05$ was deemed significant. Bars represent mean of the proportion of Ki67-expressing cells of the total crypt epithelial cell nuclei counted. Error bars represent one standard deviation from the mean. Differences between means were considered significant if the $P < 0.05$. Scale bars represent a length of 50 μm.

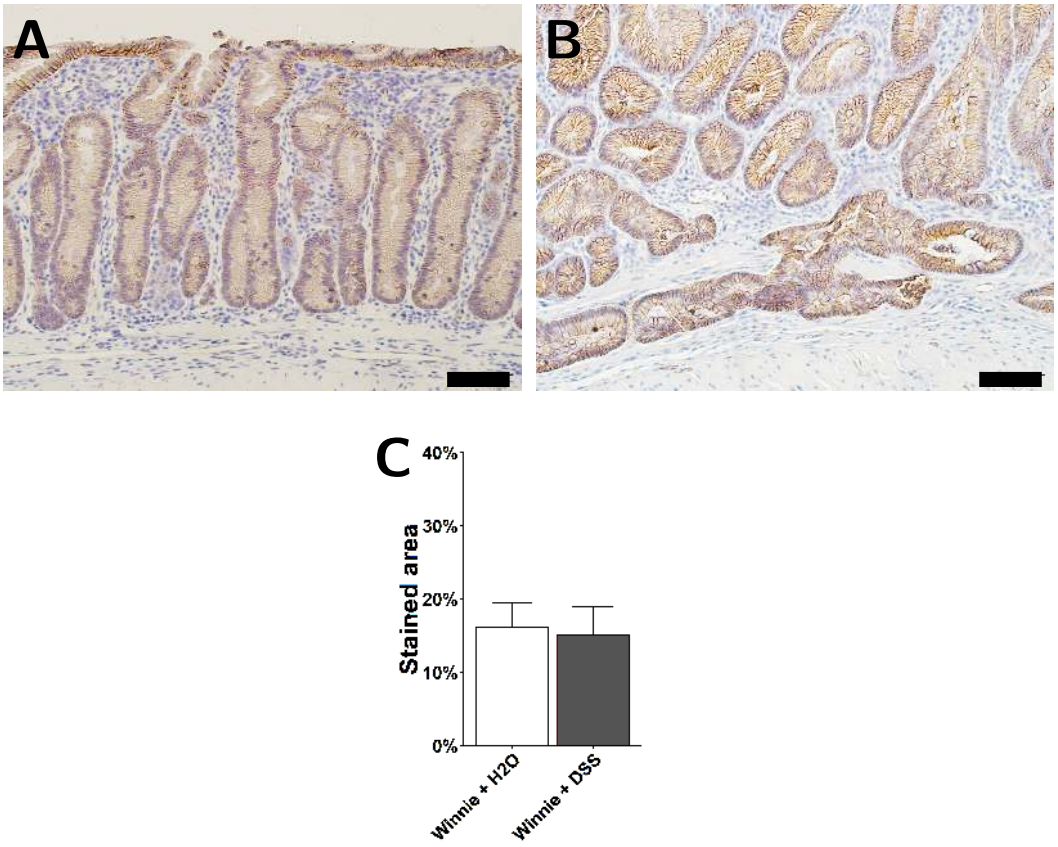

Figure 5.2: **Absence of β-catenin nuclear translocation in Winnie mucosa A**. Distal colon representative of the six untreated Winnie mice studied. Staining specific to β-catenin is localised to the cell membrane of the colonic epithelium and to the plasma membrane of endothelial and glial cells. **B**. Representative image of the distal colon Winnie mice subjected to three cycles of 1% DSS (n = 11). Expression of β-catenin was predominantly limited to the cell membrane to the cell membrane of epithelial cells without any nuclear accumulation. Scale bars represent 50 μm. **C**. Relative area area of tissue stained using anti-β-catenin antibody obtained from 10 random fields at 400× magnification. All images were drawn from untreated Winnie (n=5) and Winnie + DSS (n=7). Plotted bars represent mean of the relative area, errorbars equal to 1 SD of the mean. Differences between means for which $P < 0.05$ was deemed significant. Scale bar represents 50 μm.

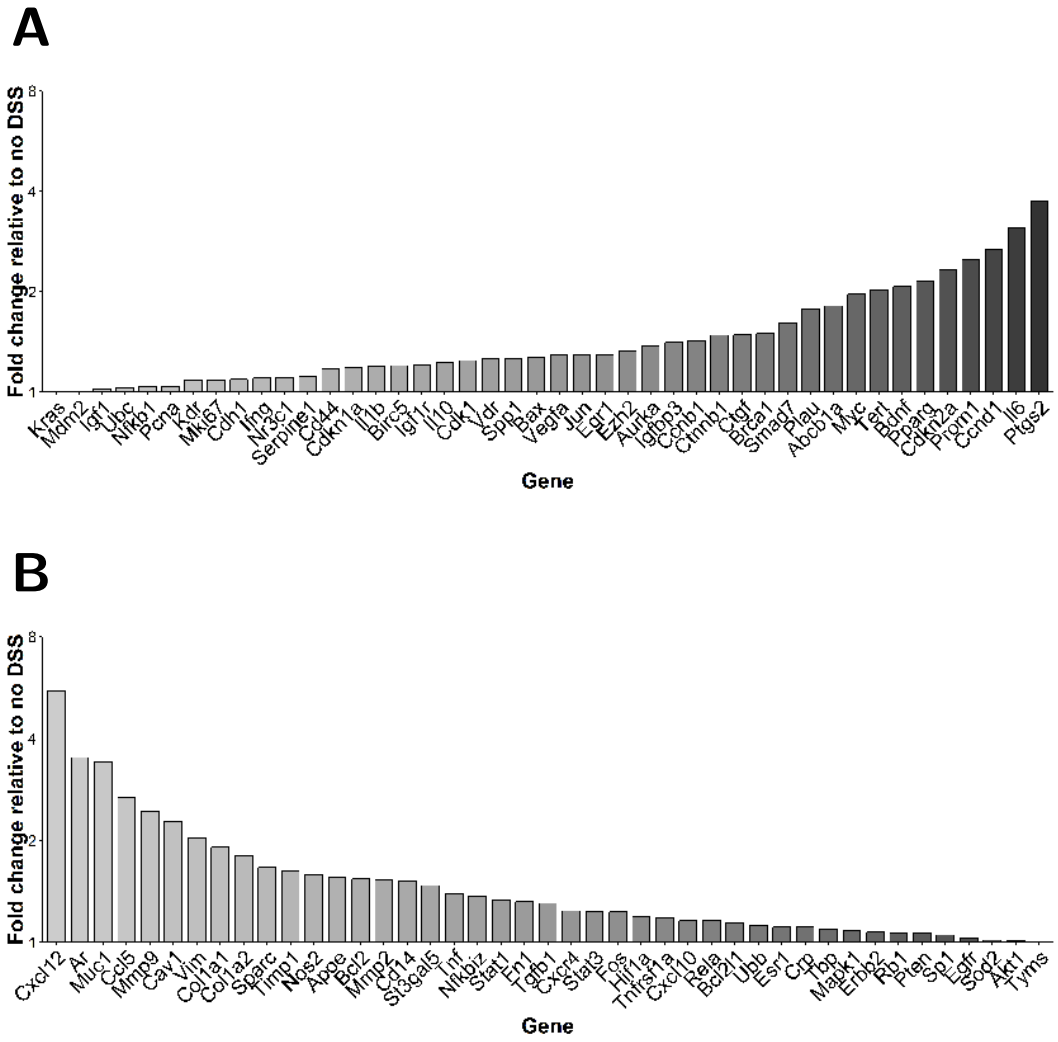

Figure 5.3: **Screening for potential markers of neoplastic transition in the Winnie colon.** Relative mRNA transcript abundance for 88 target genes on a commercially available PCR array (refer to Table A.1 for gene) between a single Winnie mouse exposed to three cycles of 1% DSS and a single age-matched Winnie mouse that had received only water. **A**. Genes for which relative abundance of mRNA transcript was increased in Winnie following three cycles of 1% DSS relative to untreated Winnie. **B**. Genes for which mRNA transcript is decreased in Winnie following three cycles of 1% DSS compared to untreated Winnie. Bars represent fold change in relative transcript abundance ($2^{-\Delta\Delta C_T}$) relative to an average of three reference genes; beta actin, (*Actb*), glyceraldehyde-3-phosphate dehydrogenase (*Gapdh*), hypoxanthine guanine phosphoribosyl transferase (*Hprt*) with all changes relative to expression in the untreated Winnie distal colon.

motif-containing chemokine ligand-5 (*Ccl5*) mRNA transcript in the Winnie distal colon relative to wild-type mice treated with DSS. Expression of *Myc* was approximately two-fold higher in the distal colon of wild-type mice after DSS compared to untreated wild-type mice. In contrast three cycles of DSS produced no detectable effect on *Myc* expression in the Winnie distal colon. Expression of murine transformation-related protein p53 (*Trp53*) in the distal colon of Winnie mice was not appreciably altered from baseline following three cycles of DSS. Treatment with DSS however induced a higher level of *Trp53* transcription in Winnie than in WT mice. None of the remaining genes displayed a detectable difference between genotype or treatment groups.

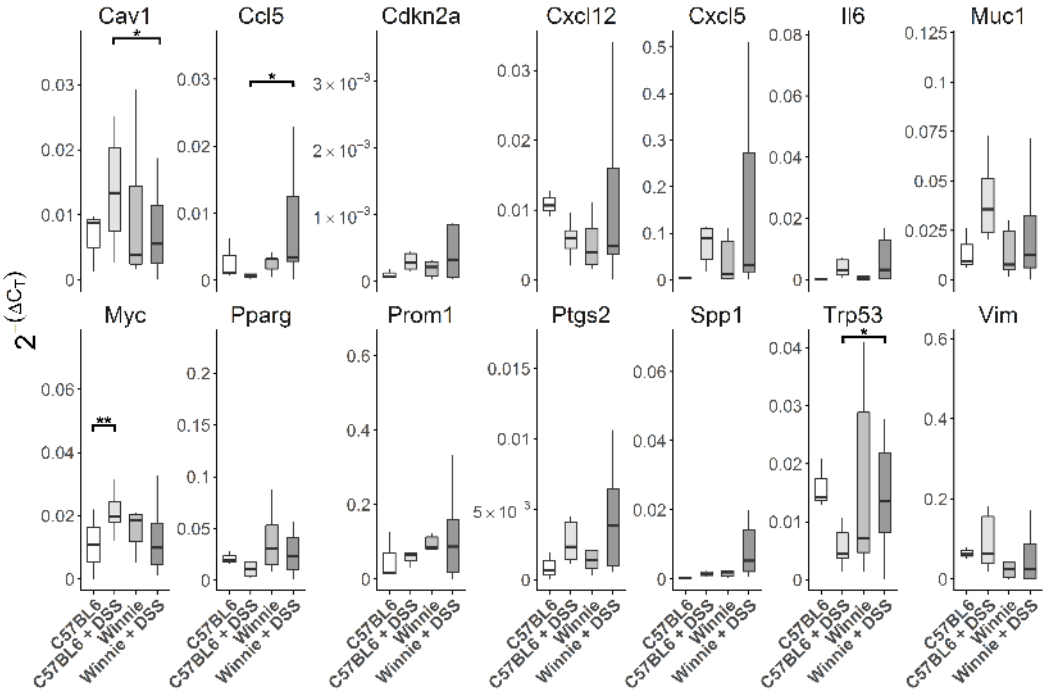

Figure 5.4: **Relative transcript abundance of genes regulating inflammation and cell proliferation.** Transcript abundance measured from 25 ng of template based on the linearised 2-ΔCT method, where each gene of interest was normalised to the relative abundance of a reference gene (Gapdh). Box plot depicts interquartile range (IQR) either side of the median for untreated C57BL/6J mice (n = 3), C57BL/6J mice exposed to three cycles of 1% DSS (n = 6), untreated Winnie mice (n = 6) and Winnie mice exposed to three cycles of 1% DSS (n = 11). Whiskers represent 1.5 IQR approximately equivalent to 5%-95% confidence intervals. *, $P < 0.05$; **, $P < 0.01$.

The existence of a potential relationship between the relative abundance of the measured mRNA transcript in the distal colon of pooled Winnie and C57BL6 mice and the grade of dysplasia was tested using Spearman's rank correlation (Table 5.5). We observed monotonic increases in the gene expression of Ccl5 (ρ = 0.46) and Spp1 (ρ = 0.40) correlated with increasing severity of dysplasia. All of the other genes analysed displayed no discernible statistical association between gene expression and histological severity.

5.3.4 Immunohistochemical detection of Cxcl5

Although Cxcl5 levels in the colon may reflect progression of colonic neoplasia, no difference in the expression of this chemokine in the colon at the gene level was observed. Since *Cxcl5* relative abundance was variable within the distal colon of Winnie mice we sought to investigate the source and distribution of the Cxcl5 protein within colonic tissue. Wild-type mice displayed a diffuse cytoplasmic staining in the colonic crypt epithelium only, with strongest staining intensity typically in the surface epithelium (Fig. 5.6A).

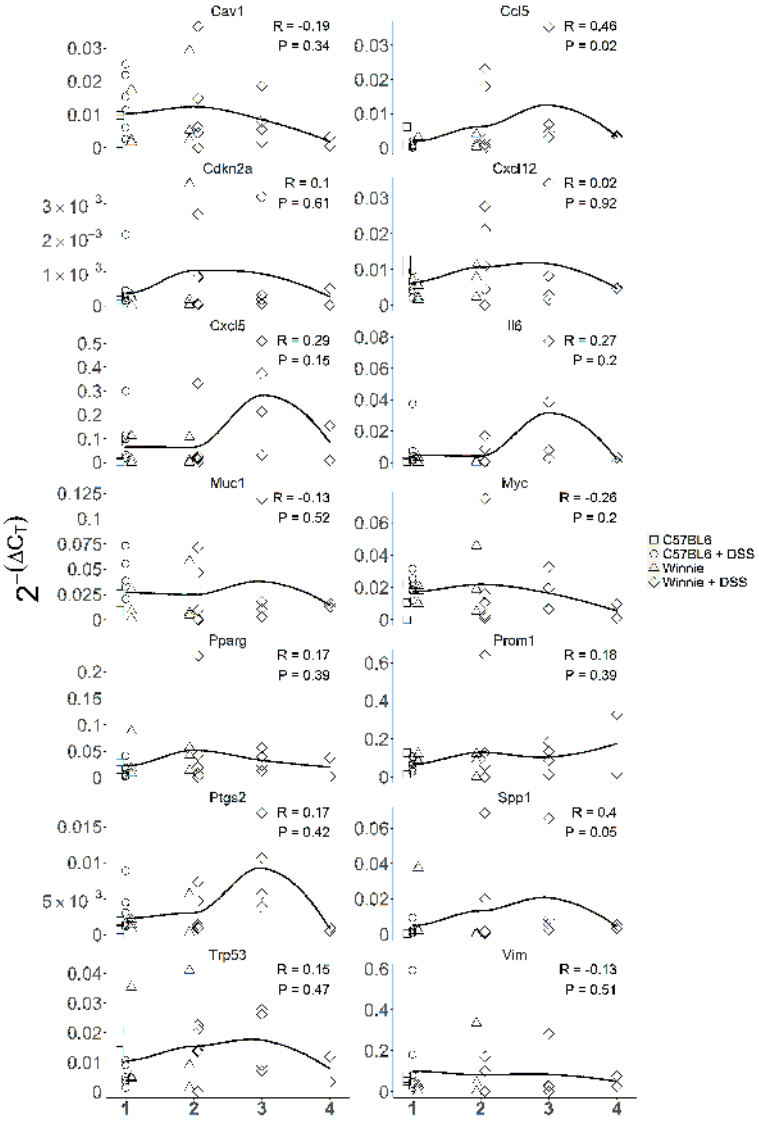

Figure 5.5: **Spearman's correlation between mRNA transcript abundance and dysplasia severity.** Relationship between relative mRNA abundance ($\Delta\Delta C_T$) and severity of dysplasia in the distal colon was tested using Spearman's rank correlation. Estimate of Spearman's co-efficient of correlation (R) and corresponding *P*-value for each gene are given.

Exposure of the distal colon of wild-type mice to three cycles of 1% DSS did not produce considerable increases in the intensity of the surface epithelium in the distal colon (Fig. 5.6B). Stronger staining intensity corresponding to Cxcl5 protein became more frequent in the top third of the colonic crypt in Winnie compared to the wild-type animals studied. Similarly, colitis induced by the Muc2 mutation in Winnie mice was associated with an increase in Cxcl5 protein levels within the intestinal epithelium (Fig. 5.6C). An additional insult of 1% DSS in Winnie mice appeared to increase the vesicular pattern of Cxcl5 staining in the distal colonic epithelium, and most notably, increased the abundance of mucosal and submucosal leukocytes (Fig. 5.6D-5.6E). Abnormal crypts induced by three cycles of DSS in Winnie often displayed a marked, focal reduction in cytoplasmic Cxcl5 staining (Fig 5.6F). One animal presenting with a lesion of extensive high-grade dysplasia displayed an abnormally low level of cytoplasmic Cxcl5 expression in the colonic epithelium whereas lamina propria leukocytes displayed intense cytoplasmic staining (Fig. 5.6F). Overall however, the relative distribution of Cxcl5 was not markedly different between any of the combinations of genotype and DSS treatment.

5.3.5 Epithelial-to-mesenchymal transition

To assess the possibility of EMT occurring in the chronically inflamed colon of Winnie mice, we analysed the immunohistochemical localisation of two mesenchymal markers, vimentin and N-cadherin. N-cadherin in the colon of six 18–20 week-old Winnie mice was observed predominantly between inner and outer coats of the tunica muscularis corresponding to location of the myenteric plexus, although an infrequent staining of an elongated cell type was also observed in the mucosal stroma (Fig. 5.7A). No discernible changes in the pattern of N-cadherin-specific staining were observed in the colon of the Winnie mice following three cycles of DSS administration (n = 11) compared to age-matched mice which never received DSS (Fig. 5.7B). No epithelial localisation was observed in Winnie mice even in crypts penetrating into the submucosa. Increased N-cadherin immunostaining was observed

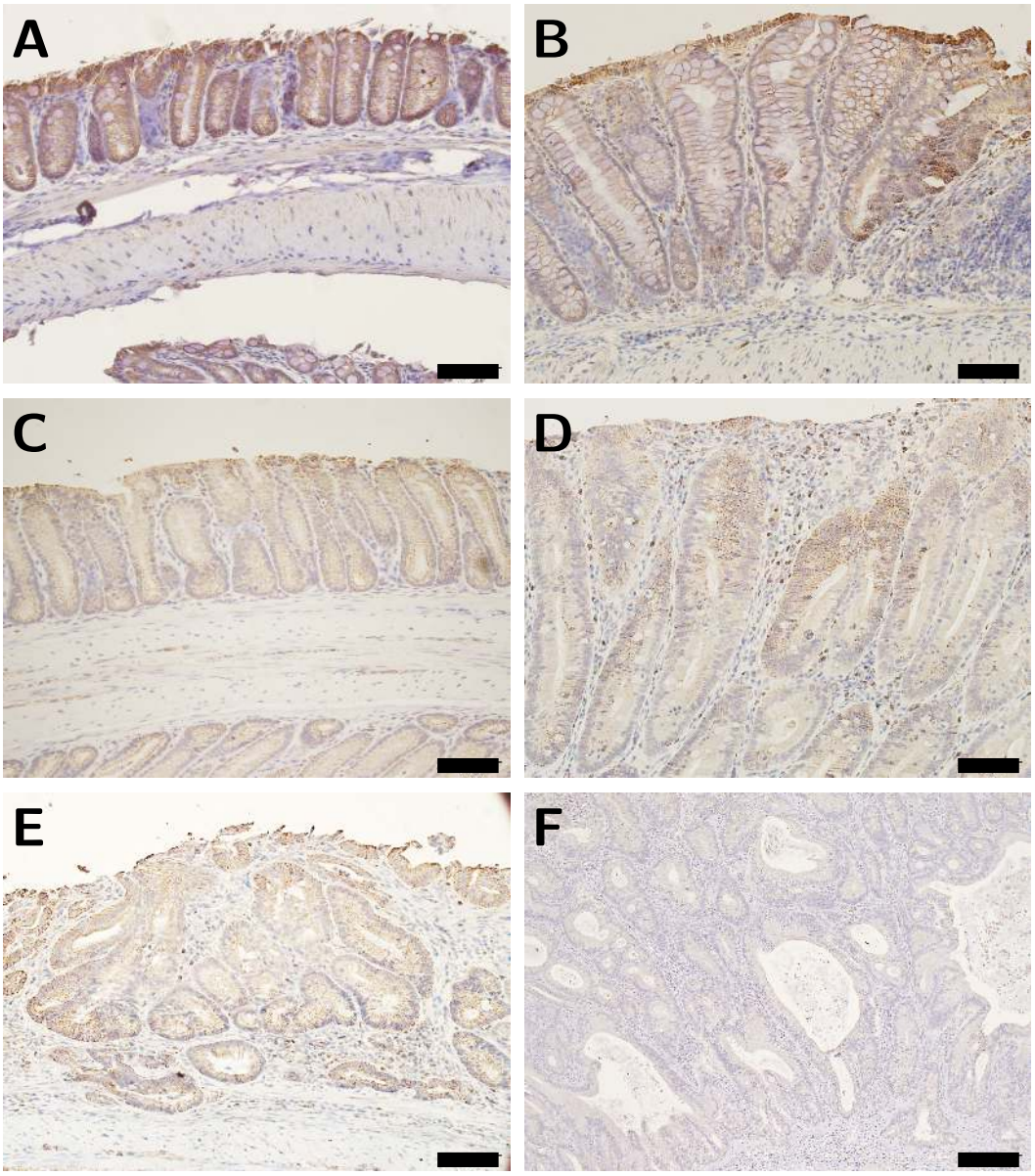
A
B
C
D
E
F

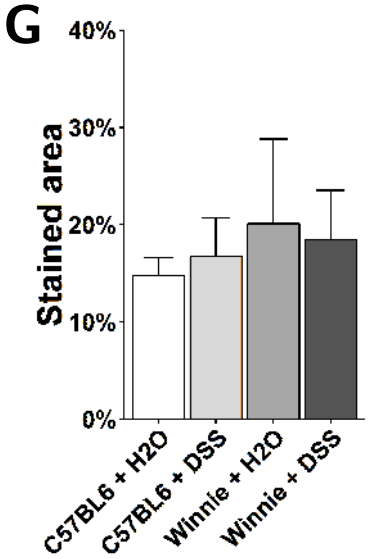
G
40%
30%
20%
10%
0%
Stained area
C57BL6 + H2O
C57BL6 + DSS
Winnie + H2O
Winnie + DSS

Figure 5.6: **Immunohistochemical detection of Cxcl5 in Winnie distal colonic mucosa** The distribution of Cxcl5 was assessed in the mucosa of both wild-type and Winnie mice, with or without prior exposure to three cycles of 1% DSS. **A**. Distal colon representative of four 18-20 week-old wild-type C57BL6 mouse without DSS exposure. **B**. Distal colon representative of six analysed wild-type C57BL6 mouse exposed to three cycles of 1% DSS. **C**. Distal colon from 18-20 week-old Winnie without DSS exposure. Cxcl5 labelling displayed a diffuse cytoplasmic pattern within the colonic epithelium. **D**. Exposure to DSS increased the intensity of epithelial staining in the hyperplastic mucosa, particularly in the top half of the crypt. Note the vesicular intracytoplasmic staining within epithelial cells. Intense cytoplasmic staining was also observed in mucosal leukocytes. **E**. Distal mucosa of Winnie exposed to DSS. Dysplastic glands displaying focal reduction in epithelial Cxcl5. Note that laterally spreading epithelium penetrating the muscularis mucosae retains Cxcl5 expression. **F**. Mucosa of distal colon in Winnie post-DSS exposure. Weak Cxcl5 immunolabelling is present within the cytoplasm of the epithelial cells lining dysplastic glands. Counterstained with haematoxylin. **G**. Average area stained by the anti-Cxcl5 antibody relative to total area obtained from 10 random fields at 400$\times$ magnification. Plotted bars represent mean of the relative area, errorbars equal to 1 SD of the mean. All images were drawn from untreated wild-type (n=2), wild-type + DSS (n=4), untreated Winnie (n=3) and Winnie + DSS (n=7). Differences between means for which $P < 0.05$ was deemed significant. Scale bar represents 50 μm.

in the submucosal stroma associated with a sporadic colonic adenoma (Fig. 5.7C). However, no epithelial staining was observed. Epithelial expression of N-cadherin was similarly absent in invasive carcinoma of the colon in both of the two patients with IBD analysed (Fig. 5.7D). Vimentin was frequently observed in the mucosa, submucosa and smooth muscle tunic of the Winnie colon, apparently localised to the cell membrane and cytoplasm of an elongated cell population (Fig. 5.8A). Occasional rounded cells displaying cytoplasmic vimentin were observed in the lamina propria and epithelial compartments, though epithelial cells were negative for vimentin. Notably smooth muscle cells did not appear to display vimentin expression, with staining in the muscularis tunica localising to myenteric neuronal/glial cells.

Exposure to three cycles of DSS in the Winnie distal colon resulted in an increase in the intensity and density of vimentin staining within the mucosal lamina propria and within the connective tissue of the submucosa (Fig. 5.8B). Again, epithelial expression was absent from the colonic epithelium. Vimentin in the two patients with IBD generally remained associated

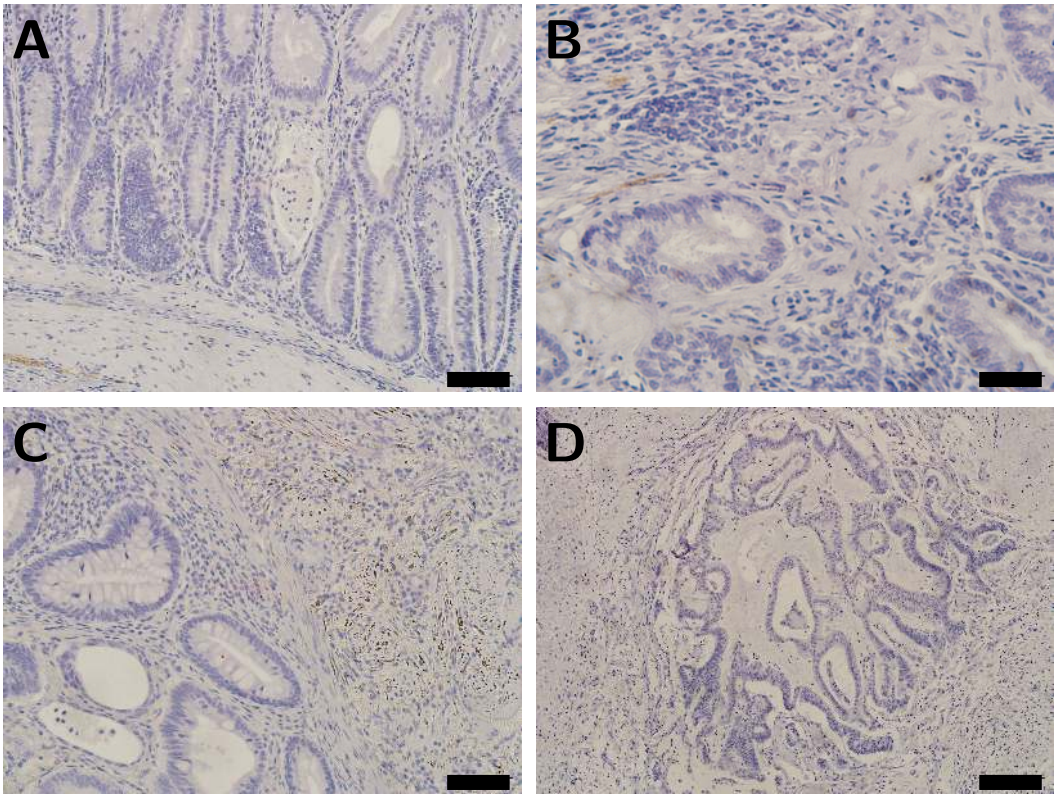

Figure 5.7: **Immunohistochemical detection of N-cadherin in Winnie distal colonic mucosa.** **A**. Distal colon of Winnie mouse having received water only. Labelling of N-cadherin is restricted to mesenchymal tissues. Occasional cytoplasmic staining is present in rare elongated pericryptal cells in the mucosa but absent in the epithelium. Prominent staining of the neuronal tissue of the tunica muscularis is visible. **B**. N-cadherin immunolabelling of the Winnie distal colon exposed to three cycles of DSS. N-cadherin present in the cytoplasm of occasional spindle-shaped cells in the mucosa and submucosa, but absent in colonic epithelium. **C**. Increased N-cadherin-positive spindle-shaped cells in the fibromuscular stalk of a polypoid adenoma arising in the uninflamed distal human colon. **D**. Adenocarcinoma arising in the colon of a patient with Crohn's disease. No staining is visible within the epithelium

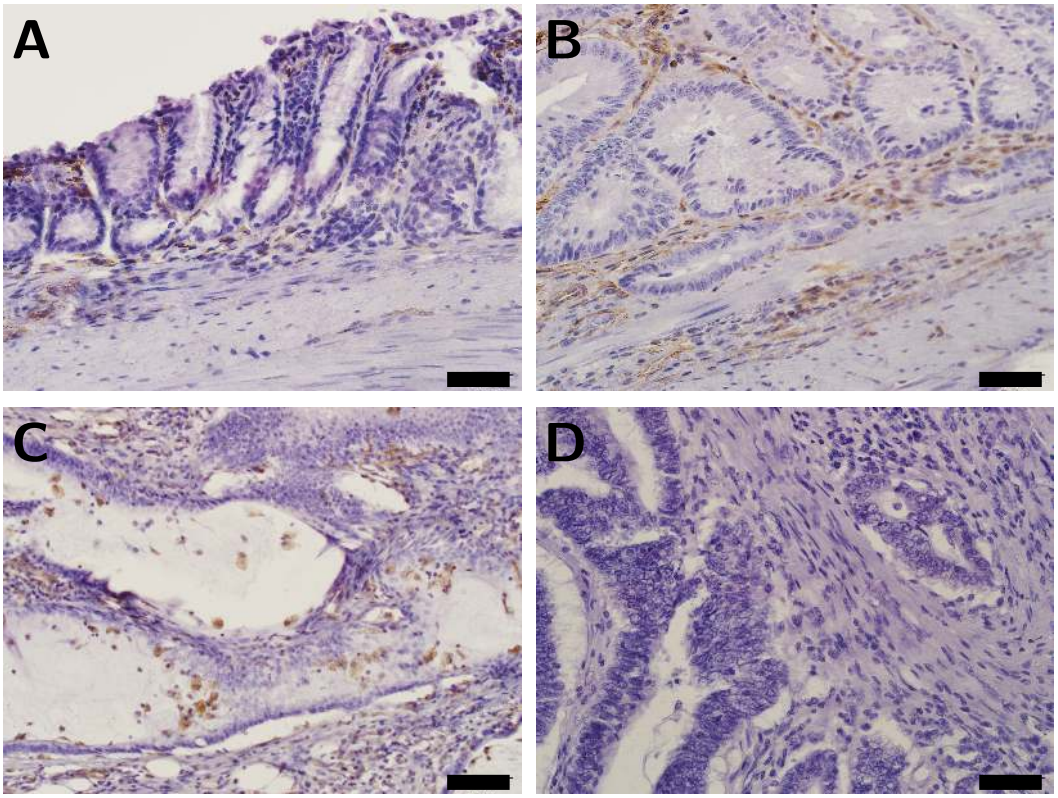

Figure 5.8: **Immunohistochemical detection of vimentin in Winnie distal colonic mucosa. A**. Distal colon of Winnie mouse having received water only. Vimentin labelling is restricted to mesenchymal tissues. Cytoplasmic staining is present in cells in the mucosal lamina propria but absent in the epithelium. **B**. Distal colon of from Winnie mouse following exposure to three cycles of DSS. Vimentin staining localises to the cytoplasm of the elongated cells residing in the connective tissue of the mucosa and submucosa and is absent in the colonic epithelium and smooth muscle layers. **C**. Adenomatous dysplasia from the distal colon of a patient with IBD. Vimentin is present in the cytoplasm of cells resident in the lamina propria. Cytoplasmic vimentin staining is also visible in a of cells with expansive cytoplasm that appear to be shed from the glandular epithelium into the lumen of several dysplastic crypts. **D**. Adenocarcinoma arising in the colon of a patient with IBD. No staining is visible within the involved epithelium or within the desmoplastic stroma.

neoplasia also displayed regions where vimentin was absent from the stroma surrounding invasive crypts (Fig. 5.8D).

5.3.6 DNA methylation

Since gene promoter methylation may establish patterns of pro-tumourigenic gene expression, pyrosequencing of bisulphite-converted promoter CpG sites was undertaken. Several genes of interest were identified from the literature describing altered methylation in human carcinogenesis or DSS-induced carcinogenesis (Primer sets are described in Table A.3). Optimisation of several primer sets designed to amplify bisulphite-converted sequences was commenced using DNA isolated from animals exposed to the three cycle DSS regimen (Fig, 5.9). Pyrosequencing of gene promoter CpG regions may detect differential methylation of the alcohol dehydrogenase-1 (*Adh1*) gene. For example methylation of promoter CpG regions may be lower in wild-type C57BL/6J (Fig. 5.9A) relative to Winnie following three cycles of 1% DSS (Fig. 5.9B).

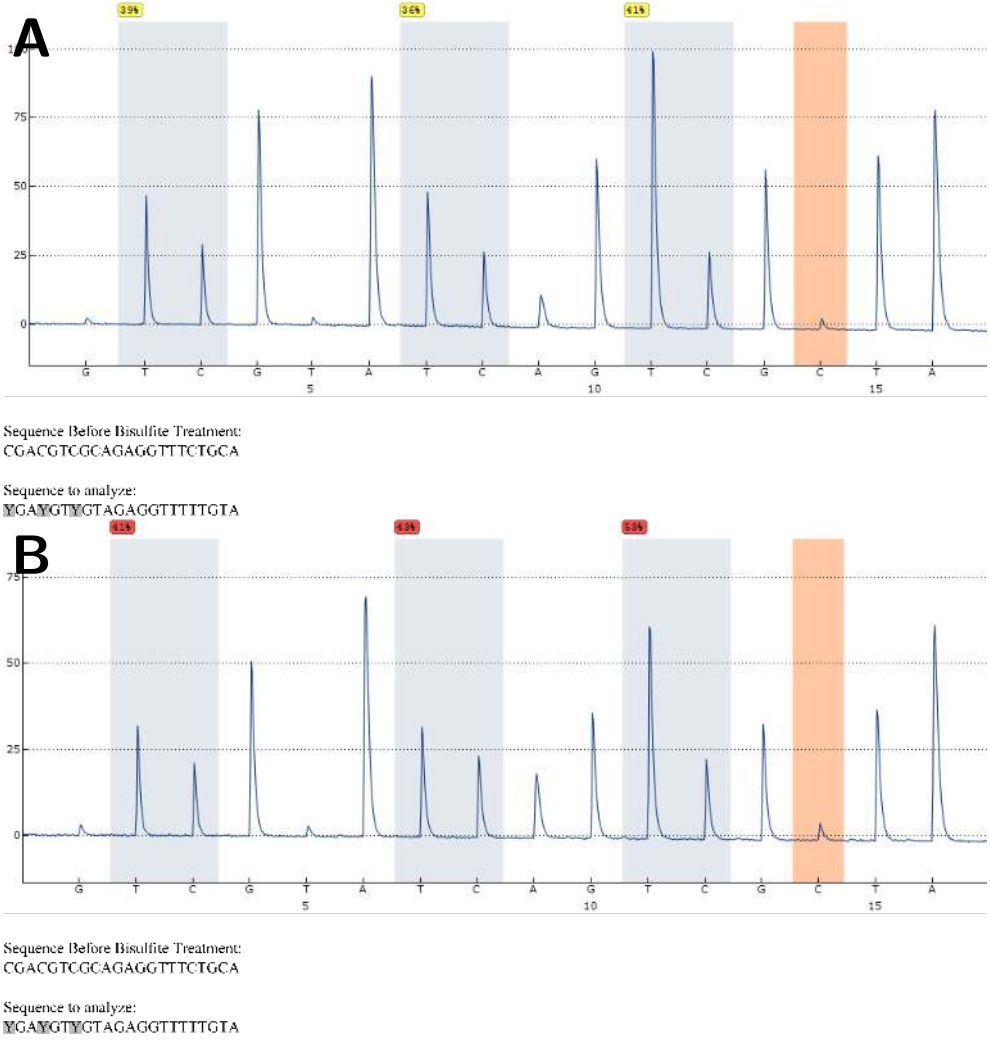

Figure 5.9: **Adh1 gene promoter CpG methylation in the distal colonic mucosa. A** Pyrogram of wild-type and **B** Winnie post-DSS, where nucleotide sequence in order of dispensation is displayed along the x-axis and y-axis represents the relative light intensity generated from incorporation of nucleotides (in arbitrary units). Grey vertical bars mark variable regions associated with CpG sites, orange bars represent the internal methylation control.

5.4 Discussion

Previous reports have suggested that histologically identifiable dysplasia in patients with UC exhibit particularly strong Ki67 expression within the surface epithelium in addition to the prominent Ki67 expression of the basal crypt epithelium similar to that observed in non-neoplastic epithelium [283, 289]. The pattern of Ki67 expression in the colonic crypts in Winnie mice displayed labelling of the crypt base but with an apical extension of the proliferative zone, as could be expected in inflammation-induced hyperplasia. The typical Ki67 distribution was expanded somewhat by three cycles of 1% DSS, however surface staining for Ki67 was not observed. A diffuse pattern of Ki67 expression was observed in a limited number of abnormal crypts, including those in the submucosa, following DSS administration. Still other foci of abnormal crypts displayed regions apparently devoid of Ki67 and were therefore potentially non-proliferative. Although pattern of diffuse epithelial Ki67 expression has been reported as the predominant pattern of Ki67 expression in invasive colorectal carcinoma, it is unclear what the cause for loss of Ki67 staining might be [283]. A loss of Ki67 has been observed at the invasive front of sporadic colonic carcinoma may indicate that the abnormal spreading of these glands may co-incide with a lack of proliferative activity.

Neutrophil recruitment, into the intestinal mucosa is a defining feature common to active inflammatory conditions in the mammalian bowel. Patients with UC typically display a diffuse neutrophilic infiltrate in the inflamed distal colon with neutrophils particularly associated with crypt epithelial abscesses [290]. Aside from acute and chronic inflammation, neutrophilic recruitment to the intestinal mucosa is observed in the stroma of colorectal neoplasms. The recruitment of neutrophils and macrophages to the neoplastic stroma has been associated with poor prognosis in patients with CRC [291, 292]. Tumour-infiltrating neutrophils may promote tumour invasion and growth through production of ROS/RNS, pro-inflammatory cytokines such as IL-6 and degradative matrix metalloproteinases [293, 294].

The abundance of neutrophils in chronic colitis and CRC begs the question of whether the presence of these cells in the chronically inflamed intestine is responsible for the rapid progression to neoplasia in patients with UC.

Recruitment of leukocytes from the circulation requires both the production of a chemotactic gradient and an alteration of the expression of surface adhesion molecules on endothelial and leukocytic cells. For this purpose a family of signalling molecules termed chemokines has evolved in mammals. Several subfamilies of chemokines exist, but two C-X-C motif-containing ligands (CXCL), CXCL5 and IL-8 (CXCL8) have been identified as the principal mediators of neutrophil recruitment in the intestine. Both CXCL5 and IL-8 contain a neutrophil-activating motif containing glutamic acid-leucine-arginine (ELR) which upon ligation with the C-X-C-motif chemokine receptor 2 (CXCR2), trigger chemotaxis, cytoskeletal re-arrangement and adhesion molecule expression in neutrophils [295].

Consistent with reports of the distribution of CXCL5 protein in the human colon, Cxcl5 in Winnie was limited primarily to enterocytes and activated monocytes in the distal colon of Winnie [296]. Increased expression of CXCL5 has been reported in the colon of patients with IBD, stimulated from epithelial cells by either increased pro-inflammatory cytokines such as IL-1β or direct exposure to pathogenic bacteria [297]. Altered expression of Cxcl5 in Winnie may therefore facilitate the massive recruitment of neutrophils to the colon during the active phases of inflammation, especially after DSS administration. Progression from early dysplasia to carcinoma corresponded with increased *Cxcl5* transcription in a combined azoxymethane/DSS model of carcinogenesis [298]. The apparent positive trend of increased CXCL5 with increased dysplastic-neoplastic progression has inspired several studies into the potential use of CXCL5 as a prognostic biomarker. Levels of mucosal and serum CXCL5 have been shown to reflect the progression of colonic neoplasms in human patients [299, 300]. Transcription of *Cxcl5* in the mucosa of the distal colon of Winnie however, displayed considerable variation in the degree of up-regulation. The basis of the variability in Cxcl5 expression was not immediately clear. Testing for a monotonic

relationship between the severity of dysplasia in each animal and the relative abundance of *Cxcl5* transcript suggested that *Cxcl5* transcription was probably unrelated to the degree of morphological complexity of the colonic crypts in the distal colon of Winnie. Visualisation of the synthesised Cxcl5 protein indicated differences in expression were associated with inflammatory activity. Animals exposed to DSS displayed more frequent mucosal erosions, and within these erosions strong expression of Cxcl5 was visible in infiltrating leukocytes. In contrast, abnormal crypts often displayed weak labelling of Cxcl5. Transcription of CXCL5 in human colorectal epithelium carcinoma lines is regulated by the binding of nuclear NF-$\varkappa$B adjacent to the *CXCL5* promoter [301]. Therefore disruption of NF-$\varkappa$B binding reduced both basal *CXCL5* transcription and IL-1β-induced up-regulation of transcription in a colonic carcinoma cell line. Since inactivation of p53 increases activation of NF-$\varkappa$B it would follow that enhanced *CXCL5* would co-incide with accumulated inactivating genetic mutations in *TP53* in the colonic epithelium.

Caveolin-1 is a membrane protein encoded by the gene *Cav1* thought to regulate trans-membrane signalling, particularly through its involvement in the formation of caveolae. Both mRNA and protein levels of caveolin-1 are markedly reduced in human colon cancers suggesting that caveolin-1 may serve to suppress tumourigenesis [302]. Homozygous *Cav1* gene deletion has been demonstrated to permit increased cell proliferation and cell cycle progression in mouse embryonic fibroblasts [303]. Modulation of proliferation is likely to be varied given the multiple signalling pathways utilising caveolae. Reduction of caveolin-1 has been associated with an increased in the cell cycle regulator cyclin D1 and a corresponding hyperproliferation and cell cycle progression [304]. Importantly, abrogation of caveolin-1 may permit escape from adhesion-dependent control of cell proliferation [305]. Though deletion of Cav1 in mice results in hyperplasia in respiratory, vascular and mammary tissues in $Cav1^{-/-}$ mice, no spontaneous carcinoma has been reported [303]. An additional event, such as mutation of Apc appears to be necessary for the initiation of colonic tumourigenesis [306]. Experimental evidence from $Apc^{Min/+}$ mice bred with Cav1 depletion supported the notion

that repression of caveolin-1 promotes expansion of neoplastic epithelial cells [307]. Due to its apparent function as modifier of pro-proliferative signalling, examination of of the status of Cav1 expression may be useful in assessing neoplastic transformation in the colon.

Detection of the accumulation of β-catenin in the epithelial cell nucleus through immunohistochemistry is typically dependent on inactivation of the APC-Axin-GSK-3β complex and is thus considered indicative of oncogenic Wnt signalling. In the inflamed mucosa of Winnie mice we failed to observe a discernible accumulation of immunoreactive β-catenin in the nuclei of the colonic epithelium. The immunohistochemical localisation of β-catenin in Winnie is comparable with the distribution of the same protein in the colonic mucosa of Swiss-Webster mice exposed to repeated administration of DSS [225, 235]. Cooper *et al.* describe nuclear accumulation detectable only in polypoid lesions arising from the inflamed colon, whereas flat lesions described in the same animals, displayed cytoplasmic β-catenin only. Polypoid adenomata induced by the combined administration of the mutagen 1,2-dimethylhydrazine and DSS frequently display immunohistochemically detectable β-catenin accumulation within the nucleus of transformed colonic epithelial cells [270]. However, it is known that 1,2-dimethylhydrazine and its metabolite AOM produce mutations in the gene encoding β-catenin when administered to mice [270, 308]. Carcinogenesis induced by mutations in β-catenin may not be especially relevant in understanding the progression of UC to CRC. Unlike sporadic neoplasms, in which nuclear beta-catenin was present in 81% of tumour cells, Aust *et al.* [309] observed nuclear beta-catenin in only 48% of tumour cells from colitis-associated neoplasms. Concordant with the reduced β-catenin accumulation, mutations in *APC* reportedly occur at a lower frequency in colitis-associated neoplasia relative to sporadic neoplasms [207, 310]. Given the difficulty in distinguishing alterations in staining density in the cytoplasm, only the presence or absence of β-catenin nuclear accumulation was asssessed. Colonic neoplasms arising from the inflamed colon of mice with *Gpx1-Gpx2*-deficient animals (mixed C57BL6 and S129Sv/J strain) displayed a high frequency of β-catenin accumulation in the ileum and colon, with 95% of HGD

and 69% of adenocarcinoma presenting with visible nuclear accumulation. Given that the majority of neoplasia arising in the Gpx double-knock-out mice was of a non-polypoid morphology, the presence of nuclear β-catenin accumulation stands in contrast with the non-polypoid lesions induced by DSS alone in the Swiss-Webster strain employed by Cooper *et al.* [225]. It is important to note that nuclear β-catenin accumulations are not homogenously distributed throughout colonic tumours. Instead nuclear β-catenin localisation may be more common at the invasive front of colonic carcinoma, where cell dedifferentiation and motility is increased [311]. Nuclear β-catenin localisation may in the case of the invasive front, be indicative of the acquisition of a relatively dedifferentiated cell phenotype.

Perhaps consistent then with the lack of nuclear β-catenin in the abnormal colonic epithelium in Winnie mice, evidence of mesenchymal-like surface markers was also absent. N-cadherin was limited to its typical expression by neuronal and other mesenchyme-derived cells in the colon of both Winnie mice, and the cases of CACC examined. While vimentin was perhaps increased in the colonic lamina propria during inflammation in Winnie and in the stroma of neoplasms from the human colon, no epithelial expression was observed. Therefore, the lack of immunohistochemical evidence for an EMT switch in the colonic epithelium in Winnie may correspond to the absence of oncogenic Wnt signalling via the canonical β-catenin pathway.

Epigenetics involves transcriptional regulation through either DNA methylation or chromatin remodelling and post-transcriptional regulation through micro-RNA (miRNA). Analysis of colectomy specimens obtained from three patients with long-standing UC (disease present for 10-20 years) revealed hypermethylation of *CDKN2A* associated with dysplasia [201]. Increased severity of dysplasia the inflamed mucosa was associated with higher levels of p16 methylation, whereas little methylation was observed in the non-dysplastic mucosa. Alternate splicing of the first exon of *CDKN2A* produces the p14 isoform ($p14^{ARF}$). Hypermethylation of p14, like p16, has also been associated with neoplasia in the chronically inflamed colon. While hypermethylation of the p14 exon is low in the non-dysplastic mucosa, paired tumour

biopsies displayed relatively high levels of p14 methylation [312]. Fifty percent of UC-associated carcinomata and 33% of dysplastic lesions displayed p14 hypermethylation. Remarkably, 60% of non-dysplastic biopsies displayed p14 hypermethylation, a feature not previously reported in the non-dysplastic mucosa of non-IBD patients, suggesting that p14 hypermethylation precedes dysplasia in the chronically inflamed colon.

5.5 Conclusion

In summary, Winnie mice displayed an abnormal pattern of epithelial proliferation that may be explained by a pattern of abnormal mucosal gene expression. Winnie mice displayed an apparent lack of *Cav1* and *Myc* up-regulation in response to DSS-induced injury in the distal colon. Conversely, while *Trp53* appeared to be down-regulated after three cycles of 1% DSS in wild-type mice, it was unaffected by DSS in Winnie. Gene expression of Ccl5 showed a positive correlation with severity of DSS-induced lesions in the distal colon of Winnie. Altogether, the absence of a immunohistochemically detectable, nuclear accumulation of β-catenin complex, and a lack of ectopic N-cadherin or vimentin localised to the cell membrane indicated that EMT was unlikely to contribute to the abnormal migration of the colonic epithelium of Winnie following DSS-induced injury. Further characterisation of the epigenetic activity in the colonic epithelium may yield further insight into the neoplastic potential of the inflamed epithelium in Winnie.

CHAPTER 6

GENERAL DISCUSSION

Colorectal cancer arising from the chronically inflamed colon represents a considerable cause of morbidity and mortality in patients with IBD. Non-specific, chronic inflammation is hypothesised to trigger and promote the transformation of the colonic epithelium to a neoplastic phenotype. The likely aetiology of IBD appears to lie in a trifecta of microbial factors; an aberrant host immune response and an impairment of the mucous barrier protecting mucosal surfaces. Experimental evidence points towards a primary defect in the integrity of the colonic mucus precipitating UC in particular. However, there is a dearth of experimental evidence which explains how such defects would transform the normal epithelium into pre-neoplastic or neoplastic cells. Investigating the pathological mechanisms in models of colitis initiated by a defect in mucus synthesis and secretion would therefore allow greater understanding of the link between IBD and colonic neoplasia.

The present study aimed to replicate the hypothetical progression from chronic UC-associated colitis to neoplasia arising as a result of a defective mucous barrier and ER stress. The Winnie strain of mice was selected for investigation as it replicates two key features of UC. Firstly, Winnie displays reduced expression of the primary mucin constituent of the colonic mucus, Muc2, a feature shared with patients with UC [256, 257]. Defective mucus secretion is further compounded by the accumulation of defective, intracellular protein within goblet cells of the colonic epithelium and the concomitant ER stress and activation of the UPR similar to that reported in patients with UC [250, 313].

6.1 Atypical regeneration in the Winnie colonic mucosa

The nature of the histopathological changes occurring in the Winnie distal colon following three cycles of 1% DSS was consistent with regeneration after repeated bouts of mucosal inflammation. The three-cycle DSS regimen was tolerated in Winnie with the expected colitic symptoms (diarrhoea, haematochaezia) and attenuated weight gain, but only a single mortality occurred due to DSS challenge. Consistent with an intact mucous barrier in the wild-type distal colon, these animals displayed little histological damage or clinical symptoms following three cycles of 1% DSS, suggesting that the concentration used was insufficient to cause substantial disease. After exposure to three cycles of 1% DSS, foci of crypts throughout the distal half of the Winnie colon, displayed an abnormal glandular architecture suggestive of dysplasia. A subset of these lesions showed changes indicative of dysplastic crypt architecture and an apparent very subtle cytological dysplasia consistent with non-polypoid HGD in human patients. Chronic insult derived from DSS to the colonic mucosa of mice has been shown to initiate and promote morphological changes indicative of neoplastic transformation [225, 226, 237]. Thus it is plausible that pre-cancerous lesions may arise in the Winnie colon with exacerbation of the pre-existing colitis using DSS.

Longer exposure to a 1% DSS solution would be expected to increase the incidence of dysplasia in Winnie. However, five cycles of 1% DSS did not produce more complex or invasive neoplasia, and no dysplasia was detected in animals allowed to lived beyond the end of the fifth cycle (up to 120 days). Although the lack of animals examined at each time-point following five cycles of DSS makes it difficult make inference about incidence of dysplasia in Winnie mice, it would suggest that the dysplasia-like pathology regresses slowly after DSS is removed.

The most well-characterised pre-cancerous, non-adenomatous lesions in the distal colon identified in rodents are the ACF visible several weeks after administration of AOM-DSS [314]. The ACF lesion may be readily identified by examining the morphology of the

crypt opening stained with methylene blue. The crypt openings within ACF will display a narrow, slit-like and distorted luminal opening. Besides the crypt opening, ACF features may include a raised profile, thickened epithelia, mucin depletion and dysplasia, all to varying degrees [315]. The abnormal crypts observed in the distal and mid-colon of Winnie exhibit some similar features to hyperplastic and dysplastic crypts. In Winnie however, mucin synthesis is reduced due to the Muc2 mutation, so a reduction in mucin is unlikely to be a useful predictor of neoplastic potential. Although dysplastic ACF are considered pre-cursors to colonic carcinoma, a considerable number of ACF may not proceed to form tumours, despite the presence of genetic mutations in genes such KRAS [316, 317]. The abnormal crypts observed in Winnie may therefore be expected to regress when the severe pro-inflammatory stimulus is removed unless tumour-suppressing Apc/β-catenin signalling is inactivated [318].

Winnie mice at the age of eighteen weeks displayed an abnormally high level of epithelial cell proliferation, even without DSS administration. Although not measured in the present study, abnormally high levels of proliferation in the Winnie colonic epithelium may be explained by increases in pro-inflammatory cytokines in response to a defective colonic mucous layer. Though the content of the environmental microbiome is likely to differ between our animal facilities and those from which previous descriptions of Winnie have originated, it might be assumed that the immune reaction to the luminal bacteria maintains an IL-1β/T_H17-dominant cytokine profile [250, 251]. Repair of the colonic epithelial barrier following DSS-induced colitis has been shown to be at least partly dependent on the mucosal production of IL-1β [319]. Also critical to the proliferation of the colonic epithelium during mucosal inflammation is the production of IL-6 [320]. Thus it is conceivable then that chronic production of cytokines such as IL-1β and IL-6 in the Winnie distal colon maintains a heightened epithelial proliferation manifesting as colonic hyperplasia, even without exposure to DSS. A persistent defect in the colonic mucus in Winnie would therefore be expected to promote the rapid accumulation of mutant epithelial cells and formation of

dysplastic lesions. While Winnie mice displayed a florid regenerative response to mucosal inflammation, this appeared to be a transient phenomenon, which would seem somewhat contrary to other murine models of mucous defects.

6.1.1 Mouse strain sensitivities to colitis and neoplasia

Interpretation of disease phenotype induced in mice through single gene deletions or insertions is complicated by the differences between the background genetics of the various inbred mouse strains used. Inbred mouse strains have demonstrated differing susceptibilities to both colitis and colonic neoplasia. It is well known for example, that the C57BL/6J mouse strain displays a comparatively higher resistance to the induction of colitis. The concentration of DSS and length/number of DSS cycles is therefore typically higher in C57BL/6J than that required to induce a similar disease severity in C3H/HeJ mice [321]. Colitis penetrance and severity is considerably increased in 129SvEv *Il10*$^{-/-}$ mice compared to C57BL/6 *Il10*$^{-/-}$ or BALB/c *Il10*$^{-/-}$ animals [239]. Continuous inbreeding of 129SvEv IL-10$^{-/-}$ over a two-year period in some cases produced mice exhibiting reduction in penetrance and severity of disease [240]. Similarly, cross-breeding of 129SvEv mice harbouring Gα_{i2} knock-out mutation with C57BL/6 mice reduced the severity of disease and produced lower rates of neoplasia that reported in pure-bred 129SvEv [246,322]. It should come as no surprise then, that colitis induced by Muc2-deficiency in C57BL/6 mice manifests in early adulthood as opposed to an onset of colitis during weaning as reported in 129Sv mice [323,324]. Background genetics in the C57BL/6J strain used as the basis for the Winnie mutation may therefore account for the lack of advanced neoplasia in Winnie. Susceptibility of the colonic epithelium to neoplastic transformation appears to be similarly modified by the mouse strain. The C57BL/6 strain has been reported to be more resistant to induction of tumours using the azoxymethane than the FVB/N and 129SvJ strains [325]. Since the original description of adenocarcinoma in the *Muc2*$^{-/-}$ was derived from a mixed C57BL/6J $\times$ 129Sv strain, the incidence of neoplasia

may therefore be higher in the colon of the mixed strain than a pure-bred C57BL/6 strain with the same deletion of both *Muc2* alleles [99].

6.1.2 ER stress

The Winnie strain offers a unique pathology for the exploration of chronic colitis due to a primary defect in protein synthesis within the colonic goblet cells. Misfolding of the Muc2 protein within the ER and secretory network of the colonic goblet cells in the Winnie colon is associated with activation of the UPR [250, 326]. All three major UPR pathways (PERK-eIF2α-ATF4, ATF6 and IRE1 pathways) display increased activity in the distal colon of Winnie mice [326]. The engagement of multiple elements of the UPR are likely to have wide-ranging effects on the physiological functioning of the colonic epithelium in Winnie mice, especially where the stress is constantly present. Chronic ER stress and UPR activation results in a global reduction in protein synthesis within the affected cell [327]. Transcription of *Muc2* may itself be the target of UPR-mediated repression as *Muc2* mRNA is reduced in Winnie mice relative to the wild-type [241, 250, 326]. Notably, differentiation of the secretory cell lineage in the Winnie colon may be impaired by the presence of a chronic ER stress since mRNA levels of the transcription factor *Spdef* are also reduced [241]. Most of the crypt lesions resembling dysplasia observed in Winnie following exposure to DSS displayed a depletion in histologically identifiable intracellular mucus. Here immunolabelling of the intestinal trefoil factor-3 (*TFF3*) would enable the measurement of terminally differentiated goblet cell numbers and assistance in determining the extent to which secretory cell maturation is impaired in the abnormal crypts in Winnie. Differentiation of the colonic epithelium is determined by interactions between Notch and Wnt/β-catenin signalling pathways. While Notch and Wnt signalling in the Winnie distal colon has not been studied in detail, Notch is known to increase the transcription of *Myc* [329]. Deletion of *Myc* within the intestinal epithelium prevents the induction of oncogenic expression of Wnt/β-catenin target genes in the absence of functional Apc [328]. Artificial over-

expression of *Myc* alone has been shown to be capable of suppressing the differentiation of intestinal goblet cells, perhaps through de-differentiation or trans-differentiation [329]. While repeated exposure of C57BL/6 mice with wild-type *Muc2* to 1% DSS appeared to induce an up-regulation in *Myc* at the transcriptional level, Winnie mice displayed no such change. While it is unclear which factors restrain *Myc* up-regulation in Winnie following DSS, it is conceivable that the stimulus for this may originate from the UPR. The Myc protein broadly regulates transcription of a number of genes and their translation through ribosome biogenesis [330]. Therefore, it would follow that the UPR, which favours decreased protein synthesis, prevents elevation of *Myc* transcription. How the UPR and expression of Myc interact to influence the survival of goblet cells is unclear and will require analysis of apoptosis and Notch/Wnt signalling. Focal hyperproliferation of goblet cells of the crypt base was detected histochemically in only a single animal exposed to three cycles of 1% DSS. Similar hyperproliferative goblet cell lesions have previously been reported as a 'transitional mucosa' induced by a variety of colonic insults including IBD, and have been observed adjacent to carcinoma [267, 268]. Although it has proved difficult to demonstrate goblet-cell hyperplasia is a precursor to dysplasia, it may suggest the clonal expansion of a cell harbouring epigenetic or genetic mutation(s) with the potential to initiate dysplasia given sufficient time. Indeed immunohistochemically detectable accumulation of p53, a phenomenon only observed when negative-feedback mechanisms that tightly regulate p53 are disrupted, have been reported in goblet cell hyperplasia [331]. Since genetic mutation of *TP53* has been identified in the non-dysplastic colonic epithelium in patients with UC, this raises the possibility that the atypical hyperplasia observed in response to chronic DSS-induced injury could represent a precursor to dysplasia.

6.2 Trp53 as regulator of cell fate in Winnie

Mutations in the *TP53* gene have been reported in approximately 85% of UC-associated cancers [171]. Cancer-associated *TP53* mutations typically involve substitution of a single

amino acid, and do not produce a truncation of the wild-type protein [170]. Oncogenic mutations in *TP53* have been associated with an increased abundance of the p53 protein in the nucleus, perhaps due to its impaired ability to up-regulate expression of the p53-repressor mouse double-minute-2 (MDM2). Inactivating mutations in one or both *Trp53* alleles render mice susceptible to colonic tumourigenesis when environmental insults are introduced. Administration of two cycles of 4% DSS induced neoplasia in up to 100% of *Trp53*$^{-/-}$ mice and 46% of *Trp53*$^{-/-}$ mice, even held under specific pathogen-free conditions [332]. Notably, the morphology of neoplasia arising in the colon of *Trp53*$^{-/-}$ mice appears to correspond to a predominantly flattened profile rather than a polypoid structure [332]. While *Trp53* mutant mice are useful for modelling the progression of tumours from *TP53* mutant clones as is believed to occur in patients with UC, these mice may not replicate the accumulation of cellular mutations preceding p53 mutation. Despite the absence of *Trp53* mutations, increased expression of the p53 protein was observed in AOM-induced colonic neoplasia [333]. Subsequent analysis of the ability of p53 to bind directly to DNA in the colonic epithelium has suggested that the p53 protein may be functionally impaired post-translation. Being that p53 is regulated at the post-transcriptional levels, it is difficult to predict the effect of the p53 up-regulation at the gene level reported in the distal colon of Winnie after three cycles of 1% DSS. In contrast to the findings of the present study, the colonic epithelium of patients with UC displays an increased IL-6-dependent p53 expression during inflammation [334]. Increased p53 expression in Winnie may then suggest that the activity of the p53-dependent DNA damage response is enhanced to prevent the accumulation of cancerous mutations resulting from DNA lesions induced by ROS/RNS. The apparently paradoxical up-regulation of *Trp53* may suggest that additional mechanisms overwhelm the effect of the surrounding chronic inflammation. Unresolved ER stress induced by accumulation of misfolded Muc2 may result in prolonged activation of the UPR in the goblet cells of the Winnie distal colon [241, 250, 326]. Induction of ER stress and the UPR through thapsigargin administration suppressed the expression of p21 (*Cdnk1a*) via

a mechanism dependent on wild-type *TP53*, making cells with wild-type p53 susceptible to DNA damage-induced apoptosis [335]. Through the activation of the PERK-eIF2α-CHOP pathway perhaps renders goblet cells vulnerable to apoptosis thus preventing the accumulation of DNA mutations induced by ROS/RNS. However, transcriptional down-regulation of Trp53 may not promote a oncogenic transformation in the Winnie epithelium without a concomitant inactivation of p21. Examination of the mutational status of both *Trp53* and *Cdkn1a*, together with an assessment of oxidative DNA damage, will therefore be crucial to understanding the mechanisms by which neoplastic transformation may be repressed in the colonic epithelium containing dysfunctional Muc2 synthesis. Overall, chronic activation of the UPR may protect against accrual of ROS-induced DNA mutation and neoplastic transformation through mechanisms that may be mediated by Trp53 and Myc (Fig. 6.1)

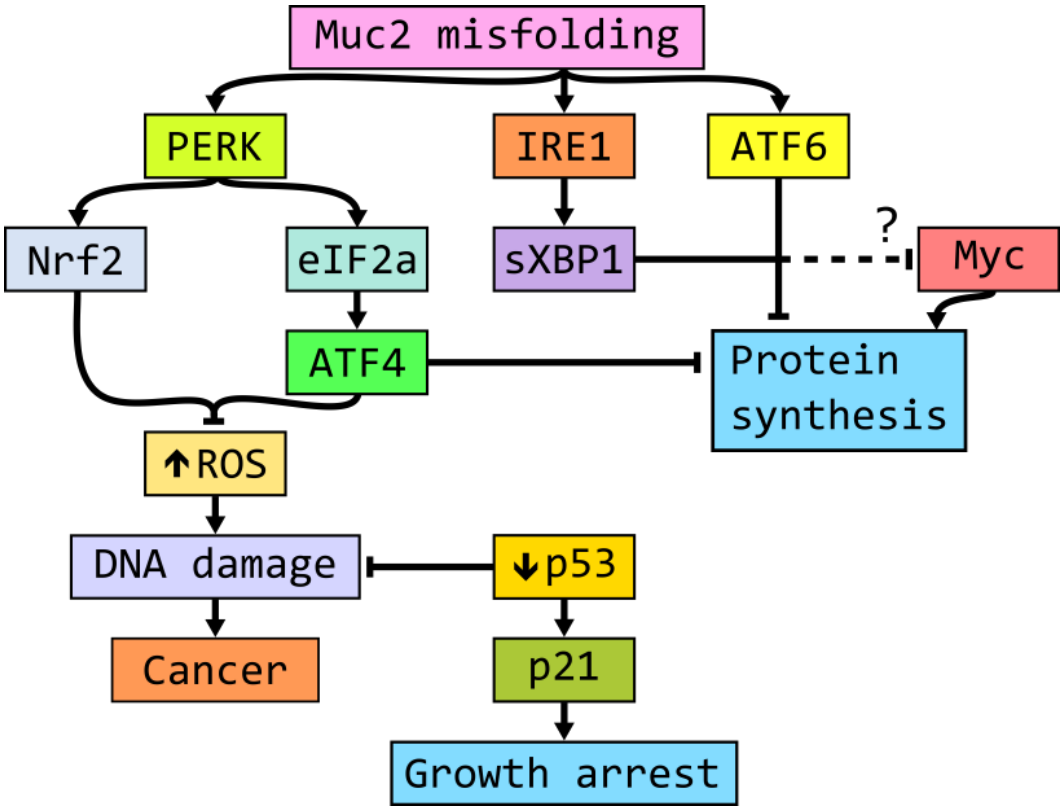

Figure 6.1: **Possible effect of chronic Muc2 misfolding on neoplastic transformation in the colon of Winnie mice.** Misfolded Muc2 accumulations in the colonic goblet cells in Winnie, activating the unfolded protein response (UPR). Activation of the UPR is characterised by increased activity of the PERK, IRE1 and ATF6 pathways. Global protein synthesis is inhibited by the UPR pathways induced by chronic Muc2 misfolding. Activation of the PERK pathway also restricts the acccumulation of reactive oxygen species (ROS) within the stressed cell, potentially limiting the amount of ROS-induced DNA damage. Chronic UPR activation may then protect against ROS-induced DNA damage when p53 transcription is suppressed in the Winnie colonic epithelium, thereby preventing oncogenic genetic mutation. Up-regulation of Myc induced by DSS in the wild-type may be repressed by engagement of the UPR in Winnie to counteract a Myc-induced increase in protein translation. Chronic UPR activation in Winnie may eventually in growth arrest via p53 and p21 or apoptosis initated by the PERK-CHOP pathway.

6.3 Colonic immune responses in Winnie

At present, many murine models of spontaneously occurring colitis exist. Several of these have since been demonstrated to display an abnormal permeability in the adherent, inner colonic mucous layer to bacterium-sized objects, thus suggesting that mucosal inflammation is initiated by bacterial colonisation of the inner mucous layer [100]. Winnie mice typically display a mild chronic colitis, both under our housing conditions and elsewhere, perhaps suggesting that the mucus defect imparted by the missense Muc2 mutation is only partial [250]. Partial abrogation of the mucous barrier in Winnie may be somewhat supported by the fact that even the relatively low 1% (w/v) concentration of DSS is capable of exacerbating the mucosal inflammation and tissue damage further in Winnie. Bacterial contact with the colonic epithelium likely triggers activation of host innate immunity through engagement with epithelial and dendritic cell Toll-like receptors [323]. Interactions with bacterial sensors at the mucosal interface result in the production of the cytokine IL-1β facilitating the release of various pro-inflammatory cytokines and chemokines [336]. Production of the chemokine Cxcl-5 by colonic epithelial cells may be stimulated by both Toll-like receptor signalling and by IL-1β and thus mediates the influx of neutrophils into the colonic mucosa. Chronic production of NF-$\varkappa$B-activating cytokines IL-1β and IL-6 by neutrophils and other phagocytes in the colonic mucosa where Muc2 secretion is impaired is likely amplified by the polarisation of $CD4^+$ T-lymphocytes toward a IL-17-dominant secretion profile [122, 294]. The combined contribution of IL-6 and members of the T_H17 cytokine family in chronic colitis may have the effect of promoting tumourigenesis in the colonic epithelium. Production of IL-6 in particular, has been studied heavily due to its ability to promote tumour growth, invasion and angiogenesis through the STAT-3 signal transduction pathway [337]. The mechanisms through which pro-inflammatory cytokines promote tumourigenesis in the colon though are likely to differ depending on the stage of tumour development. Pro-inflammatory T_H17 family members are important in the invasive stages

of tumour growth. T_H17 cytokines (IL-17A, IL-21, IL-23) are capable of increasing the release of matrix metalloproteinases, the activity of which may degrade the connective tissues underlying colonic epithelial cells, thereby promoting the invasion of the mucosa and later the submucosa by neoplastic epithelium [126, 338]. IL-6 may stimulate the early neoplastic transition in the colonic epithelium is through the activation of DNMT1, thereby increasing the methylation of tumour suppressor genes such as *TP53* [339]. The pro-inflammatory cytokine milieu in the colonic mucosa is therefore likely to facilitate the rapid progression of the colonic epithelium through to pre-malignant dysplasia and on to invasive carcinoma.

Chronic colitis of the distal colon in Winnie is dominated by a T_H17 immune profile. Expansion of activated dendritic cell populations co-incides with enhanced production of lymphoid production of the T_H17-promoting cytokines Il-1β, Il-6, Il-23 and Tgf-β1 and increased T_H17 effectors Il-17a and Il-17f [251]. Despite increased expression of IL-6 in the inflamed colonic mucosa, in our exploratory analysis of gene expression we failed to detect a difference in the expression of IL-6 between untreated Winnie mice and those having received DSS. While immunological changes were not the main focus of the thesis, several additional pro-inflammatory cytokines and chemokines were also analysed due to their potential involvement in both chronic colitis and carcinogenesis. Of the inflammatory mediators analysed at the level of mRNA transcription, only Ccl5 displayed differential expression. Expression of the lymphocyte-chemo-attractant Ccl5 at the gene level corresponded to the level of colitic inflammation and correlated with the severity of crypt distortions in the distal colon of Winnie. While increased expression of Ccl5 may simply reflect a heightened mucosal immune response and damage in the colon of Winnie, Ccl5 is known to promote tumour growth by suppressing the anti-tumour activity of cytotoxic $CD8^+$ T-lymphocytes in the colon [340]. Although production of inflammatory mediators after chronic DSS administration in Winnie is not well-known,the histopathology was somewhat similar to that induced in Winnie with mono-allelic *IL-10* gene deletion [241]. Both the naturally occurring colitis in Winnie, and the severe colitis in *IL-10*$^{-/-}$ Winnies display a prevailing T_H1/T_H17

cytokine profile suggesting that inflammation in DSS is mediated by a similar character of immune response.

6.4 Colitis-associated microbiome

A large number of commensal bacterial species are resident within the colon, normally spatially separated from the colonic epithelium [90, 341]. Although mechanisms through which an imbalance in the microbiome are able to cause IBD are not well defined, it is clear that in a permissive background, a certain microbial community may develop that is capable of producing chronic colitis. For example, goblet cell deficiency in the NLRP6 protein which forms the NLRP6 inflammasome, a complex coupling Muc2 secretion to TLR activation by microbial PAMPs, produces a colitis in mice [155, 342]. Expansion of *Prevotellaceae* in both NLRP6-deficient mice and co-housed wild-type animals was associated with colitis, suggesting that defects in the mucous barrier and innate immunity allow persistent colonisation of pathogenic bacteria to produce chronic disease [343].

In a mouse strain with defective Muc2 synthesis such as Winnie, it might therefore be expected that a defective mucous barrier would permit increased contact with potentially pathogenic bacteria. While the intestinal microbiota was not studied here, effort has already been undertaken to identify the changes in bacterial diversity associated with the spontaneous colitis in Winnie. Like the normal, uninflamed human colon, the colonic microbiota in wild-type C57BL/6 mice maintained in SPF conditions typically displays a dominance of the Bacteroidetes and Firmicutes phyla in the colon [344, 345]. In contrast, Winnie colitis may alter the microbial composition toward a reduction in the relative abundance of *Proteobacteria* in the stool of both 12 week-old Winnie mice and 15 week-old Winnie mice compared to the appendix [346].

Conversely the proportion of *Bacteroidetes* was higher in stool samples than in the appendix of 15 week-old Winnie mice. Within the *Proteobacteria* phylum, the *Helicobacteraceae* family was undetected in the appendix of wild-type C57BL/6 mice yet *Helicobacteraceae*

expanded greatly in the appendix and stool of age-matched Winnie mice [346, 347]. Future investigations will focus on the changing microbial community throughout the course of DSS administration and the period following the cessation of DSS administration using stool and mucosal tissue samples collected during these studies. The abundance of *Helicobacteraeceae* identified within the appendix raises the possibility of a colonisation of the colon by enterohepatic *Helicobacter* species.

6.4.1 Microbiome and progression of CRC

Expansion of bacterial families such as *Prevotella* in the faecal microbiome of patients with CRC have pointed to an association between certain bacteria and CRC and its precursor lesions [348]. Adenomata obtained from human patients display an increased abundance of Firmicutes, Bateroidetes and Proteobacteria families when compared to healthy patients without colonic neoplasia [349]. Since members of these bacterial groups increase in the inflamed colon it raises the question as to whether the presence of these organisms are a initiating factor in CACC. *Fusobacterium nucleatum* has been repeatedly observed at up to 100-fold higher abundance associated with human CRC [350, 351]. *F. nucleatum* expresses the cell-surface adhesin FadA that enables attachment and invasion of colonic epithelial cells via attachment to the host E-cadherin [352]. Adhesion through E-cadherin results in the nuclear translocation of β-catenin and the subsequent oncogenic up-regulation of *Myc* and *Ccnd1*. The increased abundance of *F. nucleatum* attached to colonic tumours relative to the normal epithelium may indicate an impairment in the protection provided by the colonic mucus. Therefore, defective mucus may allow attachment of similar bacteria capable of modifying molecular pathways such as Wnt-β-catenin to influence neoplastic transformation of the colonic epithelium. Bacteria in close proximity to colonic epithelium may also cause genetic mutations through the production of genotoxins. Colibactin (encoded by a gene within the *pks* pathogenicity island) is produced by *Esherichia coli* species and is capable of enhancing AOM-induced tumourigenesis by inducing DNA damage in *Il10*$^{-/-}$ mice [353].

Cytolethal distending toxin produced by *Campylobacter jejuni* exerts nuclease activity on host DNA [354].

Gentoxic ROS/RNS are also produced as by-products of bacterial metabolism, and these may also contribute to epithelial neoplastic transformation. For example, commensal *Enterococcus faecalis* produces large volumes of extracellular superoxide, thereby producing genotoxic peroxide and hydroxyl radicals [355].

Long-standing colonisation of the mucous layer may therefore, when in close proximity, subject the inflamed colonic epithelium to an additional source of DNA damage to the endogenously produced radicals. Tracing the changes in particular bacterial families thought to be associated with colonic dysplasia such as *Helicobacteria* and *Fusobacteria* may yield insight into the microbial changes influencing a possible neoplastic transition of the colonic epithelium.

6.5 Epigenetic control of neoplastic transformation in the colon

Epigenetic alterations are an appealing line of investigation when considering the stage of transition to early dysplasia. Alterations to epigenetic regulation of gene expression through DNA methylation and micro-RNA (miRNA) is likely to be present early in chronic inflammation, potentially initiating and/or promoting the transition to colonic dysplasia.

Quantification of gene promoter methylation may be undertaken through pyrosequencing of bisulphite-converted DNA. A panel of oligonucleotide primers matching the CpG-rich promoter regions of CRC-associated genes were designed based on reported methylation in UC-associated tumours and AOM and DSS-associated tumours in mice. Optimisation of all pyrosequencing primers were not completed before the time of writing the thesis. Completion of the pyrosequencing of tumour suppressors such as p16 in the colonic pathology described in this thesis may provide evidence for a field cancerisation effect in the Winnie colon. Although the sequencing of the samples obtained from the experiments described in this thesis are yet to be completed

Interactions between miRNA and mRNA facilitate the formation of an mRNA-silencing complex which leads to the degradation or inhibition of translation of the mRNA transcript. Analysis of the pattern of miRNA expression in the colonic mucosa in UC has suggested that several miRNAs are abnormally expressed in both active and inactive inflammation [356]. Particularly, miRNA-29a and miRNA-320 were found increased relative to non-IBD tissue in both inactive and active UC suggests that the targets of these miRNAs, which include the tumour suppressor *PTEN* and *DNM3TA* may be suppress DNA methylation in chronic UC [356–358]. Characterisation of differentially regulated miRNAs in the colon of Winnie relative to wild-type Muc2 and quantitative changes with disease progression would provide further mechanisms by which tumour suppressor genes may be repressed without the introduction of genetic mutation.

6.6 Study limitations

The studies described in the thesis focus on the pathology of the distal colon in Winnie mice, following three cycles of 1% DSS. Therefore all the majority of measurements were derived from mice at the same age (18 weeks old) and the same point in the recovery from chronic exposure to DSS. The lack of data collected at additional time-points definitely limits the interpretations that may be made regarding the neoplastic potential of resultant lesions. Examination of multiple time-points were considered in the five-cycle experiment however the number of mice available for each time-point was often limited to a single animal. Therefore it is possible that genuinely neoplastic lesions occurring at a low incidence would not have been detected.

Rectal prolapse was a common occurrence in the Winnie mice used in our experiments, likely arising secondary to the inherent Muc2 defect. Similarly, the original phenotypic characterisation of the Winnie mouse strain reported rectal prolapse in as many as 25% of mice by the age of 8 weeks [250]. In addition to rectal prolapse, ileo-colonic intussusception was observed simultaneously in 2/15 Winnie mice. The low incidence of intestinal intus-

susception, in addition to the relatively small sample size, makes it difficult to draw any conclusions as to the relationship between intussusception and the Winnie mutation.

The preparation of DSS may be another factor which may affect the interpretability of the studies. Though a pilot experiment comparing different commercially available DSS preparations for the full three DSS cycles was not performed, published evidence exists to support the efficacy of the DSS preparation used. Comparison of both Affymetrix-USB and MP Biomedicals DSS preparations suggested comparable levels of tissue damage over seven days of administration to C57BL/6 mice, though the effect of the housing used is unclear [359]. It is possible however that longer administration of DSS may reveal greater differences in the efficacy of the two DSS preparations.

6.7 Future directions

Animal models are useful for improving our understanding of the pathobiology of human IBD and for the testing of diagnostic methods and therapeutic interventions. Genetically engineered animal models may be used to replicate a particular aspect of the disease. To date, a range of genetically engineered models of a chronic colitis arising from defects in the intestinal barrier have been generated.

Compared to sporadic colorectal neoplasms, the neoplasia arising from the chronically inflamed colon often follows a more aggressive course and less easily treated with chemoth-reapeutic agents. Sporadic CRC typically arises from a focal polypoid dysplastic precursor lesion, whereas IBD-associated neoplasms exhibit more morphological variation. Dysplastic lesions which are flat, i.e. not raised above the height of the surrounding mucosa, are more common in patients with IBD. Flat dysplasia is more difficult to detect than visibly raised polypoid dysplasia without the use of chromo-endoscopy. Therefore, detection of multi-focal flat dysplasia, even of low-grade, in the context of chronic UC would often justify surgical resection or perhaps prophylactic colectomy. Given the movement away from a reliance on

surgical intervention in the management of UC, greater understanding of IBD-associated cancer development may refine chemotherapeutic management and neoplastic surveillance. Given the links between colonic cancer and the microbiome in rodents it may prove useful to study the changes in microbial diversity with the administration of 1% DSS in Winnie. Detailed investigations into microbial diversity within the Winnie colon, particularly with a focus on enterohepatic *Helicobacter* species *H. hepaticus* and *H. bilis* may be achievable through qPCR using stool or colonic biopsies and could provide further insight into whether such species modify the risk of neoplasia in Winnie mice.

In addition to microbiological study, it may be useful to analyse DNA modification in the distal colonic epithelium of Winnie mice following DSS. The identification of double-stranded DNA breaks through examination of markers such as the histone $H_2\gamma AX$ would provide stronger evidence supporting the initiation of carcinogenesis. Detection of oxidative DNA adducts such as the 8-OHdG lesion may also provide evidence for the existence of pre-cancerous in Winnie.

6.8 Conclusions

It is suspected that a primary defect in colonic barrier function is responsible for the chronic inflammation associated with UC. The theory of a primary defect in the effectiveness of the barrier separating the colonic mucosa from the luminal microbiota has been supported by experimental evidence derived from *Muc2* and *Il10* mutant mice. Chronic exposure to the commensal species now able to colonise the colonic mucus initiates a destructive T_H17-dominant immune response. Sustained production of ROS/RNS induced by chronic exposure of the resident mucosal immune cells to bacterial antigen, damages DNA while simultaneously inhibiting DNA repair thereby inducing initiating genetic mutations. Repeated and sustained degradation of the mucosal architecture concurrently promote the expansion of epithelial cells through the stimulation of proliferation via cytokines and growth factors, while the same pro-inflammatory milieu may suppress apoptosis of cells with DNA

damage. Additionally, pro-inflammatory signals may also influence epigenetic silencing of key tumour suppressor genes. Together, these mechanisms promote the rapid acquisition of genomic instability and malignant transformation, permitting the rapid invasion and dissemination of tumours from the chronically inflamed mucosa.

Three cycles of 1% DSS increased the severity of mucosal damage to the distal segment of the colon in Winnie mice. Repeated exposure to the insult provided by 1% DSS triggered a florid regenerative response in the colonic mucosa, where abnormal crypt foci resembling dysplasia were present in all Winnie mice exposed to the DSS regimen. Despite the abnormal epithelial cell proliferation in the distal colon and penetration of epithelium into the submucosa, no oncogenic β-catenin accumulation was detected in such lesions. However, an extended observation period after the cessation of the DSS regimen revealed the transient nature of the dysplasia-like pathology. The relatively small number of mice studied following the five-cycle DSS regimen may have made genuine neoplasia difficult to detect, thus confirmation of these results are necessary. Exploratory gene expression analysis in the distal colonic mucosa suggested transcriptional alterations in the genes encoding p53, Myc, Cav1 and Ccl5 in Winnie. In particular Ccl5 expression correlated with the severity of dysplasia-like morphology. Together, these findings may offer a starting point for further investigations into the molecular mechanisms involved in the transition of atypical hyperplastic lesions to dysplasia in colonic disease initiated by a primary secretory cell defect.

APPENDIX A

Additional Tables and Figures

A.1 Supplementary tables

Table A.1: **Gastro-intestinal neoplasia screening primer assays**

Gene Name	Gene Symbol	Assay ID	NCBI Reference
ATP-binding cassette, sub-family B (MDR/TAP), member 1A	Abcb1a	qMmuCID0027076	NC_000071.6, NT_039299.7
BCL2-like 1	Bcl2l1	qMmuCED0025041	NC_000068.7, NT_039207.8
CD14 antigen	Cd14	qMmuCED0003341	NC_000084.6, NT_039674.8
C-reactive protein, pentraxin-related	Crp	qMmuCED0003932	NC_000067.6, NT_039185.8
V-erb-b2 erythroblastic leukemia viral oncogene homolog 2, neuro/glioblastoma derived oncogene homolog (avian)	Erbb2	qMmuCID0005916	NC_000077.6, NT_096135.6
Insulin-like growth factor I receptor	Igf1r	qMmuCID0005315	NC_000073.6, NT_187035.1
Mitogen-activated protein kinase 1	Mapk1	qMmuCID0025360	NC_000082.6, NT_039624.8
Nuclear factor of kappa light polypeptide gene enhancer in B cells 1, p105	Nfkb1	qMmuCID0005357	NC_000069.6, NT_039240.8
Phosphatase and tensin homolog	Pten	qMmuCID0005543	NC_000085.6, NT_039687.8
Secreted acidic cysteine rich glycoprotein	Sparc	qMmuCID0023536	NC_000077.6, NT_096135.6
Tumor necrosis factor	Tnf	qMmuCED0004141	NC_000083.6, NT_039649.8, NT_039662.3, NT_187004.1, NT_187027.1
TATA box binding protein	Tbp	qMmuCID0040542	NC_000083.6, NT_039649.8

Gene Name	Gene Symbol	Assay ID	NCBI Reference
Actin, beta	Actb	qMmuCED0027505	NC_000071.6, NT_039316.8
Brain derived neurotrophic factor	Bdnf	qMmuCED0004519	NC_000068.7, NT_039207.8
CD44 antigen	Cd44	qMmuCID0025677	NC_000068.7, NT_039207.8
Connective tissue growth factor	Ctgf	qMmuCED0003632	NC_000076.6, NT_039492.8
Estrogen receptor 1 (alpha)	Esr1	qMmuCID0018069	NC_000076.6, NT_039490.8
Insulin-like growth factor binding protein 3	Igfbp3	qMmuCID0005232	NC_000077.6, NT_039515.7
Transformed mouse 3T3 cell double minute 2	Mdm2	qMmuCID0025320	NC_000076.6, NT_039500.8
Nuclear factor of kappa light polypeptide gene enhancer in B cells inhibitor, zeta	Nfkbiz	qMmuCID0025623	NC_000082.6, NT_039624.8
Prostaglandin-endoperoxide synthase 2	Ptgs2	qMmuCED0003742	NC_000067.6, NT_078297.7
Secreted phosphoprotein 1	Spp1	qMmuCED0040763	NC_000071.6, NT_109320.5
Tumor necrosis factor receptor superfamily, member 1a	Tnfrsf1a	qMmuCID0023110	NC_000072.6, NT_039353.8
Glyceraldehyde-3-phosphate dehydrogenase	Gapdh	qMmuCED0027497	NC_000072.6, NT_039353.8
Thymoma viral proto-oncogene 1	Akt1	qMmuCID0023089	NC_000078.6, NT_039551.8
Baculoviral IAP repeat-containing 5	Birc5	qMmuCID0006189	NC_000077.6, NT_096135.6
Cadherin 1	Cdh1	qMmuCID0005843	NC_000074.6, NT_078575.7
Catenin (cadherin associated protein), beta 1	Ctnnb1	qMmuCID0006137	NC_000075.6, NT_039482.8

Gene Name	Gene Symbol	Assay ID	NCBI Reference
Enhancer of zeste homolog 2 (Drosophila)	Ezh2	qMmuCID0015459	NC_000072.6, NT_039353.8
Interleukin 10	Il10	qMmuCID0015452	NC_000067.6, NT_078297.7
Antigen identified by monoclonal antibody Ki 67	Mki67	qMmuCID0018717	NC_000073.6, NT_039433.8
Nitric oxide synthase 2, inducible	Nos2	qMmuCID0023087	NC_000077.6, NT_096135.6
Retinoblastoma 1	Rb1	qMmuCID0005286	NC_000080.6, NT_039606.8
ST3 beta-galactoside alpha-2,3-sialyltransferase 5	St3gal5	qMmuCID0016681	NC_000072.6, NT_039353.8
Thymidylate synthase	Tyms	qMmuCID0005615	NC_000071.6, NT_165760.3
Hypoxanthine guanine phosphoribosyl transferase	Hprt	qMmuCID0005679	NC_000086.7, NT_187037.1
Apolipoprotein E	Apoe	qMmuCED0001025	NC_000073.6, NT_187034.1
Breast cancer 1	Brca1	qMmuCID0018895	NC_000077.6, NT_096135.6
Cyclin-dependent kinase 1	Cdk1	qMmuCID0015611	NC_000076.6, NT_039500.8
Chemokine (C-X-C motif) ligand 10	Cxcl10	qMmuCED0001068	NC_000071.6, NT_109320.5
Fibronectin 1	Fn1	qMmuCID0019534	NC_000067.6, NT_039170.8
Interleukin 1 beta	Il1b	qMmuCID0005641	NC_000068.7, NT_039207.8
Matrix metallopeptidase 1a (interstitial collagenase)	Mmp1a	qMmuCID0022392	NC_000075.6, NT_039471.8
Nuclear receptor subfamily 3, group C, member 1	Nr3c1	qMmuCID0016200	NC_000084.6, NT_039674.8
V-rel reticuloendotheliosis viral oncogene homolog A (avian)	Rela	qMmuCID0017564	NC_000085.6, NT_082868.6

Gene Name	Gene Symbol	Assay ID	NCBI Reference
Signal transducer and activator of transcription 1	Stat1	qMmuCID0021143	NC_000067.6, NT_039170.8
Ubiquitin B	Ubb	qMmuCED0026045	NC_000077.6, NT_096135.6
Androgen receptor	Ar	qMmuCID0005164	NC_000086.7, NT_039706.8
Caveolin 1, caveolae protein	Cav1	qMmuCID0020997	NC_000072.6, NT_039340.7
Cyclin-dependent kinase inhibitor 1A (P21)	Cdkn1a	qMmuCED0025027	NC_000083.6, NT_039649.8, NT_187005.1
Chemokine (C-X-C motif) ligand 12	Cxcl12	qMmuCID0019961	NC_000072.6, NT_039353.8
FBJ osteosarcoma oncogene	Fos	qMmuCED0001023	NC_000078.6, NT_039551.8
Interleukin 6	Il6	qMmuCID0005613	NC_000071.6, NT_165760.3
Matrix metallopeptidase 2	Mmp2	qMmuCID0021124	NC_000074.6, NT_078575.7
Proliferating cell nuclear antigen	Pcna	qMmuCED0040851	NC_000068.7, NT_039207.8
Serine (or cysteine) peptidase inhibitor, clade E, member 1	Serpine1	qMmuCID0027303	NC_000071.6, NT_039314.8
Signal transducer and activator of transcription 3	Stat3	qMmuCID0021132	NC_000077.6, NT_096135.6
Ubiquitin C	Ubc	qMmuCID0021036	NC_000071.6, NT_039313.8
Aurora kinase A	Aurka	qMmuCID0006166	NC_000068.7, NT_039207.8
Chemokine (C-C motif) ligand 5	Ccl5	qMmuCID0021047	NC_000077.6, NT_096135.6
Cyclin-dependent kinase inhibitor 2A	Cdkn2a	qMmuCED0038108	NC_000070.6, NT_187032.1

Gene Name	Gene Symbol	Assay ID	NCBI Reference
Chemokine (C-X-C motif) receptor 4	Cxcr4	qMmuCED0026325	NC_000067.6, NT_078297.7
Hypoxia inducible factor 1, alpha subunit	Hif1a	qMmuCID0005501	NC_000078.6, NT_039551.8
Jun oncogene	Jun	qMmuCED0003314	NC_000070.6, NT_039264.7
Matrix metallopeptidase 9	Mmp9	qMmuCID0021296	NC_000068.7, NT_039207.8
Plasminogen activator, urokinase	Plau	qMmuCID0022420	NC_000080.6, NT_039606.8
MAD homolog 7 (Drosophila)	Smad7	qMmuCID0016983	NC_000084.6, NT_039674.8
Telomerase reverse transcriptase	Tert	qMmuCID0018719	NC_000079.6, NT_039589.8
Vitamin D receptor	Vdr	qMmuCID0006555	NC_000081.6, NT_039621.8
BCL2-associated X protein	Bax	qMmuCID0006274	NC_000073.6, NT_187035.1
Cyclin B1	Ccnb1	qMmuCED0024590	NC_000079.6, NT_039590.8
Collagen, type I, alpha 1	Col1a1	qMmuCID0021007	NC_000077.6, NT_096135.6
Epidermal growth factor receptor	Egfr	qMmuCID0006030	NC_000077.6, NT_039515.7
Interferon gamma	Ifng	qMmuCID0006268	NC_000076.6, NT_039500.8
Kinase insert domain protein receptor	Kdr	qMmuCID0005890	NC_000071.6, NT_039306.8
Mucin 1, transmembrane	Muc1	qMmuCED0003916	NC_000069.6, NT_039240.8
Peroxisome proliferator activated receptor gamma	Pparg	qMmuCID0018821	NC_000072.6, NT_039353.8
Superoxide dismutase 2, mitochondrial	Sod2	qMmuCID0006109	NC_000083.6, NT_039638.8

Gene Name	Gene Symbol	Assay ID	NCBI Reference
Transforming growth factor, beta 1	Tgfb1	qMmuCID0017320	NC_000073.6, NT_187034.1
Vascular endothelial growth factor A	Vegfa	qMmuCED0040260	NC_000083.6, NT_039649.8
B cell leukemia/lymphoma 2	Bcl2	qMmuCED0039968	NC_000067.6, NT_078297.7
Cyclin D1	Ccnd1	qMmuCID0023518	NC_000073.6, NT_039437.8
Collagen, type I, alpha 2	Col1a2	qMmuCID0021177	NC_000072.6, NT_039340.7
Early growth response 1	Egr1	qMmuCED0039815	NC_000084.6, NT_039674.8
Insulin-like growth factor 1	Igf1	qMmuCID0005726	NC_000076.6, NT_039500.8
V-Ki-ras2 Kirsten rat sarcoma viral oncogene homolog	Kras	qMmuCID0005957	NC_000072.6, NT_039360.8, NT_166305.2
Myelocytomatosis oncogene	Myc	qMmuCID0006528	NC_000081.6, NT_039621.8
Prominin 1	Prom1	qMmuCID0021742	NC_000071.6, NT_039305.8
Trans-acting transcription factor 1	Sp1	qMmuCED0025031	NC_000081.6, NT_039621.8
Tissue inhibitor of metalloproteinase 1	Timp1	qMmuCID0025322	NC_000086.7, NT_039700.8
Vimentin	Vim	qMmuCID0005527	NC_000068.7, NT_039202.8

Table A.2: **TaqMan primer/probe assays**

Gene Name	Gene Symbol	Assay ID	NCBI Reference
Caveolin-1	Cav1	Mm00483057_m1	NM_001243064.1, NM_007616.4
C-C-motif chemokine ligand-5	Ccl5	Mm01302427_m1	NM_013653.3
Cyclin-dependent kinase inhibitor-2A	Cdkn2a	Mm00494449_m1	NM_001040654.1, NM_009877.2
C-X-C-motif chemokine ligand-5	Cxcl5	Mm00436451_g1	NM_009141.3
C-X-C-motif chemokine ligand-12	Cxcl12	Mm00445553_m1	NM_001012477.2, NM_013655.4, NM_021704.3
Interleukin-6	Il6	Mm00446190_m1	NM_031168.1
Mucin-1	Muc1	Mm00449604_m1	NM_013605.2
Myelocytomatosis oncogene	Myc	Mm00487804_m1	NM_010849.4, NM_001177352.1, NM_001177353.1, NM_001177354.1
Peroxisome proliferator-activated receptor-γ	Pparg	Mm01184322_m1	NM_011146.3, NM_001127330.1
Prominin-1	Prom1	Mm00477115_m1	NM_008935.2, NM_001163578.1, NM_001163577.1, NM_001163582.1, NM_001163583.1, NM_001163581.1, NM_001163584.1, NM_001163585.1
Prostaglandin-endoperoxide synthase 2	Ptgs2	Mm00478374_m1	NM_011198.3
Secreted phosphoprotein-1	Spp1	Mm00436767_m1	NM_001204201.1, NM_001204202.1, NM_001204203.1, NM_001204233.1, NM_009263.3
Telomerase reverse-transcriptase	Tert	Mm00436931_m1	NM_009354.1
Transformation-related protein-53	Trp53	Mm01731290_g1	NM_001127233.1, NM_011640.3
Vimentin	Vim	Mm01333430_m1	NM_011701.4

Table A.3: **Primer sequences for DNA methylation pyrosequencing**

Gene	Sequence	Amplicon	No. of CpGs
Adh	F: GGGTTAAGAGTTTAATAATTGATAGTGAG R: ATTTCAATTTAACTTTTTTTCCTAACTACT S: GTGAGAATTGGGTGTT		4
B3gnt7	F: AGTGAAGGATTTGTTGGTAATATAAGA R: CCTCTACAAAAAATCCATTCTTTTACT S: AGAGTTTTATTAGGGAGATTT		3
Cdh1	F: TGGTGGAAGAAGAGAATTGATT R: AAAAACTTCCCAACTTCCTATTC S: TGAAGGTTGTAGTTTTATTTTTATA		10
p16	F: GGGGGGAATAGTAGTGTTTTT R: CTCCATACTACTCCAAATAACTCTC S: GGAAGGAGGGATTTATTG		7
p19	F: TTGTTAAGGGGATTTTGGGTTTGA R: ACATCCCCCACTCTTCCTCTT S: GGATTTTGGGTTTGATTT		3
Kcne3	F: GTGTTTAAGATTGGTTTTGAGGGTATT R: CTCCTTCAAAACACATCCTTATTATATTA S: TTAAATTTTTTAGGAGGAGT		6
Nr5a2	F: GGGTTTTAGTATTAGTTAAAGTATGAGTGT R: CCCAAACCAAAACACTAACTTACCTTATT S: TGTTTTTGGTAAGGGAT		9
Rassf1a	F: GGGTAGGGGGAGAAGATTGGA R: ACACCCCCCCCAAAATCCA S: GAAAGGGTTTATTTTTGTG		10
Sorbs2	F: GTTTTTGTTAGTATTGGGAAGGTTTG R: ACCTCCACTAAATTCCTCCTTAAATTTCAC S: TGGTGAGTATGTTAGG		7
Smad7	F: GGGAGAGGGTGGTAGTAAT R: TCCCTCTACTCCACTAATTCCACT S: TTTTTTAAAGAGATAGGGTGTT		8
Vdr	F: AGGAATGGTTGAATGTAGATGT R: ACTAAACTCAACTTATCAATCCTAATAACA S: GAGATAAGGAATTTGGGA		6

APPENDIX B

Additional Tables and Figures

Approval permit from University of Tasmania Animal Experimental Ethics Committee

UTAS	University of Tasmania Animal Ethics Committee **ETHICS APPROVAL PERMIT**	University of Tasmania Office of Research Services Ph: 03 62267283 Fax: 03 62267148 animal.ethics@utas.edu.au

To:	Dr Raj Eri
From:	Marilyn Pugsley Ethics Officer Animal Ethics
Date:	2 July 2013
Project:	A13329 – Investigation of carcinogenesis pathways in colitis-associated colorectal cancer
Approved on:	1 July 2013
Approval expires:	1 July 2016
1st Annual Report due:	1 July 2014

Please read this permit carefully as **approval may be withdrawn** for projects that do not comply with the conditions

The Animal Ethics Committee has approved the above project. The approval is subject to the review and approval of an annual report which is due on the approval anniversary**. Please note this date in your diary.**

If the project is to continue past the expiry date, a new initial application will need to be submitted. A project can only be approved for a maximum of 3 years.

As the Responsible Investigator, you MUST ensure that:

(a) all aspects of the work conform to the requirements of the current edition of the *Australian code of practice for the care and use of animals for scientific purposes*

(b) a full record is maintained of all animals used in this project. If at any stage you anticipate the need to use additional animals this must be communicated to the committee before use. Using additional animals without AEC approval is a breach of your ethics permit.

(c) you contact the Animal Welfare Officer, Dr Sue Ottomanski (sue.ottomanski@utas.edu.au) to advise her when and where your experiments will be conducted. Sufficient notice needs to be given so that if the AWO wishes to make an inspection, this can be easily arranged.

(d) That all investigators attend Ethics training sessions every three years. The next session is scheduled for 10 am to 1 pm on 12 July 2013. Full details can be found on the website.

Histology scoresheet for assessment of colitis

Crypt Architecture		PC	MC	DC
0	Normal			
1	Irregular			
2	Moderate crypt loss (10-50%)			
3	Severe crypt loss (50-90%)			
4	Small/medium-sized ulcers ($>$10 crypt widths)			
5	Large ulcers ($>$10 crypt widths)			
Crypt Abscesses				
0	None			
1	1-5			
2	6-10			
3	$>$10			
Crypt Length				
PC	0, $<$150 μm, 1, 150-199 μm, 2, 200-249 μm, 3, 250-299 μm, 4, $\geq$300 μm			
MC	0, $<$250 μm, 1, 250-299 μm, 2, 300-349 μm, 3, 350-399 μm, 4, $\geq$400 μm			
DC	0, $<$200 μm, 1, 200-249 μm, 2, 250-299 μm, 3, 300-349 μm, 4, $\geq$350 μm			
Tissue Damage				
0	No damage			
1	Focally dilated glands and/or attenuated surface epithelium, decreased goblet cells			
2	Focally extensive gland dilation and/or surface epithelial attenuation			
3	Mucosal erosions (necrosis confined to the mucosa)			
4	Ulceration (necrosis extending into the submucosa or deeper)			
Goblet cell loss				
0	Normal			
1	$<$10% loss			
2	10-24% loss			
3	25-49%			
4	$\geq$50%			
Inflammatory cell infiltration				
0	Occasional infiltration			
1	Small, mucosal leukocyte aggregates			
2	Confluent mucosal or submucosal leukocyte aggregates			
3	Confluence of mucosal leukocytic infiltrate and mulifocal submucosal extension $\pm$ lymphoid follicle formation			
4	Severe diffuse infiltration into the mucosa, submucosa & deeper layers			
Lamina propria neutrophils				
0	0-5 neutrophils/high-power field			

BIBLIOGRAPHY

[1] Cosnes J, Gower-Rousseau C, Seksik P, Cortot A. Epidemiology and natural history of inflammatory bowel diseases. Gastroenterology. 2011;140(6):1785–94.

[2] Molodecky NA, Soon IS, Rabi DM, Ghali WA, Ferris M, Chernoff G, et al. Increasing incidence and prevalence of the inflammatory bowel diseases with time, based on systematic review. Gastroenterology. 2012;142(1):46–54 e42; quiz e30.

[3] Loftus EV. Clinical epidemiology of inflammatory bowel disease: Incidence, prevalence, and environmental influences. Gastroenterology. 2004;126:1504–1517.

[4] Gearry RB, Richardson A, Frampton CMA, Collett JA, Burt MJ, Chapman BA, et al. High incidence of Crohn's disease in Canterbury, New Zealand: results of an epidemiologic study. Inflammatory bowel diseases. 2006;12:936–943. doi:10.1097/01.mib.0000231572.88806.b9.

[5] Wilson J, Hair C, Knight R, Catto-Smith A, Bell S, Kamm M, et al. High incidence of inflammatory bowel disease in Australia: a prospective population-based Australian incidence study. Inflamm Bowel Dis. 2010;16(9):1550–6.

[6] Ng SC, Tang W, Ching JY, Wong M, Chow CM, Hui AJ, et al. Incidence and phenotype of inflammatory bowel disease based on results from the Asia-pacific Crohn's and colitis epidemiology study. Gastroenterology. 2013;145:158–165.e2. doi:10.1053/j.gastro.2013.04.007.

[7] Ng SC, Bernstein CN, Vatn MH, Lakatos PL, Loftus EV, Tysk C, et al. Geographical variability and environmental risk factors in inflammatory bowel disease. Gut. 2013;62:630–649. doi:10.1136/gutjnl-2012-303661.

[8] Thia KT, Loftus EV, Sandborn WJ, Yang SK. An update on the epidemiology of inflammatory bowel disease in Asia. The American journal of gastroenterology. 2008;103:3167–3182. doi:10.1111/j.1572-0241.2008.02158.x.

[9] Yang SK, Yun S, Kim JH, Park JY, Kim HY, Kim YH, et al. Epidemiology of inflammatory bowel disease in the Songpa-Kangdong district, Seoul, Korea, 1986-2005: a KASID study. Inflammatory bowel diseases. 2008;14:542–549. doi:10.1002/ibd.20310.

[10] Morita N, Toki S, Hirohashi T, Minoda T, Ogawa K, Kono S, et al. Incidence and prevalence of inflammatory bowel disease in Japan: nationwide epidemiological survey during the year 1991. Journal of gastroenterology. 1995;30 Suppl 8:1–4.

[11] Ekbom A, Helmick C, Zack M, Adami HO. The epidemiology of inflammatory bowel disease: a large, population-based study in Sweden. Gastroenterology. 1991;100:350–358.

[12] Loftus EV, Silverstein MD, Sandborn WJ, Tremaine WJ, Harmsen WS, Zinsmeister AR. Ulcerative colitis in Olmsted County, Minnesota, 1940-1993: incidence, prevalence, and survival. Gut. 2000;46:336–343.

[13] Hou JK, El-Serag H, Thirumurthi S. Distribution and manifestations of inflammatory bowel disease in Asians, Hispanics, and African Americans: a systematic review. The American journal of gastroenterology. 2009;104:2100–2109. doi:10.1038/ajg.2009.190.

[14] Probert CS, Jayanthi V, Pinder D, Wicks AC, Mayberry JF. Epidemiological study of ulcerative proctocolitis in Indian migrants and the indigenous population of Leicestershire. Gut. 1992;33:687–693.

[15] Carr I, Mayberry JF. The effects of migration on ulcerative colitis: a three-year prospective study among Europeans and first- and second- generation South Asians in Leicester (1991-1994). The American journal of gastroenterology. 1999;94:2918–2922. doi:10.1111/j.1572-0241.1999.01438.x.

[16] Li X, Sundquist J, Hemminki K, Sundquist K. Risk of inflammatory bowel disease in first- and second-generation immigrants in Sweden: a nationwide follow-up study. Inflammatory bowel diseases. 2011;17:1784–1791. doi:10.1002/ibd.21535.

[17] Benchimol EI, Mack DR, Guttmann A, Nguyen GC, To T, Mojaverian N, et al. Inflammatory bowel disease in immigrants to Canada and their children: a population-based cohort study. The American journal of gastroenterology. 2015;110:553–563. doi:10.1038/ajg.2015.52.

[18] Vind I, Riis L, Jess T, Knudsen E, Pedersen N, Elkjaer M, et al. Increasing incidences of inflammatory bowel disease and decreasing surgery rates in Copenhagen City and County, 2003-2005: a population-based study from the Danish Crohn colitis database. The American journal of gastroenterology. 2006;101:1274–1282. doi:10.1111/j.1572-0241.2006.00552.x.

[19] Langholz E, Munkholm P, Krasilnikoff PA, Binder V. Inflammatory bowel diseases with onset in childhood. Clinical features, morbidity, and mortality in a regional cohort. Scandinavian journal of gastroenterology. 1997;32:139–147.

[20] Molinié F, Gower-Rousseau C, Yzet T, Merle V, Grandbastien B, Marti R, et al. Opposite evolution in incidence of Crohn's disease and ulcerative colitis in Northern France (1988-1999). Gut. 2004;53:843–848.

[21] Bernstein CN, Wajda A, Svenson LW, MacKenzie A, Koehoorn M, Jackson M, et al. The epidemiology of inflammatory bowel disease in Canada: a population-based study. The American journal of gastroenterology. 2006;101:1559–1568. doi:10.1111/j.1572-0241.2006.00603.x.

[22] Loftus CG, Loftus EV, Harmsen WS, Zinsmeister AR, Tremaine WJ, Melton LJ, et al. Update on the incidence and prevalence of Crohn's disease and ulcerative colitis in Olmsted County, Minnesota, 1940-2000. Inflammatory bowel diseases. 2007;13:254–261. doi:10.1002/ibd.20029.

[23] Mahid SS, Minor KS, Soto RE, Hornung CA, Galandiuk S. Smoking and inflammatory bowel disease: a meta-analysis. Mayo Clinic proceedings. 2006;81:1462–1471. doi:10.4065/81.11.1462.

[24] Lakatos PL, Vegh Z, Lovasz BD, David G, Pandur T, Erdelyi Z, et al. Is current smoking still an important environmental factor in inflammatory bowel diseases? Results from a population-based incident cohort. Inflammatory bowel diseases. 2013;19:1010–1017. doi:10.1097/MIB.0b013e3182802b3e.

[25] Gearry RB, Richardson AK, Frampton CM, Dodgshun AJ, Barclay ML. Population-based cases control study of inflammatory bowel disease risk factors. Journal of gastroenterology and hepatology. 2010;25:325–333. doi:10.1111/j.1440-1746.2009.06140.x.

[26] Russell RK, Farhadi R, Wilson M, Drummond H, Satsangi J, Wilson DC. Perinatal passive smoke exposure may be more important than childhood exposure in the risk of developing childhood IBD. Gut. 2005;54:1500–1; author reply 1501.

[27] Baron S, Turck D, Leplat C, Merle V, Gower-Rousseau C, Marti R, et al. Environmental risk factors in paediatric inflammatory bowel diseases: a population based case control study. Gut. 2005;54:357–363. doi:10.1136/gut.2004.054353.

[28] Naganuma M, Iizuka B, Torii A, Ogihara T, Kawamura Y, Ichinose M, et al. Appendectomy protects against the development of ulcerative colitis and reduces its recurrence: results of a multicenter case-controlled study in Japan. The American journal of gastroenterology. 2001;96:1123–1126. doi:10.1111/j.1572-0241.2001.03757.x.

[29] Radford-Smith GL, Edwards JE, Purdie DM, Pandeya N, Watson M, Martin NG, et al. Protective role of appendicectomy on onset and severity of ulcerative colitis and Crohn's disease. Gut. 2002;51:808–813.

[30] Florin THJ, Pandeya N, Radford-Smith GL. Epidemiology of appendicectomy in primary sclerosing cholangitis and ulcerative colitis: its influence on the clinical behaviour of these diseases. Gut. 2004;53:973–979.

[31] Selby WS, Griffin S, Abraham N, Solomon MJ. Appendectomy protects against the development of ulcerative colitis but does not affect its course. The American journal of gastroenterology. 2002;97:2834–2838. doi:10.1111/j.1572-0241.2002.07049.x.

[32] Hallas J, Gaist D, Vach W, Sørensen HT. Appendicectomy has no beneficial effect on admission rates in patients with ulcerative colitis. Gut. 2004;53:351–354.

[33] Gardenbroek TJ, Eshuis EJ, Ponsioen CIJ, Ubbink DT, D'Haens GRAM, Bemelman WA. The effect of appendectomy on the course of ulcerative colitis: a systematic review. Colorectal disease : the official journal of the Association of Coloproctology of Great Britain and Ireland. 2012;14:545–553. doi:10.1111/j.1463-1318.2011.02600.x.

[34] Parian A, Limketkai B, Koh J, Brant SR, Bitton A, Cho JH, et al. Appendectomy does not decrease the risk of future colectomy in UC: results from a large cohort and meta-analysis. Gut. 2016;doi:10.1136/gutjnl-2016-311550.

[35] Rubin DT. The changing face of colorectal cancer in inflammatory bowel disease: progress at last! Gastroenterology. 2006;130(4):1350–2.

[36] Rao SS, Holdsworth CD, Read NW. Symptoms and stool patterns in patients with ulcerative colitis. Gut. 1988;29(3):342–5.

[37] Nikolaus S, Schreiber S. Diagnostics of inflammatory bowel disease. Gastroenterology. 2007;133(5):1670–89.

[38] Bernstein CN, Nugent Z, Blanchard JF. 5-aminosalicylate is not chemoprophylactic for colorectal cancer in IBD: a population based study. Am J Gastroenterol. 2011;106(4):731–6.

[39] van Schaik FD, van Oijen MG, Smeets HM, van der Heijden GJ, Siersema PD, Oldenburg B. Thiopurines prevent advanced colorectal neoplasia in patients with inflammatory bowel disease. Gut. 2012;61(2):235–40.

[40] Tang J, Sharif O, Pai C, Silverman AL. Mesalamine protects against colorectal cancer in inflammatory bowel disease. Dig Dis Sci. 2010;55(6):1696–703.

[41] Katzka I, Brody B. Cancer risk in ulcerative colitis. Gastroenterology. 1983;85(3):787–8.

[42] Jess T, Loftus J E V, Velayos FS, Harmsen WS, Zinsmeister AR, Smyrk TC, et al. Risk of intestinal cancer in inflammatory bowel disease: a population-based study from olmsted county, Minnesota. Gastroenterology. 2006;130(4):1039–46.

[43] Rutter MD, Saunders BP, Wilkinson KH, Rumbles S, Schofield G, Kamm MA, et al. Thirty-year analysis of a colonoscopic surveillance program for neoplasia in ulcerative colitis. Gastroenterology. 2006;130(4):1030–8.

[44] Haskell H, Andrews J C W, Reddy SI, Dendrinos K, Farraye FA, Stucchi AF, et al. Pathologic features and clinical significance of "backwash" ileitis in ulcerative colitis. Am J Surg Pathol. 2005;29(11):1472–81.

[45] Buck JL, Harned RK, Lichtenstein JE, Sobin LH. Peutz-Jeghers syndrome. Radiographics : a review publication of the Radiological Society of North America, Inc. 1992;12:365–378. doi:10.1148/radiographics.12.2.1561426.

[46] Rozenbajgier C, Ruck P, Jenss H, Kaiserling E. Filiform polyposis: a case report describing clinical, morphological, and immunohistochemical findings. The Clinical investigator. 1992;70:520–528.

[47] Oakley GJ, Schraut WH, Peel R, Krasinskas A. Diffuse filiform polyposis with unique histology mimicking familial adenomatous polyposis in a patient without inflammatory bowel disease. Archives of pathology & laboratory medicine. 2007;131:1821–1824. doi:10.1043/1543-2165(2007)131[1821:DFPWUH]2.0.CO;2.

[48] Lim YJ, Choi JH, Yang CH. What is the Clinical Relevance of Filiform Polyposis? Gut and liver. 2012;6:524–526. doi:10.5009/gnl.2012.6.4.524.

[49] Buck JL, Dachman AH, Sobin LH. Polypoid and pseudopolypoid manifestations of inflammatory bowel disease. Radiographics : a review publication of the Radiological Society of North America, Inc. 1991;11:293–304. doi:10.1148/radiographics.11.2.2028064.

[50] Kelly JK, Langevin JM, Price LM, Hershfield NB, Share S, Blustein P. Giant and symptomatic inflammatory polyps of the colon in idiopathic inflammatory bowel disease. The American journal of surgical pathology. 1986;10:420–428.

[51] Marinis A, Yiallourou A, Samanides L, Dafnios N, Anastasopoulos G, Vassiliou I, et al. Intussusception of the bowel in adults: a review. World J Gastroenterol. 2009;15(4):407–11.

[52] Warfield KL, Blutt SE, Crawford SE, Kang G, Conner ME. Rotavirus infection enhances lipopolysaccharide-induced intussusception in a mouse model. J Virol. 2006;80(24):12377–86.

[53] Yakan S, Caliskan C, Makay O, Denecli AG, Korkut MA. Intussusception in adults: clinical characteristics, diagnosis and operative strategies. World journal of gastroenterology. 2009;15:1985–1989.

[54] Azar T, Berger DL. Adult intussusception. Annals of surgery. 1997;226:134–138.

[55] Reijnen HA, Joosten HJ, de Boer HH. Diagnosis and treatment of adult intussusception. American journal of surgery. 1989;158:25–28.

[56] Coghlan E, Nadales A, Laferrere L, Terres M, Perotti JP. Colocolic intussusception in a patient with ulcerative colitis. Inflammatory bowel diseases. 2010;16:1085–1087. doi:10.1002/ibd.21123.

[57] Maldonado TS, Firoozi B, Stone D, Hiotis K. Colocolonic intussusception of a giant pseudopolyp in a patient with ulcerative colitis: a case report and review of the literature. Inflammatory bowel diseases. 2004;10:41–44.

[58] Cantarella S, Zisa M, Grasso E, Politi A, Guastella T. The intussusception in patients with Crohn's disease: the role of the surgeon. Updates in surgery. 2013;65:77–80. doi:10.1007/s13304-011-0111-6.

[59] Uchino M, Ikeuchi H, Matsuoka H, Tanaka K, Kuno T, Ohshima T, et al. Postoperative enteroenteric intussusception in patients with Crohn's disease: report of two cases. Surgery today. 2008;38:366–370. doi:10.1007/s00595-007-3624-3.

[60] Draganic B, Williamson M, Stewart P. Colonic intussusception in Crohn's disease. The Australian and New Zealand journal of surgery. 1999;69:683–684.

[61] Kihiczak D, Rosenfeld DL. Crohn's disease presenting as intermittent ileocolic intussusception. Clinical pediatrics. 1998;37:635–638. doi:10.1177/000992289803701009.

[62] Betts G, Jones E, Junaid S, El-Shanawany T, Scurr M, Mizen P, et al. Suppression of tumour-specific CD4(+) T cells by regulatory T cells is associated with progression of human colorectal cancer. Gut. 2012;61(8):1163–71.

[63] Williams GR, Jaffe S, Scott CA. Inflammatory fibroid polyp of the terminal ileum presenting in a patient with active Crohn's disease. Histopathology. 1992;20:545–547.

[64] Edwards FC, Truelove SC. The course and prognosis of ulcerative colitis. iii. complications. Gut. 1964;5:1–22.

[65] du Boulay CE, Fairbrother J, Isaacson PG. Mucosal prolapse syndrome–a unifying concept for solitary ulcer syndrome and related disorders. Journal of clinical pathology. 1983;36:1264–1268.

[66] Tendler DA, Aboudola S, Zacks JF, O'Brien MJ, Kelly CP. Prolapsing mucosal polyps: an underrecognized form of colonic polyp–a clinicopathological study of 15 cases. The American journal of gastroenterology. 2002;97:370–376. doi:10.1111/j.1572-0241.2002.05472.x.

[67] Singh B, Mortensen NJM, Warren BF. Histopathological mimicry in mucosal prolapse. Histopathology. 2007;50:97–102. doi:10.1111/j.1365-2559.2006.02552.x.

[68] Siafakas C, Vottler TP, Andersen JM. Rectal prolapse in pediatrics. Clinical pediatrics. 1999;38:63–72.

[69] Miller CL, Muthupalani S, Shen Z, Fox JG. Isolation of Helicobacter spp. from mice with rectal prolapses. Comp Med. 2014;64(3):171–8.

[70] Kraemer M, Paulus W, Kara D, Mankewitz S, Rozsnoki S. Rectal prolapse traumatizes rectal neuromuscular microstructure explaining persistent rectal dysfunction. International journal of colorectal disease. 2016;31:1855–1861. doi:10.1007/s00384-016-2649-8.

[71] Rahman AA, Robinson AM, Brookes SJH, Eri R, Nurgali K. Rectal prolapse in Winnie mice with spontaneous chronic colitis: changes in intrinsic and extrinsic innervation of the rectum. Cell and tissue research. 2016;366:285–299. doi:10.1007/s00441-016-2465-z.

[72] Miller CL, Muthupalani S, Shen Z, Drees F, Ge Z, Feng Y, et al. Lamellipodin-Deficient Mice: A Model of Rectal Carcinoma. PloS one. 2016;11:e0152940. doi:10.1371/journal.pone.0152940.

[73] Hendriksen C, Kreiner S, Binder V. Long term prognosis in ulcerative colitis–based on results from a regional patient group from the county of Copenhagen. Gut. 1985;26(2):158–63.

[74] Canavan C, Abrams KR, Mayberry J. Meta-analysis: colorectal and small bowel cancer risk in patients with Crohn's disease. Aliment Pharmacol Ther. 2006;23(8):1097–104.

[75] Herrinton LJ, Liu L, Levin TR, Allison JE, Lewis JD, Velayos F. Incidence and mortality of colorectal adenocarcinoma in persons with inflammatory bowel disease from 1998 to 2010. Gastroenterology. 2012;143(2):382–9.

[76] Jess T, Rungoe C, Peyrin-Biroulet L. Risk of colorectal cancer in patients with ulcerative colitis: a meta-analysis of population-based cohort studies. Clin Gastroenterol Hepatol. 2012;10(6):639–45.

[77] Jess T, Simonsen J, Jorgensen KT, Pedersen BV, Nielsen NM, Frisch M. Decreasing risk of colorectal cancer in patients with inflammatory bowel disease over 30 years. Gastroenterology. 2012;143(2):375–81 e1; quiz e13–4.

[78] Jess T, Riis L, Vind I, Winther KV, Borg S, Binder V, et al. Changes in clinical characteristics, course, and prognosis of inflammatory bowel disease during the last 5 decades: a population-based study from Copenhagen, Denmark. Inflamm Bowel Dis. 2007;13(4):481–9.

[79] Eaden JA, Abrams KR, Mayberry JF. The risk of colorectal cancer in ulcerative colitis: a meta-analysis. Gut. 2001;48(4):526–35.

[80] Neal RD, Din NU, Hamilton W, Ukoumunne OC, Carter B, Stapley S, et al. Comparison of cancer diagnostic intervals before and after implementation of NICE guidelines: analysis of data from the UK General Practice Research Database. Br J Cancer. 2014;110(3):584–92.

[81] Lutgens MW, Vleggaar FP, Schipper ME, Stokkers PC, van der Woude CJ, Hommes DW, et al. High frequency of early colorectal cancer in inflammatory bowel disease. Gut. 2008;57(9):1246–51.

[82] Baars JE, Kuipers EJ, van Haastert M, Nicolai JJ, Poen AC, van der Woude CJ. Age at diagnosis of inflammatory bowel disease influences early development of colorectal cancer in inflammatory bowel disease patients: a nationwide, long-term survey. J Gastroenterol. 2012;47(12):1308–22.

[83] Center MM, Jemal A. International trends in liver cancer incidence rates. Cancer epidemiology, biomarkers & prevention : a publication of the American Association for Cancer Research, cosponsored by the American Society of Preventive Oncology. 2011;20:2362–2368. doi:10.1158/1055-9965.EPI-11-0643.

[84] Young JP, Win AK, Rosty C, Flight I, Roder D, Young GP, et al. Rising incidence of early-onset colorectal cancer in Australia over two decades: report and review. J Gastroenterol Hepatol. 2015;30(1):6–13.

[85] Cleynen I, Boucher G, Jostins L, Schumm LP, Zeissig S, Ahmad T, et al. Inherited determinants of Crohn's disease and ulcerative colitis phenotypes: a genetic association study. Lancet (London, England). 2016;387:156–167. doi:10.1016/S0140-6736(15)00465-1.

[86] de la Concha EG, Fernandez-Arquero M, Lopez-Nava G, Martin E, Allcock RJ, Conejero L, et al. Susceptibility to severe ulcerative colitis is associated with polymorphism in the central MHC gene IKBL. Gastroenterology. 2000;119:1491–1495.

[87] Loftus EV, Harewood GC, Loftus CG, Tremaine WJ, Harmsen WS, Zinsmeister AR, et al. PSC-IBD: a unique form of inflammatory bowel disease associated with primary sclerosing cholangitis. Gut. 2005;54:91–96. doi:10.1136/gut.2004.046615.

[88] Jostins L, Ripke S, Weersma RK, Duerr RH, McGovern DP, Hui KY, et al. Host-microbe interactions have shaped the genetic architecture of inflammatory bowel disease. Nature. 2012;491(7422):119–24.

[89] Lees CW, Barrett JC, Parkes M, Satsangi J. New IBD genetics: common pathways with other diseases. Gut. 2011;60(12):1739–53.

[90] Johansson ME, Phillipson M, Petersson J, Velcich A, Holm L, Hansson GC. The inner of the two Muc2 mucin-dependent mucus layers in colon is devoid of bacteria. Proc Natl Acad Sci U S A. 2008;105(39):15064–9.

[91] Pelaseyed T, Bergstrom JH, Gustafsson JK, Ermund A, Birchenough GM, Schutte A, et al. The mucus and mucins of the goblet cells and enterocytes provide the first defense line of the gastrointestinal tract and interact with the immune system. Immunol Rev. 2014;260(1):8–20.

[92] Rodriguez-Pineiro AM, Bergstrom JH, Ermund A, Gustafsson JK, Schutte A, Johansson ME, et al. Studies of mucus in mouse stomach, small intestine, and colon. II. Gastrointestinal mucus proteome reveals Muc2 and Muc5ac accompanied by a set of core proteins. Am J Physiol Gastrointest Liver Physiol. 2013;305(5):G348–56.

[93] Linden SK, Florin TH, McGuckin MA. Mucin dynamics in intestinal bacterial infection. PLoS ONE. 2008;3(12):e3952.

[94] Lidell ME, Johansson ME, Morgelin M, Asker N, Gum J J R, Kim YS, et al. The recombinant C-terminus of the human MUC2 mucin forms dimers in Chinese-hamster ovary cells and heterodimers with full-length MUC2 in LS 174T cells. Biochem J. 2003;372(Pt 2):335–45.

[95] Lang T, Hansson GC, Samuelsson T. Gel-forming mucins appeared early in metazoan evolution. Proc Natl Acad Sci U S A. 2007;104(41):16209–14.

[96] Godl K, Johansson ME, Lidell ME, Morgelin M, Karlsson H, Olson FJ, et al. The N terminus of the MUC2 mucin forms trimers that are held together within a trypsin-resistant core fragment. J Biol Chem. 2002;277(49):47248–56.

[97] Ambort D, Johansson ME, Gustafsson JK, Nilsson HE, Ermund A, Johansson BR, et al. Calcium and pH-dependent packing and release of the gel-forming MUC2 mucin. Proc Natl Acad Sci U S A. 2012;109(15):5645–50.

[98] Nilsson HE, Ambort D, Backstrom M, Thomsson E, Koeck PJ, Hansson GC, et al. Intestinal MUC2 mucin supramolecular topology by packing and release resting on D3 domain assembly. J Mol Biol. 2014;426(14):2567–79.

[99] Velcich A, Yang W, Heyer J, Fragale A, Nicholas C, Viani S, et al. Colorectal cancer in mice genetically deficient in the mucin Muc2. Science. 2002;295(5560):1726–9.

[100] Johansson ME, Gustafsson JK, Holmen-Larsson J, Jabbar KS, Xia L, Xu H, et al. Bacteria penetrate the normally impenetrable inner colon mucus layer in both murine colitis models and patients with ulcerative colitis. Gut. 2014;63(2):281–91.

[101] Fritz T, Niederreiter L, Adolph T, Blumberg RS, Kaser A. Crohn's disease: NOD2, autophagy and ER stress converge. Gut. 2011;60(11):1580–8.

[102] Bibiloni R, Mangold M, Madsen KL, Fedorak RN, Tannock GW. The bacteriology of biopsies differs between newly diagnosed, untreated, Crohn's disease and ulcerative colitis patients. Journal of medical microbiology. 2006;55:1141–1149. doi:10.1099/jmm.0.46498-0.

[103] Morgan XC, Tickle TL, Sokol H, Gevers D, Devaney KL, Ward DV, et al. Dysfunction of the intestinal microbiome in inflammatory bowel disease and treatment. Genome Biol. 2012;13(9):R79.

[104] Arumugam M, Raes J, Pelletier E, Le Paslier D, Yamada T, Mende DR, et al. Enterotypes of the human gut microbiome. Nature. 2011;473:174–180. doi:10.1038/nature09944.

[105] Frank DN, St Amand AL, Feldman RA, Boedeker EC, Harpaz N, Pace NR. Molecular-phylogenetic characterization of microbial community imbalances in human inflammatory bowel diseases. Proc Natl Acad Sci U S A. 2007;104(34):13780–5.

[106] Lepage P, Häsler R, Spehlmann ME, Rehman A, Zvirbliene A, Begun A, et al. Twin study indicates loss of interaction between microbiota and mucosa of patients with ulcerative colitis. Gastroenterology. 2011;141:227–236. doi:10.1053/j.gastro.2011.04.011.

[107] Ohkusa T, Sato N, Ogihara T, Morita K, Ogawa M, Okayasu I. Fusobacterium varium localized in the colonic mucosa of patients with ulcerative colitis stimulates species-specific antibody. J Gastroenterol Hepatol. 2002;17(8):849–53.

[108] Willing BP, Dicksved J, Halfvarson J, Andersson AF, Lucio M, Zheng Z, et al. A pyrosequencing study in twins shows that gastrointestinal microbial profiles vary with inflammatory bowel disease phenotypes. Gastroenterology. 2010;139:1844–1854.e1. doi:10.1053/j.gastro.2010.08.049.

[109] Varela E, Manichanh C, Gallart M, Torrejón A, Borruel N, Casellas F, et al. Colonisation by Faecalibacterium prausnitzii and maintenance of clinical remission in patients with ulcerative colitis. Alimentary pharmacology & therapeutics. 2013;38:151–161. doi:10.1111/apt.12365.

[110] Machiels K, Joossens M, Sabino J, De Preter V, Arijs I, Eeckhaut V, et al. A decrease of the butyrate-producing species Roseburia hominis and Faecalibacterium prausnitzii defines dysbiosis in patients with ulcerative colitis. Gut. 2014;63:1275–1283. doi:10.1136/gutjnl-2013-304833.

[111] Sokol H, Pigneur B, Watterlot L, Lakhdari O, Bermúdez-Humarán LG, Gratadoux JJ, et al. Faecalibacterium prausnitzii is an anti-inflammatory commensal bacterium identified by gut microbiota analysis of Crohn disease patients. Proceedings of the National Academy of Sciences of the United States of America. 2008;105:16731–16736. doi:10.1073/pnas.0804812105.

[112] Atarashi K, Tanoue T, Shima T, Imaoka A, Kuwahara T, Momose Y, et al. Induction of colonic regulatory T cells by indigenous Clostridium species. Science (New York, NY). 2011;331:337–341. doi:10.1126/science.1198469.

[113] Yin L, Laevsky G, Giardina C. Butyrate suppression of colonocyte NF-kappa B activation and cellular proteasome activity. The Journal of biological chemistry. 2001;276:44641–44646. doi:10.1074/jbc.M105170200.

[114] Stempelj M, Kedinger M, Augenlicht L, Klampfer L. Essential role of the JAK/STAT1 signaling pathway in the expression of inducible nitric-oxide synthase in intestinal epithelial cells and its regulation by butyrate. The Journal of biological chemistry. 2007;282:9797–9804. doi:10.1074/jbc.M609426200.

[115] De Preter V, Arijs I, Windey K, Vanhove W, Vermeire S, Schuit F, et al. Impaired butyrate oxidation in ulcerative colitis is due to decreased butyrate uptake and a defect in the oxidation pathway. Inflammatory bowel diseases. 2012;18:1127–1136. doi:10.1002/ibd.21894.

[116] Lennon G, Balfe A, Earley H, Devane LA, Lavelle A, Winter DC, et al. Influences of the colonic microbiome on the mucous gel layer in ulcerative colitis. Gut microbes. 2014;5:277–285. doi:10.4161/gmic.28793.

[117] Png CW, Lindén SK, Gilshenan KS, Zoetendal EG, McSweeney CS, Sly LI, et al. Mucolytic bacteria with increased prevalence in IBD mucosa augment in vitro utilization of mucin by other bacteria. The American journal of gastroenterology. 2010;105:2420–2428. doi:10.1038/ajg.2010.281.

[118] Duchmann R, May E, Heike M, Knolle P, Neurath M, Meyer zum Buschenfelde KH. T cell specificity and cross reactivity towards enterobacteria, bacteroides, bifidobacterium, and antigens from resident intestinal flora in humans. Gut. 1999;44(6):812–8.

[119] Duchmann R, Kaiser I, Hermann E, Mayet W, Ewe K, Meyer zum Buschenfelde KH. Tolerance exists towards resident intestinal flora but is broken in active inflammatory bowel disease (IBD). Clin Exp Immunol. 1995;102(3):448–55.

[120] Kamada N, Hisamatsu T, Okamoto S, Chinen H, Kobayashi T, Sato T, et al. Unique CD14 intestinal macrophages contribute to the pathogenesis of Crohn disease via IL-23/IFN-gamma axis. J Clin Invest. 2008;118(6):2269–80.

[121] Boden EK, Snapper SB. Regulatory T cells in inflammatory bowel disease. Curr Opin Gastroenterol. 2008;24(6):733–41.

[122] Wang R, Hasnain SZ, Tong H, Das I, Che-Hao Chen A, Oancea I, et al. Neutralizing IL-23 is superior to blocking IL-17 in suppressing intestinal inflammation in a spontaneous murine colitis model. Inflamm Bowel Dis. 2015;21(5):973–84.

[123] Bogaert S, Laukens D, Peeters H, Melis L, Olievier K, Boon N, et al. Differential mucosal expression of Th17-related genes between the inflamed colon and ileum of patients with inflammatory bowel disease. BMC Immunol. 2010;11:61.

[124] Fujino S, Andoh A, Bamba S, Ogawa A, Hata K, Araki Y, et al. Increased expression of interleukin 17 in inflammatory bowel disease. Gut. 2003;52(1):65–70.

[125] Mangan PR, Harrington LE, O'Quinn DB, Helms WS, Bullard DC, Elson CO, et al. Transforming growth factor-beta induces development of the T(H)17 lineage. Nature. 2006;441(7090):231–4.

[126] Grivennikov SI, Wang K, Mucida D, Stewart CA, Schnabl B, Jauch D, et al. Adenoma-linked barrier defects and microbial products drive IL-23/IL-17-mediated tumour growth. Nature. 2012;491(7423):254–8.

[127] Jauch D, Martin M, Schiechl G, Kesselring R, Schlitt HJ, Geissler EK, et al. Interleukin 21 controls tumour growth and tumour immunosurveillance in colitis-associated tumorigenesis in mice. Gut. 2011;60(12):1678–86.

[128] Chalaris A, Schmidt-Arras D, Yamamoto K, Rose-John S. Interleukin-6 trans-signaling and colonic cancer associated with inflammatory bowel disease. Dig Dis. 2012;30(5):492–9.

[129] Maihofner C, Charalambous MP, Bhambra U, Lightfoot T, Geisslinger G, Gooderham NJ. Expression of cyclooxygenase-2 parallels expression of interleukin-1beta, interleukin-6 and NF-kappaB in human colorectal cancer. Carcinogenesis. 2003;24(4):665–71.

[130] Ahn B, Ohshima H. Suppression of intestinal polyposis in Apc(Min/+) mice by inhibiting nitric oxide production. Cancer Res. 2001;61(23):8357–60.

[131] Hanahan D, Weinberg RA. The hallmarks of cancer. Cell. 2000;100(1):57–70.

[132] Bressenot A, Cahn V, Danese S, Peyrin-Biroulet L. Microscopic features of colorectal neoplasia in inflammatory bowel diseases. World J Gastroenterol. 2014;20(12):3164–72.

[133] Fearon ER, Vogelstein B. A genetic model for colorectal tumorigenesis. Cell. 1990;61(5):759–67.

[134] Atkin WS, Morson BC, Cuzick J. Long-term risk of colorectal cancer after excision of rectosigmoid adenomas. N Engl J Med. 1992;326(10):658–62.

[135] Rubin DT, Rothe JA, Hetzel JT, Cohen RD, Hanauer SB. Are dysplasia and colorectal cancer endoscopically visible in patients with ulcerative colitis? Gastrointest Endosc. 2007;65(7):998–1004.

[136] Farraye FA, Odze RD, Eaden J, Itzkowitz SH. AGA technical review on the diagnosis and management of colorectal neoplasia in inflammatory bowel disease. Gastroenterology. 2010;138(2):746–74, 774 e1–4; quiz e12–3.

[137] Ullman TA, Itzkowitz SH. Intestinal inflammation and cancer. Gastroenterology. 2011;140(6):1807–16.

[138] Bedard K, Krause KH. The NOX family of ROS-generating NADPH oxidases: physiology and pathophysiology. Physiological reviews. 2007;87:245–313. doi:10.1152/physrev.00044.2005.

[139] Perner A, Andresen L, Pedersen G, Rask-Madsen J. Superoxide production and expression of NAD(P)H oxidases by transformed and primary human colonic epithelial cells. Gut. 2003;52:231–236.

[140] Szanto I, Rubbia-Brandt L, Kiss P, Steger K, Banfi B, Kovari E, et al. Expression of NOX1, a superoxide-generating NADPH oxidase, in colon cancer and inflammatory bowel disease. The Journal of pathology. 2005;207:164–176. doi:10.1002/path.1824.

[141] Nathan C, Xie QW. Nitric oxide synthases: roles, tolls, and controls. Cell. 1994;78:915–918.

[142] MacMicking JD, Nathan C, Hom G, Chartrain N, Fletcher DS, Trumbauer M, et al. Altered responses to bacterial infection and endotoxic shock in mice lacking inducible nitric oxide synthase. Cell. 1995;81:641–650.

[143] Mastroeni P, Vazquez-Torres A, Fang FC, Xu Y, Khan S, Hormaeche CE, et al. Antimicrobial actions of the NADPH phagocyte oxidase and inducible nitric oxide synthase in experimental salmonellosis. II. Effects on microbial proliferation and host survival in vivo. The Journal of experimental medicine. 2000;192:237–248.

[144] Shiloh MU, MacMicking JD, Nicholson S, Brause JE, Potter S, Marino M, et al. Phenotype of mice and macrophages deficient in both phagocyte oxidase and inducible nitric oxide synthase. Immunity. 1999;10:29–38.

[145] Rachmilewitz D, Karmeli F, Okon E, Bursztyn M. Experimental colitis is ameliorated by inhibition of nitric oxide synthase activity. Gut. 1995;37(2):247–55.

[146] Segui J, Gironella M, Sans M, Granell S, Gil F, Gimeno M, et al. Superoxide dismutase ameliorates TNBS-induced colitis by reducing oxidative stress, adhesion molecule expression, and leukocyte recruitment into the inflamed intestine. J Leukoc Biol. 2004;76(3):537–44.

[147] Heyworth PG, Curnutte JT, Nauseef WM, Volpp BD, Pearson DW, Rosen H, et al. Neutrophil nicotinamide adenine dinucleotide phosphate oxidase assembly. Translocation of p47-phox and p67-phox requires interaction between p47-phox and cytochrome b558. The Journal of clinical investigation. 1991;87:352–356. doi:10.1172/JCI114993.

[148] Xie QW, Kashiwabara Y, Nathan C. Role of transcription factor NF-kappa B/Rel in induction of nitric oxide synthase. The Journal of biological chemistry. 1994;269:4705–4708.

[149] Kamijo R, Harada H, Matsuyama T, Bosland M, Gerecitano J, Shapiro D, et al. Requirement for transcription factor IRF-1 in NO synthase induction in macrophages. Science (New York, NY). 1994;263:1612–1615.

[150] Pacelli R, Wink DA, Cook JA, Krishna MC, DeGraff W, Friedman N, et al. Nitric oxide potentiates hydrogen peroxide-induced killing of Escherichia coli. The Journal of experimental medicine. 1995;182:1469–1479.

[151] Schapiro JM, Libby SJ, Fang FC. Inhibition of bacterial DNA replication by zinc mobilization during nitrosative stress. Proceedings of the National Academy of Sciences of the United States of America. 2003;100:8496–8501. doi:10.1073/pnas.1033133100.

[152] Lloyd DR, Carmichael PL, Phillips DH. Comparison of the formation of 8-hydroxy-2'-deoxyguanosine and single- and double-strand breaks in DNA mediated by fenton reactions. Chemical research in toxicology. 1998;11:420–427. doi:10.1021/tx970156l.

[153] Kawahara T, Kuwano Y, Teshima-Kondo S, Takeya R, Sumimoto H, Kishi K, et al. Role of nicotinamide adenine dinucleotide phosphate oxidase 1 in oxidative burst response to Toll-like receptor 5 signaling in large intestinal epithelial cells. Journal of immunology (Baltimore, Md : 1950). 2004;172:3051–3058.

[154] Kojim Si, Ikeda M, Shibukawa A, Kamikawa Y. Modification of 5-hydroxytryptophan-evoked 5-hydroxytryptamine formation of guinea pig colonic mucosa by reactive oxygen species. Japanese journal of pharmacology. 2002;88:114–118.

[155] Birchenough GM, Nystrom EE, Johansson ME, Hansson GC. A sentinel goblet cell guards the colonic crypt by triggering Nlrp6-dependent Muc2 secretion. Science. 2016;352(6293):1535–42.

[156] Kruidenier L, Kuiper I, Van Duijn W, Mieremet-Ooms MA, van Hogezand RA, Lamers CB, et al. Imbalanced secondary mucosal antioxidant response in inflammatory bowel disease. J Pathol. 2003;201(1):17–27.

[157] Kimura H, Hokari R, Miura S, Shigematsu T, Hirokawa M, Akiba Y, et al. Increased expression of an inducible isoform of nitric oxide synthase and the formation of peroxynitrite in colonic mucosa of patients with active ulcerative colitis. Gut. 1998;42(2):180–7.

[158] Kruidenier L, Kuiper I, Lamers CB, Verspaget HW. Intestinal oxidative damage in inflammatory bowel disease: semi-quantification, localization, and association with mucosal antioxidants. J Pathol. 2003;201(1):28–36.

[159] Gushima M, Hirahashi M, Matsumoto T, Fujita K, Fujisawa R, Mizumoto K, et al. Altered expression of MUTYH and an increase in 8-hydroxydeoxyguanosine are early events in ulcerative colitis-associated carcinogenesis. J Pathol. 2009;219(1):77–86.

[160] Shibutani S, Takeshita M, Grollman AP. Insertion of specific bases during DNA synthesis past the oxidation-damaged base 8-oxodG. Nature. 1991;349(6308):431–4.

[161] Wink DA, Kasprzak KS, Maragos CM, Elespuru RK, Misra M, Dunams TM, et al. DNA deaminating ability and genotoxicity of nitric oxide and its progenitors. Science. 1991;254(5034):1001–3.

[162] Nguyen T, Brunson D, Crespi CL, Penman BW, Wishnok JS, Tannenbaum SR. DNA damage and mutation in human cells exposed to nitric oxide in vitro. Proc Natl Acad Sci U S A. 1992;89(7):3030–4.

[163] Yermilov V, Rubio J, Ohshima Hk. Formation of 8-nitroguanine in DNA treated with peroxynitrite in vitro and its rapid removal from DNA by depurination. FEBS Lett. 1995;376(3):207–10.

[164] Phoa N, Epe B. Influence of nitric oxide on the generation and repair of oxidative DNA damage in mammalian cells. Carcinogenesis. 2002;23(3):469–75.

[165] Krokan HE, Nilsen H, Skorpen F, Otterlei M, Slupphaug G. Base excision repair of DNA in mammalian cells. FEBS Lett. 2000;476(1-2):73–7.

[166] Farrington SM, Tenesa A, Barnetson R, Wiltshire A, Prendergast J, Porteous M, et al. Germline susceptibility to colorectal cancer due to base-excision repair gene defects. Am J Hum Genet. 2005;77(1):112–9.

[167] Jaiswal M, LaRusso NF, Nishioka N, Nakabeppu Y, Gores GJ. Human Ogg1, a protein involved in the repair of 8-oxoguanine, is inhibited by nitric oxide. Cancer Res. 2001;61(17):6388–93.

[168] Liu L, Xu-Welliver M, Kanugula S, Pegg AE. Inactivation and degradation of O(6)-alkylguanine-DNA alkyltransferase after reaction with nitric oxidel. Cancer Res. 2002;62(11):3037–43.

[169] Liao J, Seril DN, Lu GG, Zhang M, Toyokuni S, Yang AL, et al. Increased susceptibility of chronic ulcerative colitis-induced carcinoma development in DNA repair enzyme Ogg1 deficient mice. Mol Carcinog. 2008;47(8):638–46.

[170] Cooks T, Harris CC, Oren M. Caught in the cross fire: p53 in inflammation. Carcinogenesis. 2014;35(8):1680–90.

[171] Burmer GC, Rabinovitch PS, Haggitt RC, Crispin DA, Brentnall TA, Kolli VR, et al. Neoplastic progression in ulcerative colitis: histology, DNA content, and loss of a p53 allele. Gastroenterology. 1992;103(5):1602–10.

[172] Yin J, Harpaz N, Tong Y, Huang Y, Laurin J, Greenwald BD, et al. p53 point mutations in dysplastic and cancerous ulcerative colitis lesions. Gastroenterology. 1993;104(6):1633–9.

[173] Hussain SP, Amstad P, Raja K, Ambs S, Nagashima M, Bennett WP, et al. Increased p53 mutation load in noncancerous colon tissue from ulcerative colitis: a cancer-prone chronic inflammatory disease. Cancer Res. 2000;60(13):3333–7.

[174] Brentnall TA, Crispin DA, Rabinovitch PS, Haggitt RC, Rubin CE, Stevens AC, et al. Mutations in the p53 gene: an early marker of neoplastic progression in ulcerative colitis. Gastroenterology. 1994;107(2):369–78.

[175] Forrester K, Ambs S, Lupold SE, Kapust RB, Spillare EA, Weinberg WC, et al. Nitric oxide-induced p53 accumulation and regulation of inducible nitric oxide synthase expression by wild-type p53. Proc Natl Acad Sci U S A. 1996;93(6):2442–7.

[176] Robles AI, Traverso G, Zhang M, Roberts NJ, Khan MA, Joseph C, et al. Whole-Exome Sequencing Analyses of Inflammatory Bowel Disease-Associated Colorectal Cancers. Gastroenterology. 2016;150(4):931–43.

[177] Lengauer C, Kinzler KW, Vogelstein B. Genetic instabilities in human cancers. Nature. 1998;396(6712):643–9.

[178] Willenbucher RF, Aust DE, Chang CG, Zelman SJ, Ferrell LD, Moore n D H, et al. Genomic instability is an early event during the progression pathway of ulcerative-colitis-related neoplasia. Am J Pathol. 1999;154(6):1825–30.

[179] Barbera VM, Martin M, Marinoso L, Munne A, Carrato A, Real FX, et al. The 18q21 region in colorectal and pancreatic cancer: independent loss of DCC and DPC4 expression. Biochim Biophys Acta. 2000;1502(2):283–96.

[180] Rapozo DC, Grinmann AB, Carvalho AT, de Souza HS, Soares-Lima SC, de Almeida Simao T, et al. Analysis of mutations in TP53, APC, K-ras, and DCC genes in the non-dysplastic mucosa of patients with inflammatory bowel disease. Int J Colorectal Dis. 2009;24(10):1141–8.

[181] Lei J, Zou TT, Shi YQ, Zhou X, Smolinski KN, Yin J, et al. Infrequent DPC4 gene mutation in esophageal cancer, gastric cancer and ulcerative colitis-associated neoplasms. Oncogene. 1996;13(11):2459–62.

[182] Terdiman JP, Aust DE, Chang CG, Willenbucher RF, Baretton GB, Waldman FM. High resolution analysis of chromosome 18 alterations in ulcerative colitis-related colorectal cancer. Cancer Genet Cytogenet. 2002;136(2):129–37.

[183] De Angelis PM, Clausen OP, Schjolberg A, Stokke T. Chromosomal gains and losses in primary colorectal carcinomas detected by CGH and their associations with tumour DNA ploidy, genotypes and phenotypes. Br J Cancer. 1999;80(3-4):526–35.

[184] Holzmann K, Klump B, Borchard F, Gregor M, Porschen R. Flow cytometric and histologic evaluation in a large cohort of patients with ulcerative colitis: correlation with clinical characteristics and impact on surveillance. Dis Colon Rectum. 2001;44(10):1446–55.

[185] Gerling M, Meyer KF, Fuchs K, Igl BW, Fritzsche B, Ziegler A, et al. High Frequency of Aneuploidy Defines Ulcerative Colitis-Associated Carcinomas: A Prognostic Comparison to Sporadic Colorectal Carcinomas. Ann Surg. 2010;252(1):74–83.

[186] Friis-Ottessen M, Bendix L, Kolvraa S, Norheim-Andersen S, De Angelis PM, Clausen OP. Telomere shortening correlates to dysplasia but not to DNA aneuploidy in longstanding ulcerative colitis. BMC Gastroenterol. 2014;14:8.

[187] Risques RA, Lai LA, Brentnall TA, Li L, Feng Z, Gallaher J, et al. Ulcerative colitis is a disease of accelerated colon aging: evidence from telomere attrition and DNA damage. Gastroenterology. 2008;135(2):410–8.

[188] O'Sullivan JN, Bronner MP, Brentnall TA, Finley JC, Shen WT, Emerson S, et al. Chromosomal instability in ulcerative colitis is related to telomere shortening. Nat Genet. 2002;32(2):280–4.

[189] Artandi SE, Attardi LD. Pathways connecting telomeres and p53 in senescence, apoptosis, and cancer. Biochem Biophys Res Commun. 2005;331(3):881–90.

[190] Dietmaier W, Wallinger S, Bocker T, Kullmann F, Fishel R, Ruschoff J. Diagnostic microsatellite instability: definition and correlation with mismatch repair protein expression. Cancer Res. 1997;57(21):4749–56.

[191] Goel A, Boland CR. Epigenetics of colorectal cancer. Gastroenterology. 2012;143(6):1442–1460 e1.

[192] Lyda MH, Noffsinger A, Belli J, Fenoglio-Preiser CM. Microsatellite instability and K-ras mutations in patients with ulcerative colitis. Hum Pathol. 2000;31(6):665–71.

[193] Cawkwell L, Sutherland F, Murgatroyd H, Jarvis P, Gray S, Cross D, et al. Defective hMSH2/hMLH1 protein expression is seen infrequently in ulcerative colitis associated colorectal cancers. Gut. 2000;46(3):367–9.

[194] Fleisher AS, Esteller M, Harpaz N, Leytin A, Rashid A, Xu Y, et al. Microsatellite instability in inflammatory bowel disease-associated neoplastic lesions is associated with hypermethylation and diminished expression of the DNA mismatch repair gene, hMLH1. Cancer Res. 2000;60(17):4864–8.

[195] Schulmann K, Mori Y, Croog V, Yin J, Olaru A, Sterian A, et al. Molecular phenotype of inflammatory bowel disease-associated neoplasms with microsatellite instability. Gastroenterology. 2005;129(1):74–85.

[196] Ozaki K, Nagasaka T, Notohara K, Kambara T, Takeda M, Sasamoto H, et al. Heterogeneous microsatellite instability observed within epithelium of ulcerative colitis. Int J Cancer. 2006;119(11):2513–9.

[197] Gloria L, Cravo M, Pinto A, de Sousa LS, Chaves P, Leitao CN, et al. DNA hypomethylation and proliferative activity are increased in the rectal mucosa of patients with long-standing ulcerative colitis. Cancer. 1996;78(11):2300–6.

[198] Feinberg AP, Gehrke CW, Kuo KC, Ehrlich M. Reduced genomic 5-methylcytosine content in human colonic neoplasia. Cancer Res. 1988;48(5):1159–61.

[199] Fujii S, Katake Y, Tanaka H. Increased expression of DNA methyltransferase-1 in non-neoplastic epithelium helps predict colorectal neoplasia risk in ulcerative colitis. Digestion. 2010;82(3):179–86.

[200] Li Y, Deuring J, Peppelenbosch MP, Kuipers EJ, de Haar C, van der Woude CJ. IL-6-induced DNMT1 activity mediates SOCS3 promoter hypermethylation in ulcerative colitis-related colorectal cancer. Carcinogenesis. 2012;33(10):1889–96.

[201] Hsieh CJ, Klump B, Holzmann K, Borchard F, Gregor M, Porschen R. Hypermethylation of the p16INK4a promoter in colectomy specimens of patients with long-standing and extensive ulcerative colitis. Cancer Res. 1998;58(17):3942–5.

[202] Garrity-Park MM, Loftus J E V, Sandborn WJ, Bryant SC, Smyrk TC. Methylation status of genes in non-neoplastic mucosa from patients with ulcerative colitis-associated colorectal cancer. Am J Gastroenterol. 2010;105(7):1610–9.

[203] Azarschab P, Porschen R, Gregor M, Blin N, Holzmann K. Epigenetic control of the E-cadherin gene (CDH1) by CpG methylation in colectomy samples of patients with ulcerative colitis. Genes Chromosomes Cancer. 2002;35(2):121–6.

[204] Konishi K, Shen L, Wang S, Meltzer SJ, Harpaz N, Issa JP. Rare CpG island methylator phenotype in ulcerative colitis-associated neoplasias. Gastroenterology. 2007;132(4):1254–60.

[205] Mikami T, Yoshida T, Numata Y, Shiraishi H, Araki K, Guiot MC, et al. Low frequency of promoter methylation of O6-methylguanine DNA methyltransferase and hMLH1 in ulcerative colitis-associated tumors: comparison with sporadic colonic tumors. Am J Clin Pathol. 2007;127(3):366–73.

[206] Toyota M, Ahuja N, Ohe-Toyota M, Herman JG, Baylin SB, Issa JP. CpG island methylator phenotype in colorectal cancer. Proc Natl Acad Sci U S A. 1999;96(15):8681–6.

[207] Aust DE, Terdiman JP, Willenbucher RF, Chang CG, Molinaro-Clark A, Baretton GB, et al. The APC/beta-catenin pathway in ulcerative colitis-related colorectal carcinomas: a mutational analysis. Cancer. 2002;94(5):1421–7.

[208] Coopman P, Djiane A. Adherens Junction and E-Cadherin complex regulation by epithelial polarity. Cell Mol Life Sci. 2016;.

[209] Ikeda S, Kishida S, Yamamoto H, Murai H, Koyama S, Kikuchi A. Axin, a negative regulator of the Wnt signaling pathway, forms a complex with GSK-3beta and beta-catenin and promotes GSK-3beta-dependent phosphorylation of beta-catenin. Embo J. 1998;17(5):1371–84.

[210] Tetsu O, McCormick F. Beta-catenin regulates expression of cyclin D1 in colon carcinoma cells. Nature. 1999;398(6726):422–6.

[211] He TC, Sparks AB, Rago C, Hermeking H, Zawel L, da Costa LT, et al. Identification of c-MYC as a target of the APC pathway. Science. 1998;281(5382):1509–12.

[212] Phesse TJ, Buchert M, Stuart E, Flanagan DJ, Faux M, Afshar-Sterle S, et al. Partial inhibition of gp130-Jak-Stat3 signaling prevents Wnt-beta-catenin-mediated intestinal tumor growth and regeneration. Sci Signal. 2014;7(345):ra92.

[213] Schwitalla S, Fingerle AA, Cammareri P, Nebelsiek T, Goktuna SI, Ziegler PK, et al. Intestinal tumorigenesis initiated by dedifferentiation and acquisition of stem-cell-like properties. Cell. 2013;152(1-2):25–38.

[214] Takagi Y, Kohmura H, Futamura M, Kida H, Tanemura H, Shimokawa K, et al. Somatic alterations of the DPC4 gene in human colorectal cancers in vivo. Gastroenterology. 1996;111(5):1369–72.

[215] Salovaara R, Roth S, Loukola A, Launonen V, Sistonen P, Avizienyte E, et al. Frequent loss of SMAD4/DPC4 protein in colorectal cancers. Gut. 2002;51(1):56–9.

[216] Miyaki M, Iijima T, Konishi M, Sakai K, Ishii A, Yasuno M, et al. Higher frequency of Smad4 gene mutation in human colorectal cancer with distant metastasis. Oncogene. 1999;18(20):3098–103.

[217] Maitra A, Molberg K, Albores-Saavedra J, Lindberg G. Loss of Dpc4 expression in colonic adenocarcinomas correlates with the presence of metastatic disease. Am J Pathol. 2000;157(4):1105–11.

[218] Zhang B, Halder SK, Kashikar ND, Cho YJ, Datta A, Gorden DL, et al. Antimetastatic role of Smad4 signaling in colorectal cancer. Gastroenterology. 2010;138(3):969–80 e1–3.

[219] Reinacher-Schick A, Baldus SE, Romdhana B, Landsberg S, Zapatka M, Monig SP, et al. Loss of Smad4 correlates with loss of the invasion suppressor E-cadherin in advanced colorectal carcinomas. J Pathol. 2004;202(4):412–20.

[220] Woodford-Richens KL, Rowan AJ, Gorman P, Halford S, Bicknell DC, Wasan HS, et al. SMAD4 mutations in colorectal cancer probably occur before chromosomal instability, but after divergence of the microsatellite instability pathway. Proc Natl Acad Sci U S A. 2001;98(17):9719–23.

[221] Hoque AT, Hahn SA, Schutte M, Kern SE. DPC4 gene mutation in colitis associated neoplasia. Gut. 1997;40(1):120–2.

[222] Kitajima S, Morimoto M, Sagara E. A model for dextran sodium sulfate (DSS)-induced mouse colitis: bacterial degradation of DSS does not occur after incubation with mouse cecal contents. Exp Anim. 2002;51(2):203–6.

[223] Okayasu I, Hatakeyama S, Yamada M, Ohkusa T, Inagaki Y, Nakaya R. A novel method in the induction of reliable experimental acute and chronic ulcerative colitis in mice. Gastroenterology. 1990;98(3):694–702.

[224] Perse M, Cerar A. Dextran sodium sulphate colitis mouse model: traps and tricks. J Biomed Biotechnol. 2012;2012:718617.

[225] Cooper HS, Murthy S, Kido K, Yoshitake H, Flanigan A. Dysplasia and cancer in the dextran sulfate sodium mouse colitis model. Relevance to colitis-associated neoplasia in the human: a study of histopathology, B-catenin and p53 expression and the role of inflammation. Carcinogenesis. 2000;21(4):757–68.

[226] Okayasu I, Yamada M, Mikami T, Yoshida T, Kanno J, Ohkusa T. Dysplasia and carcinoma development in a repeated dextran sulfate sodium-induced colitis model. J Gastroenterol Hepatol. 2002;17(10):1078–83.

[227] Ni J, Chen SF, Hollander D. Effects of dextran sulphate sodium on intestinal epithelial cells and intestinal lymphocytes. Gut. 1996;39(2):234–41.

[228] Rath HC, Schultz M, Freitag R, Dieleman LA, Li F, Linde HJ, et al. Different Subsets of Enteric Bacteria Induce and Perpetuate Experimental Colitis in Rats and Mice. Infection and Immunity. 2001;69(4):2277–2285.

[229] Laroui H, Ingersoll SA, Liu HC, Baker MT, Ayyadurai S, Charania MA, et al. Dextran sodium sulfate (DSS) induces colitis in mice by forming nano-lipocomplexes with medium-chain-length fatty acids in the colon. PLoS ONE. 2012;7(3):e32084.

[230] Johansson ME, Gustafsson JK, Sjoberg KE, Petersson J, Holm L, Sjovall H, et al. Bacteria penetrate the inner mucus layer before inflammation in the dextran sulfate colitis model. PLoS ONE. 2010;5(8):e12238.

[231] Axelsson LG, Landstrom E, Goldschmidt TJ, Gronberg A, Bylund-Fellenius AC. Dextran sulfate sodium (DSS) induced experimental colitis in immunodeficient mice: effects in CD4(+) -cell depleted, athymic and NK-cell depleted SCID mice. Inflamm Res. 1996;45(4):181–91.

[232] Dieleman LA, Ridwan BU, Tennyson GS, Beagley KW, Bucy RP, Elson CO. Dextran sulfate sodium-induced colitis occurs in severe combined immunodeficient mice. Gastroenterology. 1994;107(6):1643–52.

[233] Sainathan SK, Hanna EM, Gong Q, Bishnupuri KS, Luo Q, Colonna M, et al. Granulocyte macrophage colony-stimulating factor ameliorates DSS-induced experimental colitis. Inflamm Bowel Dis. 2008;14(1):88–99.

[234] Melgar S, Karlsson A, Michaelsson E. Acute colitis induced by dextran sulfate sodium progresses to chronicity in C57BL/6 but not in BALB/c mice: correlation between symptoms and inflammation. Am J Physiol Gastrointest Liver Physiol. 2005;288(6):G1328–38.

[235] Cooper HS, Everley L, Chang WC, Pfeiffer G, Lee B, Murthy S, et al. The role of mutant Apc in the development of dysplasia and cancer in the mouse model of dextran sulfate sodium-induced colitis. Gastroenterology. 2001;121(6):1407–16.

[236] Seril DN, Liao J, Ho KL, Warsi A, Yang CS, Yang GY. Dietary iron supplementation enhances DSS-induced colitis and associated colorectal carcinoma development in mice. Dig Dis Sci. 2002;47(6):1266–78.

[237] Kim YJ, Hong KS, Chung JW, Kim JH, Hahm KB. Prevention of colitis-associated carcinogenesis with infliximab. Cancer Prev Res (Phila). 2010;3(10):1314–33.

[238] Chromik AM, Muller AM, Albrecht M, Rottmann S, Otte JM, Herdegen T, et al. Oral administration of taurolidine ameliorates chronic DSS colitis in mice. J Invest Surg. 2007;20(5):273–82.

[239] Berg DJ, Davidson N, Kuhn R, Muller W, Menon S, Holland G, et al. Enterocolitis and colon cancer in interleukin-10-deficient mice are associated with aberrant cytokine production and CD4(+) TH1-like responses. J Clin Invest. 1996;98(4):1010–20.

[240] Ostanin DV, Bao J, Koboziev I, Gray L, Robinson-Jackson SA, Kosloski-Davidson M, et al. T cell transfer model of chronic colitis: concepts, considerations, and tricks of the trade. Am J Physiol Gastrointest Liver Physiol. 2009;296(2):G135–46.

[241] Hasnain SZ, Tauro S, Das I, Tong H, Chen AC, Jeffery PL, et al. IL-10 promotes production of intestinal mucus by suppressing protein misfolding and endoplasmic reticulum stress in goblet cells. Gastroenterology. 2013;144(2):357–368 e9.

[242] Panwala CM, Jones JC, Viney JL. A novel model of inflammatory bowel disease: mice deficient for the multiple drug resistance gene, mdr1a, spontaneously develop colitis. J Immunol. 1998;161(10):5733–44.

[243] Crowe A. The role of P-glycoprotein and breast cancer resistance protein (BCRP) in bacterial attachment to human gastrointestinal cells. J Crohns Colitis. 2011;5(6):531–42.

[244] Ufer M, Hasler R, Jacobs G, Haenisch S, Lachelt S, Faltraco F, et al. Decreased sigmoidal ABCB1 (P-glycoprotein) expression in ulcerative colitis is associated with disease activity. Pharmacogenomics. 2009;10(12):1941–53.

[245] Yamada T, Mori Y, Hayashi R, Takada M, Ino Y, Naishiro Y, et al. Suppression of intestinal polyposis in Mdr1-deficient ApcMin/+ mice. Cancer Res. 2003;63(5):895–901.

[246] Rudolph U, Finegold MJ, Rich SS, Harriman GR, Srinivasan Y, Brabet P, et al. Ulcerative colitis and adenocarcinoma of the colon in G alpha i2-deficient mice. Nat Genet. 1995;10(2):143–50.

[247] Uhlig HH, Hultgren Hornquist E, Ohman Bache L, Rudolph U, Birnbaumer L, Mothes T. Antibody response to dietary and autoantigens in G alpha i2-deficient mice. Eur J Gastroenterol Hepatol. 2001;13(12):1421–9.

[248] Gotlind YY, Raghavan S, Bland PW, Hornquist EH. CD4+FoxP3+ regulatory T cells from Galphai2-/- mice are functionally active in vitro, but do not prevent colitis. PLoS ONE. 2011;6(9):e25073.

[249] Van der Sluis M, De Koning BAE, De Bruijn ACJM, Velcich A, Meijerink JPP, Van Goudoever JB, et al. Muc2-Deficient Mice Spontaneously Develop Colitis, Indicating That MUC2 Is Critical for Colonic Protection. Gastroenterology. 2006;131(1):117–129.

[250] Heazlewood CK, Cook MC, Eri R, Price GR, Tauro SB, Taupin D, et al. Aberrant mucin assembly in mice causes endoplasmic reticulum stress and spontaneous inflammation resembling ulcerative colitis. PLoS Med. 2008;5(3):e54.

[251] Eri RD, Adams RJ, Tran TV, Tong H, Das I, Roche DK, et al. An intestinal epithelial defect conferring ER stress results in inflammation involving both innate and adaptive immunity. Mucosal Immunol. 2011;4(3):354–64.

[252] Moolenbeek C, Ruitenberg EJ. The "Swiss roll": a simple technique for histological studies of the rodent intestine. Lab Anim. 1981;15(1):57–9.

[253] Rasband WS. ImageJ, U. S. National Institutes of Health, Bethesda, Maryland, USA; 1997-2016. https://imagej.nih.gov/ij/.

[254] Ruifrok AC, Johnston DA. Quantification of histochemical staining by color deconvolution. Analytical and quantitative cytology and histology. 2001;23:291–299.

[255] Livak KJ, Schmittgen TD. Analysis of relative gene expression data using real-time quantitative PCR and the 2(-Delta Delta C(T)) Method. Methods. 2001;25(4):402–8.

[256] Moehle C, Ackermann N, Langmann T, Aslanidis C, Kel A, Kel-Margoulis O, et al. Aberrant intestinal expression and allelic variants of mucin genes associated with inflammatory bowel disease. J Mol Med (Berl). 2006;84(12):1055–66.

[257] Longman RJ, Poulsom R, Corfield AP, Warren BF, Wright NA, Thomas MG. Alterations in the composition of the supramucosal defense barrier in relation to disease severity of ulcerative colitis. J Histochem Cytochem. 2006;54(12):1335–48.

[258] Bettington M, Walker N, Clouston A, Brown I, Leggett B, Whitehall V. The serrated pathway to colorectal carcinoma: current concepts and challenges. Histopathology. 2013;62(3):367–86.

[259] Endo A, Koizumi H, Takahashi M, Tamura T, Tatsunami S, Watanabe Y, et al. A significant imbalance in mitosis versus apoptosis accelerates the growth rate of sessile serrated adenoma/polyps. Virchows Archiv : an international journal of pathology. 2013;462:131–139. doi:10.1007/s00428-012-1365-1.

[260] Arai N, Mitomi H, Ohtani Y, Igarashi M, Kakita A, Okayasu I. Enhanced epithelial cell turnover associated with p53 accumulation and high p21WAF1/CIP1 expression in ulcerative colitis. Modern pathology : an official journal of the United States and Canadian Academy of Pathology, Inc. 1999;12:604–611.

[261] Leedham SJ, Graham TA, Oukrif D, McDonald SAC, Rodriguez-Justo M, Harrison RF, et al. Clonality, founder mutations, and field cancerization in human ulcerative colitis-associated neoplasia. Gastroenterology. 2009;136:542–50.e6. doi:10.1053/j.gastro.2008.10.086.

[262] Allen DC, Biggart JD. Misplaced epithelium in ulcerative colitis and Crohn's disease of the colon and its relationship to malignant mucosal changes. Histopathology. 1986;10(1):37–52.

[263] Boivin GP, Washington K, Yang K, Ward JM, Pretlow TP, Russell R, et al. Pathology of mouse models of intestinal cancer: consensus report and recommendations. Gastroenterology. 2003;124(3):762–77.

[264] Ochiai M, Hippo Y, Izumiya M, Watanabe M, Nakagama H. Newly defined aberrant crypt foci as a marker for dysplasia in the rat colon. Cancer Sci. 2014;105(8):943–50.

[265] Sugihara K, Jass JR. Colorectal goblet cell sialomucin heterogeneity: its relation to malignant disease. J Clin Pathol. 1986;39(10):1088–95.

[266] Ehsanullah M, Filipe MI, Gazzard B. Mucin secretion in inflammatory bowel disease: correlation with disease activity and dysplasia. Gut. 1982;23(6):485–9.

[267] Kilgore SP, Sigel JE, Goldblum JR. Hyperplastic-like mucosal change in Crohn's disease: an unusual form of dysplasia? Mod Pathol. 2000;13(7):797–801.

[268] Lee YS. Background mucosal changes in colorectal carcinomas. Cancer. 1988;61(8):1563–70.

[269] Neufert C, Becker C, Neurath MF. An inducible mouse model of colon carcinogenesis for the analysis of sporadic and inflammation-driven tumor progression. Nat Protoc. 2007;2(8):1998–2004.

[270] Kohno H, Suzuki R, Sugie S, Tanaka T. Beta-Catenin mutations in a mouse model of inflammation-related colon carcinogenesis induced by 1,2-dimethylhydrazine and dextran sodium sulfate. Cancer Sci. 2005;96(2):69–76.

[271] O'Toole SM, Pegg AE, Swenberg JA. Repair of O6-methylguanine and O4-methylthymidine in F344 rat liver following treatment with 1,2-dimethylhydrazine and O6-benzylguanine. Cancer research. 1993;53:3895–3898.

[272] Tanaka T, Kohno H, Suzuki R, Yamada Y, Sugie S, Mori H. A novel inflammation-related mouse colon carcinogenesis model induced by azoxymethane and dextran sodium sulfate. Cancer science. 2003;94:965–973.

[273] Suzuki R, Kohno H, Sugie S, Nakagama H, Tanaka T. Strain differences in the susceptibility to azoxymethane and dextran sodium sulfate-induced colon carcinogenesis in mice. Carcinogenesis. 2006;27(1):162–9.

[274] Nolte T, Brander-Weber P, Dangler C, Deschl U, Elwell MR, Greaves P, et al. Nonproliferative and Proliferative Lesions of the Gastrointestinal Tract, Pancreas and Salivary Glands of the Rat and Mouse. J Toxicol Pathol. 2016;29(1 Suppl):1S–125S.

[275] Nissan A, Zhang JM, Lin Z, Haskel Y, Freund HR, Hanani M. The contribution of inflammatory mediators and nitric oxide to lipopolysaccharide-induced intussusception in mice. J Surg Res. 1997;69(1):205–7.

[276] Killoran KE, Miller AD, Uray KS, Weisbrodt NW, Pautler RG, Goyert SM, et al. Role of innate immunity and altered intestinal motility in LPS- and MnCl2-induced intestinal intussusception in mice. Am J Physiol Gastrointest Liver Physiol. 2014;306(5):G445–53.

[277] Rahman AA, Robinson AM, Jovanovska V, Eri R, Nurgali K. Alterations in the distal colon innervation in Winnie mouse model of spontaneous chronic colitis. Cell Tissue Res. 2015;362l(3):497–512.

[278] Robinson AM, Rahman AA, Carbone SE, Randall-Demllo S, Filippone R, Bornstein JC, et al. Alterations of colonic function in the Winnie mouse model of spontaneous chronic colitis. American journal of physiology Gastrointestinal and liver physiology. 2017;312:G85–G102. doi:10.1152/ajpgi.00210.2016.

[279] Roberts JA, Durnin L, Sharkey KA, Mutafova-Yambolieva VN, Mawe GM. Oxidative stress disrupts purinergic neuromuscular transmission in the inflamed colon. The Journal of physiology. 2013;591:3725–3737. doi:10.1113/jphysiol.2013.254136.

[280] Park JH, Kwon JG, Kim SJ, Song DK, Lee SG, Kim ES, et al. Alterations of colonic contractility in an interleukin-10 knockout mouse model of inflammatory bowel disease. Journal of neurogastroenterology and motility. 2015;21:51–61. doi:10.5056/jnm14008.

[281] Birner P, Ritzi M, Musahl C, Knippers R, Gerdes J, Voigtlander T, et al. Immunohistochemical detection of cell growth fraction in formalin-fixed and paraffin-embedded murine tissue. Am J Pathol. 2001;158(6):1991–6.

[282] Gerdes J, Lemke H, Baisch H, Wacker HH, Schwab U, Stein H. Cell cycle analysis of a cell proliferation-associated human nuclear antigen defined by the monoclonal antibody Ki-67. J Immunol. 1984;133(4):1710–5.

[283] Noffsinger AE, Miller MA, Cusi MV, Fenoglio-Preiser CM. The pattern of cell proliferation in neoplastic and nonneoplastic lesions of ulcerative colitis. Cancer. 1996;78(11):2307–12.

[284] Yang J, Weinberg RA. Epithelial-mesenchymal transition: at the crossroads of development and tumor metastasis. Dev Cell. 2008;14(6):818–29.

[285] Gottardi CJ, Wong E, Gumbiner BM. E-cadherin suppresses cellular transformation by inhibiting beta-catenin signaling in an adhesion-independent manner. J Cell Biol. 2001;153(5):1049–60.

[286] Gao D, Vahdat LT, Wong S, Chang JC, Mittal V. Microenvironmental regulation of epithelial-mesenchymal transitions in cancer. Cancer Res. 2012;72(19):4883–9.

[287] Zeisberg M, Neilson EG. Biomarkers for epithelial-mesenchymal transitions. J Clin Invest. 2009;119(6):1429–37.

[288] McInroy L, Maatta A. Down-regulation of vimentin expression inhibits carcinoma cell migration and adhesion. Biochem Biophys Res Commun. 2007;360(1):109–14.

[289] Andersen SN, Rognum TO, Bakka A, Clausen OP. Ki-67: a useful marker for the evaluation of dysplasia in ulcerative colitis. Mol Pathol. 1998;51(6):327–32.

[290] Sasaki Y, Tanaka M, Kudo H. Differentiation between ulcerative colitis and Crohn's disease by a quantitative immunohistochemical evaluation of T lymphocytes, neutrophils, histiocytes and mast cells. Pathol Int. 2002;52(4):277–85.

[291] Galizia G, Lieto E, Zamboli A, De Vita F, Castellano P, Romano C, et al. Neutrophil to lymphocyte ratio is a strong predictor of tumor recurrence in early colon cancers: A propensity score-matched analysis. Surgery. 2015;158(1):112–20.

[292] Turner N, Wong HL, Templeton A, Tripathy S, Whiti Rogers T, Croxford M, et al. Analysis of local chronic inflammatory cell infiltrate combined with systemic inflammation improves prognostication in stage II colon cancer independent of standard clinicopathologic criteria. Int J Cancer. 2016;138(3):671–8.

[293] Fridlender ZG, Albelda SM. Tumor-associated neutrophils: friend or foe? Carcinogenesis. 2012;33(5):949–55.

[294] Wang Y, Wang K, Han GC, Wang RX, Xiao H, Hou CM, et al. Neutrophil infiltration favors colitis-associated tumorigenesis by activating the interleukin-1 (IL-1)/IL-6 axis. Mucosal Immunol. 2014;7(5):1106–15.

[295] Walz A, Burgener R, Car B, Baggiolini M, Kunkel SL, Strieter RM. Structure and neutrophil-activating properties of a novel inflammatory peptide (ENA-78) with homology to interleukin 8. J Exp Med. 1991;174(6):1355–62.

[296] Keates S, Keates AC, Mizoguchi E, Bhan A, Kelly CP. Enterocytes are the primary source of the chemokine ENA-78 in normal colon and ulcerative colitis. Am J Physiol. 1997;273(1 Pt 1):G75–82.

[297] Yang SK, Eckmann L, Panja A, Kagnoff MF. Differential and regulated expression of C-X-C, C-C, and C-chemokines by human colon epithelial cells. Gastroenterology. 1997;113(4):1214–23.

[298] Tang A, Li N, Li X, Yang H, Wang W, Zhang L, et al. Dynamic activation of the key pathways: linking colitis to colorectal cancer in a mouse model. Carcinogenesis. 2012;33(7):1375–83.

[299] Kawamura M, Toiyama Y, Tanaka K, Saigusa S, Okugawa Y, Hiro J, et al. CXCL5, a promoter of cell proliferation, migration and invasion, is a novel serum prognostic marker in patients with colorectal cancer. Eur J Cancer. 2012;48(14):2244–51.

[300] Rubie C, Frick VO, Wagner M, Schuld J, Graber S, Brittner B, et al. ELR+ CXC chemokine expression in benign and malignant colorectal conditions. BMC Cancer. 2008;8:178.

[301] Keates AC, Keates S, Kwon JH, Arseneau KO, Law DJ, Bai L, et al. ZBP-89, Sp1, and nuclear factor-kappa B regulate epithelial neutrophil-activating peptide-78 gene expression in Caco-2 human colonic epithelial cells. J Biol Chem. 2001;276(47):43713–22.

[302] Bender FC, Reymond MA, Bron C, Quest AF. Caveolin-1 levels are down-regulated in human colon tumors, and ectopic expression of caveolin-1 in colon carcinoma cell lines reduces cell tumorigenicity. Cancer Res. 2000;60(20):5870–8.

[303] Razani B, Engelman JA, Wang XB, Schubert W, Zhang XL, Marks CB, et al. Caveolin-1 null mice are viable but show evidence of hyperproliferative and vascular abnormalities. J Biol Chem. 2001;276(41):38121–38.

[304] Hulit J, Bash T, Fu M, Galbiati F, Albanese C, Sage DR, et al. The cyclin D1 gene is transcriptionally repressed by caveolin-1. J Biol Chem. 2000;275(28):21203–9.

[305] Cerezo A, Guadamillas MC, Goetz JG, Sanchez-Perales S, Klein E, Assoian RK, et al. The absence of caveolin-1 increases proliferation and anchorage- independent growth by a Rac-dependent, Erk-independent mechanism. Mol Cell Biol. 2009;29(18):5046–59.

[306] Roy UK, Henkhaus RS, Ignatenko NA, Mora J, Fultz KE, Gerner EW. Wild-type APC regulates caveolin-1 expression in human colon adenocarcinoma cell lines via FOXO1a and C-myc. Mol Carcinog. 2008;47(12):947–55.

[307] Friedrich T, Richter B, Gaiser T, Weiss C, Janssen KP, Einwachter H, et al. Deficiency of caveolin-1 in Apc(min/+) mice promotes colorectal tumorigenesis. Carcinogenesis. 2013;34(9):2109–18.

[308] Takahashi M, Nakatsugi S, Sugimura T, Wakabayashi K. Frequent mutations of the beta-catenin gene in mouse colon tumors induced by azoxymethane. Carcinogenesis. 2000;21(6):1117–20.

[309] Aust DE, Terdiman JP, Willenbucher RF, Chew K, Ferrell L, Florendo C, et al. Altered distribution of beta-catenin, and its binding proteins E-cadherin and APC, in ulcerative colitis-related colorectal cancers. Mod Pathol. 2001;14(1):29–39.

[310] Odze RD, Brien T, Brown CA, Hartman CJ, Wellman A, Fogt F. Molecular alterations in chronic ulcerative colitis-associated and sporadic hyperplastic polyps: a comparative analysis. Am J Gastroenterol. 2002;97(5):1235–42.

[311] Brabletz T, Jung A, Reu S, Porzner M, Hlubek F, Kunz-Schughart LA, et al. Variable beta-catenin expression in colorectal cancers indicates tumor progression driven by the tumor environment. Proc Natl Acad Sci U S A. 2001;98(18):10356–61.

[312] Sato F, Harpaz N, Shibata D, Xu Y, Yin J, Mori Y, et al. Hypermethylation of the p14(ARF) gene in ulcerative colitis-associated colorectal carcinogenesis. Cancer Res. 2002;62(4):1148–51.

[313] Treton X, Pedruzzi E, Cazals-Hatem D, Grodet A, Panis Y, Groyer A, et al. Altered endoplasmic reticulum stress affects translation in inactive colon tissue from patients with ulcerative colitis. Gastroenterology. 2011;141(3):1024–35.

[314] De Robertis M, Massi E, Poeta ML, Carotti S, Morini S, Cecchetelli L, et al. The AOM/DSS murine model for the study of colon carcinogenesis: From pathways to diagnosis and therapy studies. J Carcinog. 2011;10:9.

[315] Wargovich MJ, Brown VR, Morris J. Aberrant crypt foci: the case for inclusion as a biomarker for colon cancer. Cancers. 2010;2:1705–1716. doi:10.3390/cancers2031705.

[316] Carter JW, Lancaster HK, Hardman WE, Cameron IL. Distribution of intestine-associated lymphoid tissue, aberrant crypt foci, and tumors in the large bowel of 1,2-dimethylhydrazine-treated mice. Cancer research. 1994;54:4304–4307.

[317] Jen J, Powell SM, Papadopoulos N, Smith KJ, Hamilton SR, Vogelstein B, et al. Molecular determinants of dysplasia in colorectal lesions. Cancer research. 1994;54:5523–5526.

[318] Alrawi SJ, Schiff M, Carroll RE, Dayton M, Gibbs JF, Kulavlat M, et al. Aberrant crypt foci. Anticancer Res. 2006;26(1A):107–19.

[319] Bersudsky M, Luski L, Fishman D, White RM, Ziv-Sokolovskaya N, Dotan S, et al. Non-redundant properties of IL-1alpha and IL-1beta during acute colon inflammation in mice. Gut. 2013;.

[320] Kuhn KA, Manieri NA, Liu TC, Stappenbeck TS. IL-6 stimulates intestinal epithelial proliferation and repair after injury. PLoS ONE. 2014;9(12):e114195.

[321] Mahler M, Bristol IJ, Sundberg JP, Churchill GA, Birkenmeier EH, Elson CO, et al. Genetic analysis of susceptibility to dextran sulfate sodium-induced colitis in mice. Genomics. 1999;55(2):147–56.

[322] Hornquist CE, Lu X, Rogers-Fani PM, Rudolph U, Shappell S, Birnbaumer L, et al. G(alpha)i2-deficient mice with colitis exhibit a local increase in memory CD4+ T cells and proinflammatory Th1-type cytokines. J Immunol. 1997;158(3):1068–77.

[323] Wenzel UA, Magnusson MK, Rydstrom A, Jonstrand C, Hengst J, Johansson ME, et al. Spontaneous colitis in Muc2-deficient mice reflects clinical and cellular features of active ulcerative colitis. PLoS ONE. 2014;9(6):e100217.

[324] Burger-van Paassen N, van der Sluis M, Bouma J, Korteland-van Male AM, Lu P, Van Seuningen I, et al. Colitis development during the suckling-weaning transition in mucin Muc2-deficient mice. Am J Physiol Gastrointest Liver Physiol. 2011;301(4):G667–78.

[325] Nambiar PR, Girnun G, Lillo NA, Guda K, Whiteley HE, Rosenberg DW. Preliminary analysis of azoxymethane induced colon tumors in inbred mice commonly used as transgenic/knockout progenitors. Int J Oncol. 2003;22(1):145–50.

[326] Das I, Png CW, Oancea I, Hasnain SZ, Lourie R, Proctor M, et al. Glucocorticoids alleviate intestinal ER stress by enhancing protein folding and degradation of misfolded proteins. J Exp Med. 2013;.

[327] Walter P, Ron D. The unfolded protein response: from stress pathway to homeostatic regulation. Science. 2011;334(6059):1081–6.

[328] Sansom OJ, Meniel VS, Muncan V, Phesse TJ, Wilkins JA, Reed KR, et al. Myc deletion rescues Apc deficiency in the small intestine. Nature. 2007;446(7136):676–9.

[329] Finch AJ, Soucek L, Junttila MR, Swigart LB, Evan GI. Acute overexpression of Myc in intestinal epithelium recapitulates some but not all the changes elicited by Wnt/beta-catenin pathway activation. Mol Cell Biol. 2009;29(19):5306–15.

[330] van Riggelen J, Yetil A, Felsher DW. MYC as a regulator of ribosome biogenesis and protein synthesis. Nat Rev Cancer. 2010;10(4):301–9.

[331] Vaiphei K, Saha M, Sharma BC, Bhasin DK, Singh K. Goblet cell status in idiopathic ulcerative colitis–implication in surveillance program. Indian J Pathol Microbiol. 2004;47(1):16–21.

[332] Fujii S, Fujimori T, Kawamata H, Takeda J, Kitajima K, Omotehara F, et al. Development of colonic neoplasia in p53 deficient mice with experimental colitis induced by dextran sulphate sodium. Gut. 2004;53(5):710–6.

[333] Nambiar PR, Giardina C, Guda K, Aizu W, Raja R, Rosenberg DW. Role of the alternating reading frame (P19)-p53 pathway in an in vivo murine colon tumor model. Cancer Res. 2002;62(13):3667–74.

[334] Brighenti E, Calabrese C, Liguori G, Giannone FA, Trere D, Montanaro L, et al. Interleukin 6 downregulates p53 expression and activity by stimulating ribosome biogenesis: a new pathway connecting inflammation to cancer. Oncogene. 2014;33(35):4396–406.

[335] Mlynarczyk C, Fahraeus R. Endoplasmic reticulum stress sensitizes cells to DNA damage-induced apoptosis through p53-dependent suppression of p21(CDKN1A). Nat Commun. 2014;5:5067.

[336] Coccia M, Harrison OJ, Schiering C, Asquith MJ, Becher B, Powrie F, et al. IL-1beta mediates chronic intestinal inflammation by promoting the accumulation of IL-17A secreting innate lymphoid cells and CD4(+) Th17 cells. J Exp Med. 2012;209(9):1595–609.

[337] Fisher DT, Appenheimer MM, Evans SS. The two faces of IL-6 in the tumor microenvironment. Semin Immunol. 2014;26(1):38–47.

[338] Yagi Y, Andoh A, Inatomi O, Tsujikawa T, Fujiyama Y. Inflammatory responses induced by interleukin-17 family members in human colonic subepithelial myofibroblasts. J Gastroenterol. 2007;42(9):746–53.

[339] Hodge DR, Peng B, Cherry JC, Hurt EM, Fox SD, Kelley JA, et al. Interleukin 6 supports the maintenance of p53 tumor suppressor gene promoter methylation. Cancer Res. 2005;65(11):4673–82.

[340] Chang LY, Lin YC, Mahalingam J, Huang CT, Chen TW, Kang CW, et al. Tumor-derived chemokine CCL5 enhances TGF-beta-mediated killing of CD8(+) T cells in colon cancer by T-regulatory cells. Cancer Res. 2012;72(5):1092–102.

[341] Bergstrom KS, Kissoon-Singh V, Gibson DL, Ma C, Montero M, Sham HP, et al. Muc2 protects against lethal infectious colitis by disassociating pathogenic and commensal bacteria from the colonic mucosa. PLoS Pathog. 2010;6(5):e1000902.

[342] Wlodarska M, Thaiss CA, Nowarski R, Henao-Mejia J, Zhang JP, Brown EM, et al. NLRP6 inflammasome orchestrates the colonic host-microbial interface by regulating goblet cell mucus secretion. Cell. 2014;156(5):1045–59.

[343] Elinav E, Strowig T, Kau AL, Henao-Mejia J, Thaiss CA, Booth CJ, et al. NLRP6 inflammasome regulates colonic microbial ecology and risk for colitis. Cell. 2011;145(5):745–57.

[344] Gu S, Chen D, Zhang JN, Lv X, Wang K, Duan LP, et al. Bacterial community mapping of the mouse gastrointestinal tract. PLoS ONE. 2013;8(10):e74957.

[345] Lozupone CA, Stombaugh JI, Gordon JI, Jansson JK, Knight R. Diversity, stability and resilience of the human gut microbiota. Nature. 2012;489(7415):220–30.

[346] Alkadhi S, Kunde D, Cheluvappa R, Randall-Demllo S, Eri R. The murine appendiceal microbiome is altered in spontaneous colitis and its pathological progression. Gut Pathog. 2014;6:25.

[347] Robinson AM, Gondalia SV, Karpe AV, Eri R, Beale DJ, Morrison PD, et al. Fecal Microbiota and Metabolome in a Mouse Model of Spontaneous Chronic Colitis: Relevance to Human Inflammatory Bowel Disease. Inflammatory bowel diseases. 2016;22:2767–2787. doi:10.1097/MIB.0000000000000970.

[348] Sobhani I, Tap J, Roudot-Thoraval F, Roperch JP, Letulle S, Langella P, et al. Microbial dysbiosis in colorectal cancer (CRC) patients. PloS one. 2011;6:e16393. doi:10.1371/journal.pone.0016393.

[349] Sanapareddy N, Legge RM, Jovov B, McCoy A, Burcal L, Araujo-Perez F, et al. Increased rectal microbial richness is associated with the presence of colorectal adenomas in humans. The ISME journal. 2012;6:1858–1868. doi:10.1038/ismej.2012.43.

[350] Castellarin M, Warren RL, Freeman JD, Dreolini L, Krzywinski M, Strauss J, et al. Fusobacterium nucleatum infection is prevalent in human colorectal carcinoma. Genome Res. 2012;22(2):299–306.

[351] Kostic AD, Chun E, Robertson L, Glickman JN, Gallini CA, Michaud M, et al. Fusobacterium nucleatum potentiates intestinal tumorigenesis and modulates the tumor-immune microenvironment. Cell Host Microbe. 2013;14(2):207–15.

[352] Rubinstein MR, Wang X, Liu W, Hao Y, Cai G, Han YW. Fusobacterium nucleatum promotes colorectal carcinogenesis by modulating E-cadherin/beta-catenin signaling via its FadA adhesin. Cell Host Microbe. 2013;14(2):195–206.

[353] Arthur JC, Perez-Chanona E, Muhlbauer M, Tomkovich S, Uronis JM, Fan TJ, et al. Intestinal inflammation targets cancer-inducing activity of the microbiota. Science. 2012;338(6103):120–3.

[354] Lara-Tejero M, Galan JE. A bacterial toxin that controls cell cycle progression as a deoxyribonuclease I-like protein. Science. 2000;290(5490):354–7.

[355] Huycke MM, Abrams V, Moore DR. Enterococcus faecalis produces extracellular superoxide and hydrogen peroxide that damages colonic epithelial cell DNA. Carcinogenesis. 2002;23(3):529–36.

[356] Fasseu M, Treton X, Guichard C, Pedruzzi E, Cazals-Hatem D, Richard C, et al. Identification of restricted subsets of mature microRNA abnormally expressed in inactive colonic mucosa of patients with inflammatory bowel disease. PLoS ONE. 2010;5(10).

[357] Motoyama K, Inoue H, Takatsuno Y, Tanaka F, Mimori K, Uetake H, et al. Over- and under-expressed microRNAs in human colorectal cancer. Int J Oncol. 2009;34(4):1069–75.

[358] Bronisz A, Godlewski J, Wallace JA, Merchant AS, Nowicki MO, Mathsyaraja H, et al. Reprogramming of the tumour microenvironment by stromal PTEN-regulated miR-320. Nat Cell Biol. 2012;14(2):159–67.

[359] Bamba S, Andoh A, Ban H, Imaeda H, Aomatsu T, Kobori A, et al. The severity of dextran sodium sulfate-induced colitis can differ between dextran sodium sulfate preparations of the same molecular weight range. Dig Dis Sci. 2012;57(2):327–34.